

Pattern Kerfing for Responsive Wooden Surfaces

A formal approach to produce flexible panels with acoustic performance

Andreas Holterman



GRADUATION THESIS

Student

A. M. (Andreas) Holterman

Studentnumber 4156013

Mentors

Dr. S. (Serdar) Aşut

Architectural Engineering + Technology

Chair Design Informatics

Ir. C.J. (Christien) Janssen

Architectural Engineering + Technology

Chair Building Physics and Services

Examiner of Graduation Committee

Dr. Ir. M. (Marjolein) Spaans

AR3B025 Sustainable Design Graduation

Master Track of Building Technology

Faculty of Architecture and the Built Environment

Delft University of Technology

ABSTRACT

The aim of this thesis is to present the outputs of a project in which pattern kerfing techniques are explored for producing responsive freeform panels out of wooden plates. Relevant research such as the ones presented by Ivanišević, (2014), Zarrinmehr et al. (2017) and Ohshima et al. (2013) have shown that it is possible to bend a wooden plate by carving patterns on one or two sides of it. By this means, the plate is able to perform both single and double curved surfaces depending on the pattern design.

The main objective of this research is to find out the relationships between the geometric parameters of the pattern and the bending capabilities of the plate and to put forward a formalized method for the design and fabrication of three-dimensional, freeform and responsive surfaces. These findings lead to complex pattern designs which enable the plates to perform three dimensional and freeform curved surfaces. Moreover, these panels can be actuated as responsive building components which answer the changing performance requirements in a space. In this research, acoustic performance is addressed by designing panels which respond to the changing acoustic needs of a lecture room.

The applied research methods on the flexibility involve experiments with physical models and a simulation in which the effect of the geometric parameters of the pattern on the bending capabilities are further elaborated. The acoustic performance is measured and calculated by means of multiple acoustic measurements.

This research outputs three main items. The first one is a parametric definition which was used to design pattern variations in order to achieve various three-dimensional freeform surfaces produced by pattern kerfing out of wooden plates. This definition is applicable in different design problems in which the design of such surfaces is needed. The second output is a series of prototypes which are produced using laser cutting and CNC milling in order to test the actual bending capabilities of the produced panels and to measure the acoustic performance based on the defined parameters related to the geometry and composition of the panels. The last output is a case study in which the developed design and fabrication techniques are demonstrated for designing a teaching environment with better acoustic performance.

TABLE OF CONTENTS

	List of Figures	10
	List of Graphs	14
1.	INTRODUCTION	17
1.1.	Background	17
1.2.	Problem statement	18
1.3.	Objectives	19
1.4.	Research questions	20
1.5.	Approach and methodology	20
	1.5.1. Research Method	20
	1.5.2. Boundary Conditions	21
1.6.	Relevance	22
1.7.	Time planning	23
2.	FLEXIBILITY	27
2.1.	Introduction	27
2.2.	Literature study	28
	2.2.1. Flexible patterns	28
	2.2.2. Surface curvature	31
	2.2.3. Cutting techniques	33
2.3.	Pattern design	36
	2.3.1. Introduction	36
	2.3.2. Linear pattern	36
	2.3.3. Meander pattern	37
	2.3.4. Parameters	39
2.4.	Parametric model	45
	2.4.1. Introduction	45
	2.4.2. Parameters	45
	2.4.3. Algorithm	46

2.5.	Analyses on flexibility	48
2.5.1.	Introduction	48
2.5.2.	Observations	48
2.5.3.	Simulations	53
2.6.	Conclusions	64
2.6.1.	Simulations	64
2.6.2.	Final Remarks	64
3.	ACOUSTICS	67
3.1.	Introduction	67
3.2.	Literature study	68
3.2.1.	Principles	68
3.2.2.	Porous absorption	73
3.2.3.	Resonant absorbers	75
3.2.4.	Architectural acoustics	76
3.2.5.	Classroom scenario	79
3.3.	Acoustic design	81
3.3.1.	Introduction	81
3.3.2.	Acoustic parameters	81
3.3.3.	Space definition	82
3.4.	Measurements	84
3.4.1.	Introduction	84
3.4.2.	Impedance Tube	84
3.4.3.	Impulse Response	100
3.5.	Conclusions	112
3.5.1.	Impedance Tube	112
3.5.2.	Impulse Response	113
3.5.3.	Final remarks	114
4.	DESIGN	117
4.1.	Introduction	117

4.2.	Concept	118
4.2.1.	Material aspects	120
4.2.2.	Manufacturing	121
4.2.3.	Assembly	122
4.2.4.	Transformation	125
4.3.	Prototyping	127
4.3.1.	Design concept	127
4.3.2.	Proceeding to a final product	134
4.4.	Case study	135
4.4.1.	Introduction	135
4.4.2.	Scenarios	135
4.5.	Conclusions	140
4.5.1.	Prototype	140
4.5.2.	Design	140
4.5.3.	Final Remarks	141
5.	CONCLUSIONS	143
5.1.	Conclusions	143
5.1.1.	Flexibility	143
5.1.2.	Acoustics	143
5.1.3.	Design	144
5.1.4.	Final remarks	144
5.2.	Recommendations for future work	146
6.	REFLECTION	149
7.	BIBLIOGRAPHY	153

APPENDICES	159
A. Acoustic data and measurement results	159
A.1. Project setup impedance tube - Large samples	159
A.2. Project setup impedance tube - Small samples	160
A.3. Individual graphs impedance tube measurement	161

LIST OF FIGURES

Figure 1.	Japanese art of kirigami (MaterialDistrict, 2017).	17
Figure 2.	The wooden knot shows the flexibility of the dukta method (dukta, 2018b).	18
Figure 3.	Global time schedule for the entire research.	24
Figure 4.	Linear pattern allows for flexibility in one direction (Couden, 2013).	28
Figure 5.	A flexible 2D Meander pattern discovered by Ivanišević (2014).	29
Figure 6.	Other symmetric meander patterns motivated by the original pattern by Ivanišević: Pattern attributed to Robert Lang (a), pattern introduced by an anonymous person (b) and a circular pattern by M. S. Raynolds (c) (Zarrinmehr, Akleman, Ettehad, Kalantar, & Borhani, 2017).	29
Figure 7.	Local flexibility by manipulating the number of iterations locally, by means of a control image (Zarrinmehr, Akleman, Ettehad, Kalantar, & Borhani, 2017).	30
Figure 8.	Plywood is constructed of multiple layers of wood veneer, giving it isotropic properties (US Craft Company, Unknown).	31
Figure 9.	Bending changes the mean but not the Gaussian curvature (adapted from Callens and Zadpoor (2017))	32
Figure 10.	Non-zero Gaussian curvatures (adapted from Callens and Zadpoor (2017))	32
Figure 11.	Developable surfaces with zero Gaussian curvature (adapted from Callens and Zadpoor (2017))	33
Figure 12.	A laser cutting machine in operation. (Kingston University London, Unknown)	34
Figure 13.	A laser cut pattern (Porterfield, 2014).	34
Figure 14.	Cutting wood with a CNC milling machine (Nieweglowski).	35
Figure 15.	Kerfing a linear pattern in plywood ("Cutting Plywood," Unknown).	35
Figure 16.	Connected lengths of a linear pattern.	36
Figure 17.	Cross-section A-A'. The kerf width determines possible rotation of segments.	37
Figure 18.	Linear patterns: A standard parallel orientation (a) and linear patterns with manipulated orientation (b & c).	37
Figure 19.	A [4,2] meander unit is repeated to create the final pattern, where each branch interlocks with a branch of a different spiral tree.	38
Figure 20.	The subtracted meander pattern divides the surface into multiple interconnected segments, which are subjected to bending and/or torsion.	38
Figure 21.	Relations between the different pattern and material parameters for a meander pattern.	39

Figure 22. The three main pattern variables: Unit size (a), number of iterations (b) and kerf width (c).	40
Figure 23. Flexibility can be increased by a higher number of iterations (b) or a larger kerf width (c).	41
Figure 24. Expectations for changes in stiffness when manipulating the segment parameters.	41
Figure 25. Grid distortion by randomizing or stretching.	42
Figure 26. Variable kerf width based on a line attractor (a), point attractor (b) or shape attractor (c).	43
Figure 27. Local flexibility obtained by varying number of iterations based on a point attractor. Regular (a) and inverted (b).	44
Figure 28. Parametric model from Grasshopper based on the pattern parameters.	45
Figure 29. The three main steps in the process: Interlocking branches (a) are projected onto the grid (b) and given an offset to be merged together (c).	46
Figure 30. Flowchart of the meander pattern algorithm in Grasshopper.	47
Figure 31. Bending tool to examine the bending behavior of different patterns. Here a non-uniform pattern is displayed, as shown in Figure 26a.	49
Figure 32. Close-up from protruding segments.	49
Figure 33. Angle of displacement between the colored regions.	50
Figure 34. Segments subjected to bending (red) and torsion (green) when a bending moment is applied about the y-axis.	51
Figure 35. Deformation of a shell structure with axial stresses, due to a bending moment.	53
Figure 36. Conversion of a panel into a Karamba model. A regular meander pattern (a), centerlines of all segments (b) and beams created from the centerlines (c).	54
Figure 37. Karamba flowchart for the constructed algorithm.	54
Figure 38. The model is supported on two opposite sides, with green arrows indicating the fixed translation along that particular axis.	55
Figure 39. Deformation of the model, built up of interconnected beams.	55
Figure 40. Model with gradually increased uniformly distributed load.	56
Figure 41. Axial stresses on the top and bottom surface.	56
Figure 42. Bending moments (M_x) about the local x-axis (torsional moment).	57
Figure 43. Bending moments (M_y) about the local y-axis.	57
Figure 44. Base model, used for finding the maximum displacement	58
Figure 45. Load diagram of the supported model.	58
Figure 46. Maximum displacement of 257 mm for the model supported on both ends, with a span of 1,20 m.	59

Figure 47. Maximum displacement of 21 mm for the model supported at both ends, with a span of 0,60m.	62
Figure 48. Maximum displacement of 10 mm for the model supported at both ends and in the middle, with a total span of 1,20 m.	62
Figure 49. Loosening one of the cables causes large deformations of the panel and a different force-flow.	63
Figure 50. Relation between sound level and sound pressure, at a single frequency (Ermann, 2014, p. 3).	68
Figure 51. Acoustic Waveform for pure tones, harmonics and complex sounds (adapted from Ermann (2014)).	70
Figure 52. Wavelength vs. frequency.	71
Figure 53. Incident sound will be distributed into transmission, absorption or reflection.	71
Figure 54. Schematic representation of closed (top) and open (bottom) pore structures (adapted from Cremer and Muller (1982)).	73
Figure 55. Oscillatory viscous flow over a surface (Godbold, 2008, p. 15).	74
Figure 56. Typical construction for a Helmholtz absorber (Cox & D'Antonio, 2009, p. 197).	75
Figure 57. Variable room acoustics in l'Espace de Projection, IRCAM, Paris (Panier des Touches, 2014).	77
Figure 58. Jones Hall, Houston, Texas (adapted from Arie, 2013; Downtown Houston, 2010).	78
Figure 59. E. J. Thomas Hall, Akron, Ohio (Dionne, 2012).	78
Figure 60. Acoustic parameters: Type of pattern (a), open surface area (b), air cavity (c) and surface curvature (d).	81
Figure 61. Three different scenarios: Classroom with a single speaker (a), classroom with round-table discussion (b) and classroom with small groups (c).	83
Figure 62. Setup for Impedance Tube measurement.	85
Figure 63. Setup of Impedance Tube. Top: Large tube setting for measurements from 50 to 1600 Hz. Bottom: Small tube setting for measurements from 500 to 6400 Hz.	85
Figure 64. Acoustic samples with different pattern parameters.	87
Figure 65. Sample with surface curvature (L24-40 Curved).	87
Figure 66. The given codename for each sample is composed of the dimensions of the kerfs and segments.	88
Figure 67. An acoustical Impulse Response (Rational Acoustics, 2015).	100
Figure 68. Setup of the equipment for the Impulse Response measurement.	102
Figure 69. Two different frames have been used for the Impulse Response measurement. An enclosed box (left) and an open frame (right).	103

Figure 70.	The room that is used to perform the measurement (left) and the removed panels of the suspended ceiling (right).	104
Figure 71.	Floorplan of the measurement room with the two different setups.	104
Figure 72.	Panel positions, three with a surface curvature, four inside the box and the frame at different air cavity depths.	105
Figure 73.	Design concept: Responsive panels mounted on the ceiling with a retractable cable system that is controlled by an automatic system.	118
Figure 74.	A single panel is attached to 20 cables, which can be individually extended or retracted to deform the panel into a double-curved surface.	119
Figure 75.	The support locations on the surface and the used pattern parameters.	120
Figure 76.	Detail from the support at the acoustic panel.	122
Figure 77.	Actuator positions are placed in a grid structure onto the ceiling, above the panel.	123
Figure 78.	The predefined shapes for the responsive panels, flat and the three compositions for the described scenarios.	124
Figure 79.	Transformation from flat to curved surface.	125
Figure 80.	Transformation from panel composition 2 to 3.	126
Figure 81.	Pattern design for the constructed prototype.	127
Figure 82.	Close-up from the constructed panel, directly coming from the milling machine.	128
Figure 83.	Simulation model of the built prototype has a maximum displacement of 12 mm.	129
Figure 84.	The radius of the maximum surface curvature of this prototype is approximately 70 cm.	129
Figure 85.	Completed prototype laid down flat.	130
Figure 86.	Completed prototype laid down with curved surface.	130
Figure 87.	Completed prototype with the absorbent layer fixed by bolts and nuts.	131
Figure 88.	Close-up from the support point at the completed prototype.	131
Figure 89.	Hanging prototype with a convex surface.	132
Figure 90.	Hanging prototype with a concave surface.	132
Figure 91.	Hanging prototype with a freeform surface.	133
Figure 92.	Close-up from the hanging prototype with a freeform surface.	133
Figure 93.	The four basic panel compositions: Flat, half parabolic, full parabolic and sinusoidal.	135
Figure 94.	Acoustic panels applied in the lecture room, with a flat surface.	136
Figure 95.	Acoustic panels applied in the lecture room, with a half parabolic surface.	137
Figure 96.	Acoustic panels applied in the lecture room, with a full parabolic surface.	138
Figure 97.	Acoustic panels applied in the lecture room, with a sinusoidal surface.	139

LIST OF GRAPHS

Graph 1.	Maximum displacement with constant segment width of 10 mm.	60
Graph 2.	Maximum displacement for a pattern with 4 iterations.	61
Graph 3.	Absorption coefficient for L25-50 and M24-50. (Note: graph is in logarithmic scale)	90
Graph 4.	Absorption coefficient for L44-68 and M44-68. (Note: graph is in logarithmic scale)	91
Graph 5.	Absorption coefficient for L24-50 and L44-50. (Note: graph is in logarithmic scale)	92
Graph 6.	Absorption coefficient for L24-50 and L48-50. (Note: graph is in logarithmic scale)	93
Graph 7.	Absorption coefficient for L24-40 large and curved. (Note: graph is in logarithmic scale)	94
Graph 8.	Absorption coefficient for L24-40 small. (Note: graph is in linear scale)	95
Graph 9.	Absorption coefficient for L24-40 large and small. (Note: graph is in logarithmic scale)	96
Graph 10.	Absorption coefficient for various open surface areas. (Note: graph is in logarithmic scale)	97
Graph 11.	Absorption coefficient for various open surface areas. (Note: graph is in linear scale)	98
Graph 12.	Average absorption coefficient for L24-40. (Note: graph is in linear scale)	99
Graph 13.	The reverberation time can be determined by using different intervals.	106
Graph 14.	Reverberation Time for setup A at T_{20}	109
Graph 15.	Reverberation Time for setup B at T_{20}	109
Graph 16.	Absorption Coefficient for setup A at T_{20}	111
Graph 17.	Absorption Coefficient for setup B at T_{20}	111

1. INTRODUCTION

1.1. BACKGROUND

The aim of this research is to present the outputs of an ongoing project in which pattern cutting (kerfing) techniques are explored for producing responsive freeform panels out of wooden plates.

Relative simple forms of pattern cutting can be seen in the art of kirigami, a variation to origami (Figure 1). This technique is also named as the art of paper cutting, which combines paper cutting and folding to create three-dimensional objects. T. C. Shyu and other researchers at the University of Michigan, also looked into this Japanese technique and used it to develop flexible electronic conductors, opening up possibilities for transformable electronics (Shyu et al., 2015).

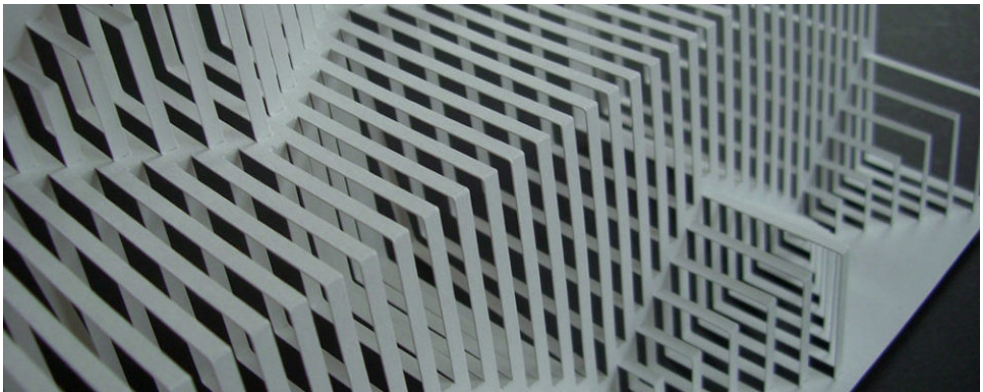


Figure 1. Japanese art of kirigami (MaterialDistrict, 2017).

This technique of pattern cutting to create freeform surfaces out of a flat layer of material, can also be applied on other, solid materials with a higher bending stiffness such as wood. Relevant research such as the ones presented by Ivanišević (2014), Zarrinmehr et al. (2017) and Ohshima et al. (2013) have shown that it is possible to bend a wooden plate by kerfing patterns on one or two sides of it. They showed that precise pattern kerfs in a solid plate will change the geometric properties in such a way that it decreases the bending stiffness. It gives the wooden plate a higher flexibility, enhancing the plate to perform both single and double curved surfaces depending on the pattern design.

The company dukta is currently a leading company when it comes to this type of incision processes to make wood and engineered wood, such as plywood and MDF, flexible. They initiated their first experiments of this technique in Switzerland back

in 2007 (See Figure 2). Since 2015, products based on dukta processes have been manufactured and shipped throughout Europe (dukta, 2018a).

These findings lead to complex pattern designs which enable the plates to perform three dimensional and freeform curved surfaces. Moreover, these panels can be actuated as responsive building components which can react to the changing performance requirements in a space. In this research, acoustic performance is addressed by designing panels which respond to the changing acoustic needs of a lecture room.

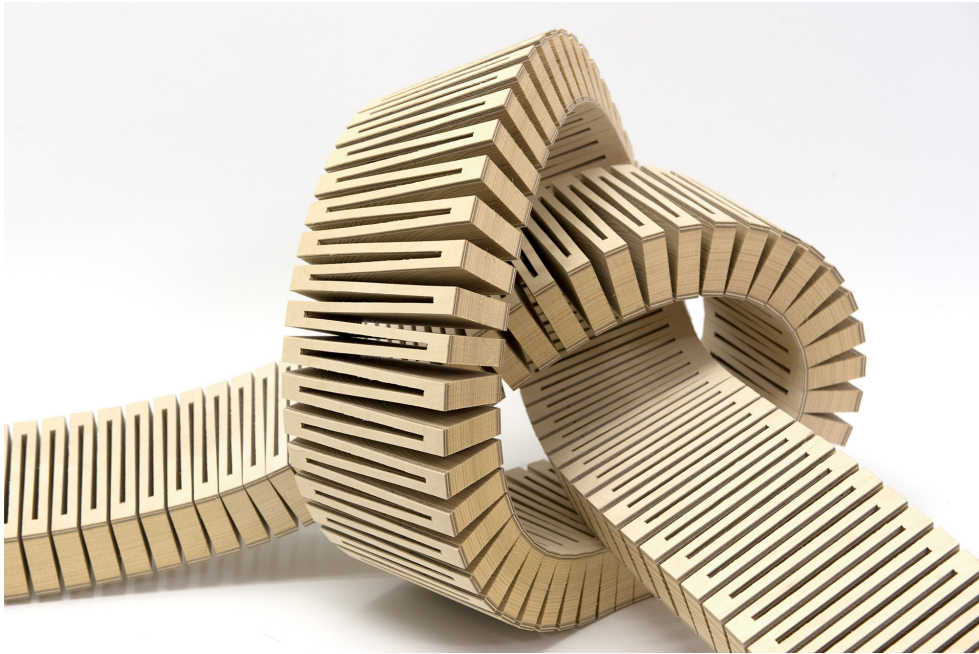


Figure 2. The wooden knot shows the flexibility of the dukta method (dukta, 2018b).

1.2. PROBLEM STATEMENT

Kerfing patterns can be applied in various shapes and sizes, giving the material not only a different appearance, but more importantly a change in bending capabilities. The deformation caused by cuts in the material decreases the stiffness of the material and increases its flexibility, in one or two directions, depending on the pattern design.

Apart from manipulating the bending stiffness, a pattern cut into a solid plate is also beneficial for acoustic performances. The effect of the kerfing pattern is expected to be similar to the perforated plates that are used for existing acoustic panels (see Figure 56 on page 75). The main difference with this approach is that the shape of the panel can be changed, which allows for development of a responsive acoustic panel with variable

acoustic properties in terms of absorption and reflection.

Freeform and responsive surfaces are potentially beneficial for several performance criteria in architecture. However, the manufacturing of building components with such geometric properties is still a challenging task. This research aims to address this problem.

The objective of this research is to put forward a formalized method for the design and fabrication of three-dimensional, freeform and responsive surfaces. The formalization of the design and fabrication means proposing a well defined statement to design and fabricate kerf patterns using parametric models. To this end, pattern kerfing techniques on wooden plates will be explored. The influences of the geometric parameters of the pattern on the attainable surface curvatures of the panel will be explained. Additionally, an approach for the design and production of responsive panels which adapts the changing acoustic needs of a space will be proposed by using this method.

1.3. OBJECTIVES

The main objective for this research is:

To determine a formal approach for the design and fabrication of responsive wooden surfaces by using pattern kerfing techniques towards better acoustic performance.

As there are several aspects involved, they are divided in four sub-objectives:

To explain the relationships between the parameters of a pattern and the attainable curvature of a surface.

To explain the relationships between the parameters of a pattern and the acoustic performance of a surface.

To explain the relationships between the curvature of a surface and its acoustical performance.

To investigate which architectural possibilities are available for responsive acoustic panels.

The following outcomes emerge by the conclusion of this research:

1. A parametric model for the pattern design in which multiple parameters are included to manipulate the design for flexibility adjustments.
2. Physical scale models for testing the physical behavior of different panels with certain kerfing patterns. Similar samples are made for acoustic measurements to determine the relation between the pattern parameters and the acoustic performance.

3. A one-to-one scaled prototype.
4. Results of the Impedance Tube measurement.
5. Results of the Impulse Response measurement.
6. Results of the simulations on the flexibility of a panel.
7. Visual representation of the design.

1.4. RESEARCH QUESTIONS

Since it is known that a kerfing pattern can generate flexibility out of solid and rigid panels, and additionally is expected to improve the acoustic performance, the following research question came up:

How can we formalize the pattern kerfing techniques in order to produce responsive wooden surfaces for better acoustic performance?

In order to answer the main research question, it has been divided into several sub-questions, which relate to the pattern and acoustic aspects to realize suitable architectural applications:

How does pattern kerfing influence the attainable curvature of a panel?

How does pattern kerfing influence the acoustic performance of a panel?

What effect has a curved surface of a panel on its acoustic performance?

What are potential uses of responsive surfaces on acoustic performance?

1.5. APPROACH AND METHODOLOGY

1.5.1. RESEARCH METHOD

This research is divided into 5 phases, starting with a literature study, elaborating on flexibility, acoustics and concept and prototype design, to finish with a conclusion.

Phase 1 Literature study

The first chapter of pattern kerfing starts with a literature study on the short history and development of pattern design to create flexible materials. It continues with a description of surface curvatures and ends with the available manufacturing techniques.

The chapter of acoustics contains a literature study which explains the basic principles of acoustics and gives an understanding of the functioning of acoustic panels.

Furthermore, a description on variable acoustics will be given. Architectural acoustics describes the architectural applications and requirements to be used in the case study.

Phase 2 Elaborations on flexibility

Creating a pattern comes with multiple parameters to manipulate the design. An elaboration on both linear and meander patterns will explain how these parameters relate and influence the flexible behavior of a panel. The parametric model which includes the pattern parameters is then visualized and explained by means of flowcharts.

Subtractive manufacturing techniques like laser cutting and CNC milling are used to make several physical models. These models are used for observations and measurements on flexibility to provide feedback to optimize the parametric model. Studies on both physical and digital models form the basis for the prototype design of a responsive surface.

Phase 3 Elaborations on acoustics

The parameters that are used for the pattern design are now defined in relation to the acoustic properties. This is done by measuring acoustic samples, each of which having a different combination of pattern parameters, on their acoustic absorbing and reflecting qualities. The results show which pattern variables are relevant and how these relate to the acoustic properties.

Phase 4 Concept and Prototype Design

The results of the acoustic measurements are combined with the results of the flexibility analyses, to create a substantiated concept for a responsive acoustic panel. The design is subject to several boundary conditions that simplify the design in this conceptual phase. The resulting acoustic panel is used for the case study concerning a lecture room at the Faculty of Architecture in Delft, The Netherlands.

Phase 5 Conclusions

The last phase is to present conclusions on the studies being done on pattern design and acoustics.

1.5.2. BOUNDARY CONDITIONS

Pattern

A short introduction will be given on the basic linear pattern, as the meander pattern is derived from it. But the main focus lies on the meander pattern, as it has more potentials than the basic linear pattern in creating three-dimensional freeform building components.

Material

Developing responsive acoustic panels comes with multiple aspects that influence the design, some of which are excluded from this research, like the effects of surface treatment, and environmental conditions such as humidity and temperature. The material is limited to plywood.

Manufacturing technique

Not all techniques are well suited for pattern kerfing. In order to initiate flexibility to a solid and rigid material, parts of the material have to be removed, a technique called subtractive manufacturing. This research focuses on two common types of subtractive manufacturing that are appropriate for machining engineered wood, such as plywood: Laser Cutting and CNC Milling.

Scale

At first small scale physical models with different patterns are examined. Next, patterns will be applied to panels containing larger dimensions with a surface area up to one square meter for the final model. The minimum scale of the pattern depends on the applied manufacturing technique. A laser cutter is able to create smaller patterns than a CNC milling machine, because the diameter of the rotary cutter determines the minimum width of the kerfs.

Other aspects that are excluded from this research are the production costs and a detailed structural analysis.

1.6. RELEVANCE

Responsive panels are not yet widely available because the technique to produce flexible panels is relatively new and still under development. More research is needed to realize this technique for additional functional applications and higher cost efficiency. The actual behavior of patterns regarding flexibility and acoustic performance has not yet been elaborated completely, as there are only few literature studies available on this topic. A further exploration is recommended to improve the design in terms of flexibility and acoustic performance.

Responsive panels can be used in various spaces to improve the acoustic performance and aesthetic appearance. As the panels contain kinetic elements and are vulnerable for environmental impacts like wind and rain, the main use would be for indoor applications.

In spaces where higher sound volumes are reached or where the requirements for acoustic design are of high importance, acoustic panels offer a solution. Concert halls or theaters are examples of spaces that require an advanced acoustic design to achieve the best acoustic experience for the audience. Such multi-purpose spaces are used for different kinds of events, with different types of music, that need an acoustic design that is adaptable, to meet the acoustic requirements. On smaller scale, conference halls or lecture rooms may also be used for different scenarios where an adaptable acoustic design is desired. For example, a traditional classroom setup with a single speaker at the front would require a different acoustic design than using the same space for discussions in smaller groups spread across the room. The advantage of this responsive

panel is that it can change its surface curvature to adjust its acoustic performance in order to answer the needs of the different usages of the room.

Furthermore, the panels can be manufactured from flat plates of material which are relatively easy to make at low costs and convenient when using of laser cutters and CNC milling machines. Starting out with flat plates of wood to create transformable three-dimensional and freeform geometries, is highly efficient in terms of costs and waste, compared to the production of such elements directly in 3D. An additional advantage is that the manufactured panels can be positioned in their original flat shape which makes transport and storage simple and efficient.

1.7. TIME PLANNING

One month after P1, I decided to change topics and start over from scratch, as the former subject did not embody what was expected. This four-week delay caused a lot of work in the time prior to the P2 presentation. The content that was developed from the literature study and theoretical background on flexibility and acoustics was presented at the P2 presentation. It appeared to be sufficient to continue with this research.

After P2, the literature study continued, in order to supplement the theoretical backgrounds on the chapters of flexibility and acoustics. Existing patterns were examined to define the input parameters of the parametric model of the pattern design. The first samples with various combinations of pattern parameters were created by means of laser cutting, in order for further elaboration on the flexibility of such patterns.

The time after P3 included the continuation of design and kerfing of multiple patterns. Bending simulations were done to provide more detailed information on the influence of the defined pattern parameters on the stiffness and flexibility of a panel. The design and fabrication of a full-scale prototype were conducted, to be used for flexibility and acoustic measurements. The acoustic design had its conceptual setup and included the results of the measurements with the Impedance Tube.

The official P4 presentation had been postponed, due to the amount of work to be done in relation to the available time. This resulted in a few additional months to continue working on this research. The current information on flexibility and acoustics resulted in a design concept. Right before the holidays in July and August the results of the first acoustic measurements were elaborated and the second set of acoustic measurements were performed. This time by means of an Impulse Response measurement, which involved the use of the constructed prototype.

After the holidays and prior to the actual P4 presentation, the final results and conclusions were completed for the flexibility and acoustic parts. The overall conclusion on the research and final design were completed in the period before P5 (see Figure 3).

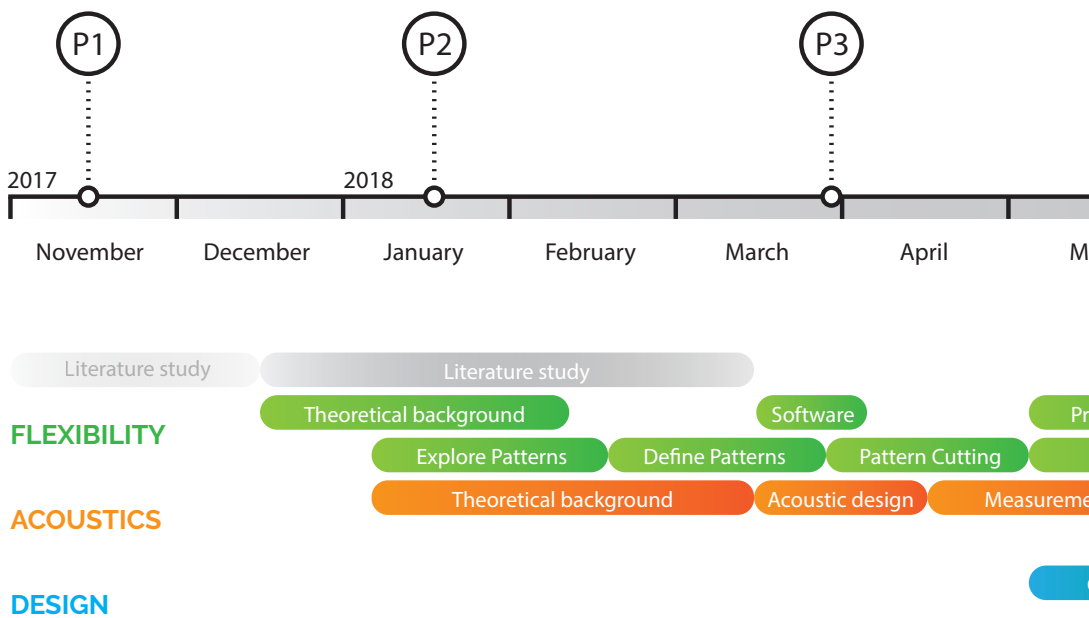
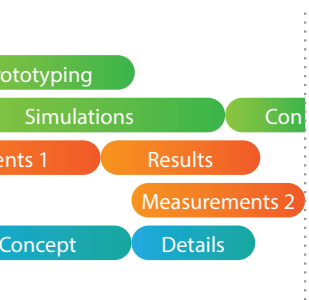
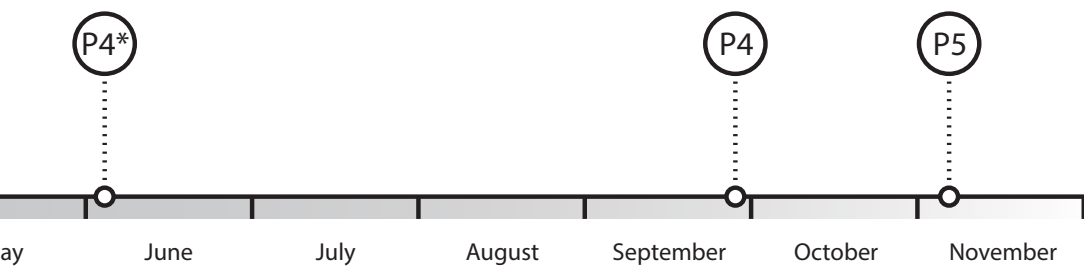
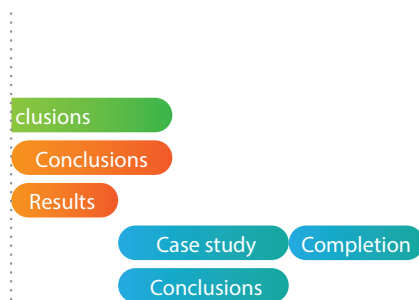


Figure 3. Global time schedule for the entire research.



HOLIDAYS



2. FLEXIBILITY

2.1. INTRODUCTION

The rational design of the cut patterns enables the shape-shifting of solid plates or sheets into geometries with apparent intrinsic curvature (Callens & Zadpoor, 2017). Transformation of these flat materials into three-dimensional and freeform objects has multiple advantages. One of them is that adjustments are made onto flat starting materials, which is a cost-efficient way to create transformable three-dimensional and freeform geometries. Flat wooden plates are relatively easy to make at low costs and convenient when using laser cutters and CNC milling tools. Furthermore, the manufactured panels can be positioned in their original flat shape which makes transportation and storage simple and efficient.

This chapter will first investigate existing literature on the design and manufacturing of flexible patterns. Next, the different parameters influencing the attainable curvature of a panel will be explained. They either relate to the material or the pattern design and need to be altered in a controllable manner. Then the configuration of the parametric model is explained and visualized. The second last paragraph will focus on the analyses on flexibility by means of small scale physical models and simulations, giving insights in the behavior of the different parameters. The chapter will conclude with a conclusion of the studies that have been done.

The corresponding sub-question that will be answered in this chapter, is:

How does pattern kerfing influence the attainable curvature of a panel?

2.2. LITERATURE STUDY

2.2.1. FLEXIBLE PATTERNS

Rigid planar panels can be turned into flexible ones by applying a technique called relief cutting, which goes by the name kerfing in architectural practice (Zarrinmehr, Ettehad, et al., 2017). Kerfing is nothing more than precisely removing material at specific locations. The early designs with this method were made by applying linear slits which are staggered relative to each other. Due to the linear pattern, the wooden pieces obtain flexibility in one direction but preserve their stiffness in the other. The kerfs divide the surface into a series of slender segments, which can easily be twisted and are interconnected at fixed points (Figure 4).



Figure 4. Linear pattern allows for flexibility in one direction (Couden, 2013).

It was Dujam Ivanišević who discovered in 2014 the 2D meander pattern to be used as relief cuts, making a rigid material flexible in two directions (Zarrinmehr, Akleman, Ettehad, Kalantar, Haghighi, et al., 2017). He turned the linear elements into interlocking rectangular spirals, whose segments twist in two directions (Ivanišević, 2014). This type of pattern shown in Figure 5 is called meander, named after the “Menderes” rivers in Turkey, describing their twisting and turning paths throughout the landscape. But usually the term is used for decorative motifs with straight lines and right angles, which appear numerously in Greek and Roman art (Wikipedia contributors, 2018).

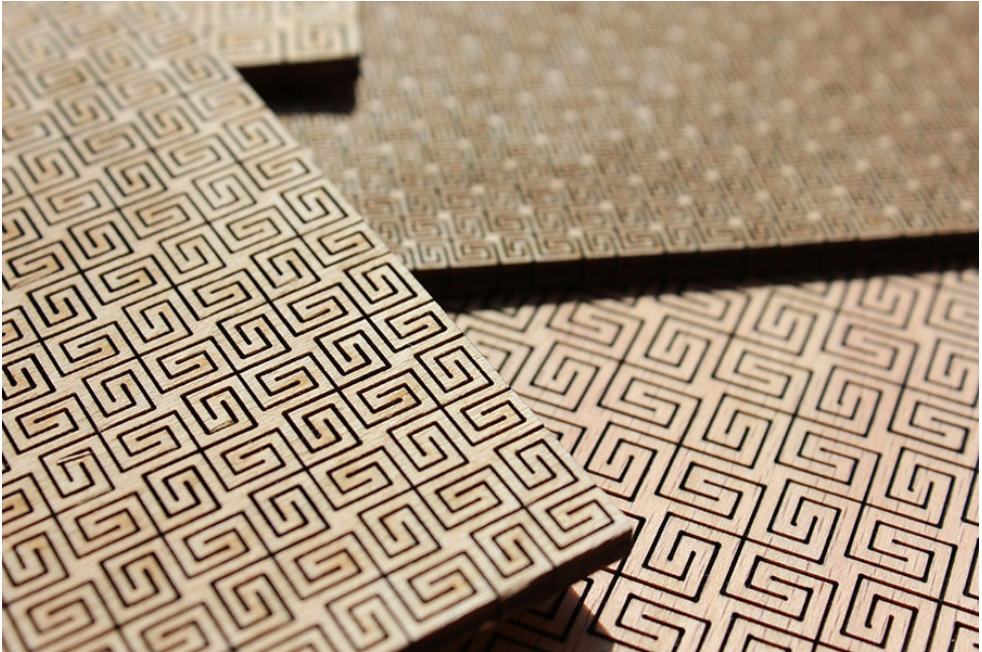


Figure 5. A flexible 2D Meander pattern discovered by Ivanišević (2014).

Other designers used the meander pattern from Ivanišević as inspiration and created similar patterns, aiming to obtain flexible panels as well (See Figure 6). The resulting kerfing patterns however, were less flexible than the original pattern as visually demonstrated by Ivanišević (Zarrinmehr, Ettehad, et al., 2017).

These 2D meander patterns are called wallpaper patterns that can be generated using basic symmetry operations such as rotation and translation (Schattschneider, 1978). This method only allows for exact copies of a single motif and makes it hard to differ from the original wallpaper pattern, finding varying patterns. Another issue with this approach is that it is difficult to change the local properties of a panel, making certain regions more rigid and other more flexible.



Figure 6. Other symmetric meander patterns motivated by the original pattern by Ivanišević: Pattern attributed to Robert Lang (a), pattern introduced by an anonymous person (b) and a circular pattern by M. S. Reynolds (c) (Zarrinmehr, Akleman, Ettehad, Kalantar, & Borhani, 2017).

Classification

Meander patterns can be classified by two numbers as [N,K]: where N is the number of spiral branches in a given spiral tree and K the number of interlocking spirals (Zarrinmehr, Akleman, Etehad, Kalantar, & Borhani, 2017). According to this principle, [4,2] refers to the original meander pattern discovered by Ivanišević. The patterns in Figure 6b and c are respectively noted as [6,2] and [3,3]. This notation only includes the number of spiral branches and interlocking spirals, which means that there will be other patterns with the same classification but with a different appearance.

Local flexibility

A panel obtains its flexibility mainly by the segments that are subjected to torsion. A single segment can only take a small amount of torsion, but multiple segments together result in a significantly larger angle of displacement for the panel as a whole.

Local flexibility can be manipulated by changing the parameters of the pattern locally. But one cannot simply change the size of individual units to obtain local flexibility. A 2D meander pattern follows a certain grid, made by the basic symmetry operations of translation and rotation. This means that the size of a single meander unit should match the grid cells and is therefore unable to be adjusted independently. However, there is a certain way to influence the local flexibility by scaling down individual units, which will be explained further on .

A more sophisticated way to obtain local flexibility is by increasing the number of iterations of two interlocking spiral branches. The number of iterations is the number of repeated rotations for a spiral branch. This approach can be used for each set of interlocking spirals, as they are located in a single grid cell. A spiral tree can therefore have branches with varying numbers of iterations, because each branch is not directly related to other branches of the same tree. Figure 7 shows an example of this technique, where they used a control image to determine the density of the pattern in specific areas.

Besides the number of iterations for individual branches, the local flexibility can also

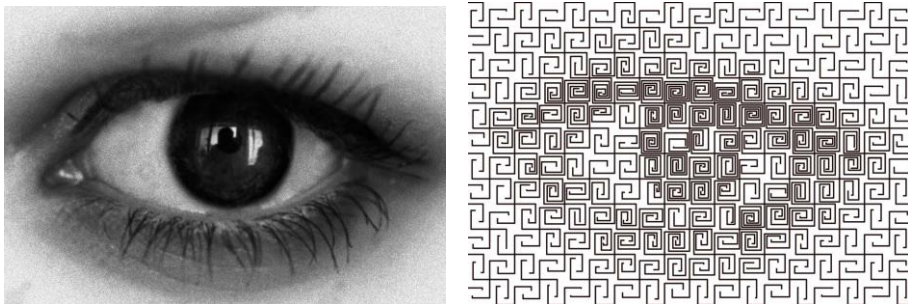


Figure 7. Local flexibility by manipulating the number of iterations locally, by means of a control image (Zarrinmehr, Akleman, Etehad, Kalantar, & Borhani, 2017).

be manipulated by changing the kerf width of the individual branches. This second approach leaves the amount of branch iterations and segments untouched, but it only modifies the local dimensions of the segments. The width of the kerf is directly related to the width and length of the adjacent segments. This means that an increase of the kerf width automatically results in a decrease of the material width of the segments.

Material

"Pattern material should be cheap and readily available. It should be hard, strong and light weight with resistance to corrosion. It should be capable of taking good surface finish. And it should be easy to work upon by normal manufacturing methods used in making the pattern out of it. [...] Wood is commonly used because it is cheap, easily available, can be shaped easily, light in weight and can have good surface finish."
(Kaushish, 2010)

Based on the advantages mentioned by Kaushish and the available subtractive manufacturing techniques, plywood appears to be an appropriate material for the construction of flexible wooden panels. This material is manufactured from thin layers of wood veneer that are glued together, with each layer having its wood grain rotated 90 degrees (Figure 8). The grain alternation gives the panel isotropic properties, which means that the material is uniform in all directions. In other words, the orientation of the panel is not important when a pattern will be applied on the surface in order to generate flexibility.



Figure 8. Plywood is constructed of multiple layers of wood veneer, giving it isotropic properties (US Craft Company, Unknown).

2.2.2. SURFACE CURVATURE

A surface curvature can be defined by the principal curvatures κ_1 and κ_2 , at a given point on the surface, which are the minimum and maximum of all the normal curvatures at

that point. Two well-known measures of curvature at a given point on the surface can be obtained by combining the principal curvatures (Callens & Zadpoor, 2017). The first one is the mean of both curvatures, simply called the mean curvature H :

$$H = \frac{\kappa_1 + \kappa_2}{2}$$

A flat plane has no curvatures, thus the mean curvature is equal to zero. When the plane is bent along a single axis, the value for the mean curvature is no longer zero, since one of the principal curvatures has changed.

The second measure is the product of the principal curvatures, called the Gaussian curvature K :

$$K = \kappa_1 \cdot \kappa_2$$

The plane in Figure 9 is bent along a single axis. One of the principal curvatures changed, but since the second principal curvature is zero, the Gaussian curvature is also zero. When both principal curvatures are non-zero, the value for the Gaussian curvature is non-zero (Figure 10).

Both the mean and the Gaussian curvatures can be derived from the principal

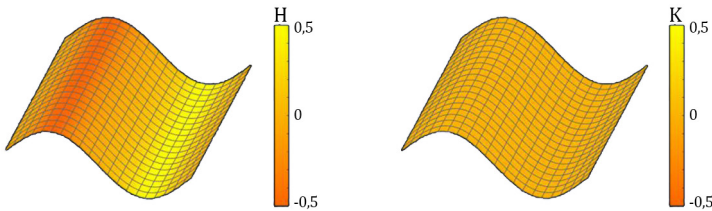


Figure 9. Bending changes the mean but not the Gaussian curvature (adapted from Callens and Zadpoor (2017))

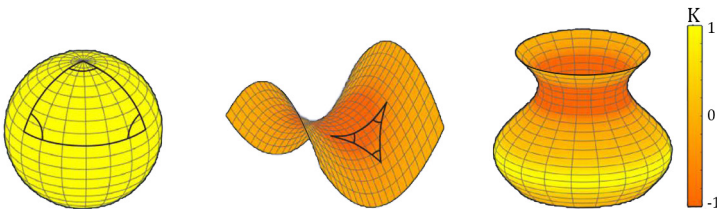


Figure 10. Non-zero Gaussian curvatures (adapted from Callens and Zadpoor (2017))

curvatures, but they represent a different perspective on surface curvature. The mean curvature can be stated as an extrinsic measure, meaning that it depends on the way the surface is embedded in the surrounding 3D space. The Gaussian curvature can be stated as an intrinsic measure, which means that it does not depend on the surrounding space but can be determined by looking at the surface itself (Callens & Zadpoor, 2017).

The difference between the mean and the Gaussian curvature is essential, as surfaces can have an extrinsic curvature while they are intrinsically flat. A surface like the one in Figure 11, is called a developable surface, having zero Gaussian curvature at any given point on the surface (Callens & Zadpoor, 2017). The characteristic of a developable surface is that it can be formed by bending a planar surface without deformation (stretching or compressing). And vice versa, that a developable surface can be flattened on a plane without extensional deformations.

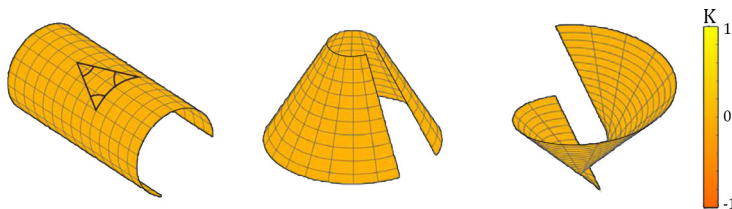


Figure 11. *Developable surfaces with zero Gaussian curvature (adapted from Callens and Zadpoor (2017))*

2.2.3. CUTTING TECHNIQUES

Several machining processes are available to make a kerfing pattern into a solid plate of wood. The technique of removing excess material to create a three-dimensional object is called subtractive manufacturing.

Available techniques for subtractive manufacturing are cutting by means of a laser and milling performed on CNC machines. Both are usable for pattern kerfing in wooden plates, but come with different limitations. A basic understanding of these techniques will be given in the next paragraph, combined with certain specifications.

Laser cutting

Laser cutting is a technique that goes back to the early 1960s when it was developed. By the 1970s this process of laser cutting has been introduced into the aerospace industry and other industries worldwide followed.

Belforte and Jafferson (2016) give three requirements for cutting nonmetal: (1) a focused beam of energy at a wavelength that will be absorbed by the material to be cut so that melting, chemical degradation, or vaporization can occur, (2) a gas jet to remove by-

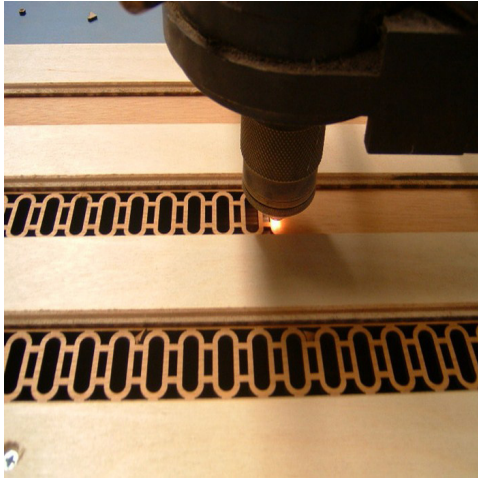


Figure 12. A laser cutting machine in operation. (Kingston University London, Unknown)

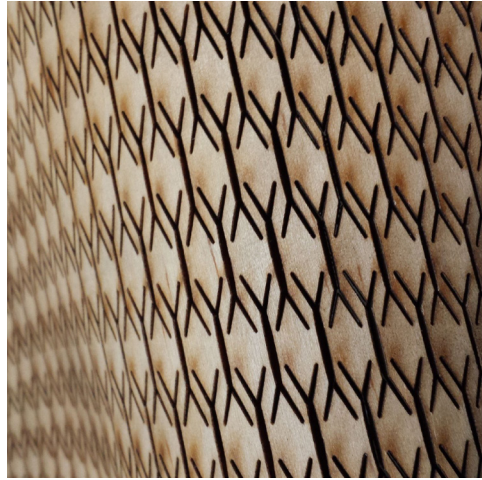


Figure 13. A laser cut pattern (Porterfield, 2014).

products from the cut area and (3) a means of generating cuts in straight lines or curved patterns.

There is no exact limitation on cut thickness because of the moderate amounts of power needed for the nonmetal cutting process. But to obtain a certain quality of the cut, in practice, the majority of cutting applications occur in material less than 12 mm thick (Belforte & Jafferson, 2016). The thickness of the material, the quality of the laser with gas assist and the process rate determine the width of the cut (kerf). Characteristic for nonmetal cutting is a narrow kerf width of 0,1 – 1,0 mm, making it possible to make complex cuts in small scale (Sharma & Yadava, 2017, p. 265).

To cut sheet materials there are three main types of advanced sheet cutting processes (ASCP's): Plasma beam cutting (PBC), abrasive water jet cutting (AWJC) and laser beam cutting (LBC) (Sharma & Yadava, 2017, p. 265). Laser beam cutting is a well suited method for cutting materials with low thermal diffusivity and conductivity, such as wood. An assist gas jet blows the material vapor out of the kerf, in order to avoid the hot gaseous emissions to precipitate on the workpiece (Sharma & Yadava, 2017, p. 266).

CNC Milling

Milling by means of Computer Numeric Control (CNC) is a sophisticated technique that makes use of precise cutting tools. It can be used for shaping various solid materials by means of a rotating cylindrical cutting tool. Unlike regular drilling machines, the cutter in a CNC milling machine is able to move along multiple axes, and can create a variety of shapes, slots and holes (Thomasnet, 2018). Most machines offer movement in 3 axes, horizontal movement in the X and Y plane and vertical movement along the Z axis.

Current technology allows the process to be also performed by advanced industrial



Figure 14. Cutting wood with a CNC milling machine (Niewegłowski).

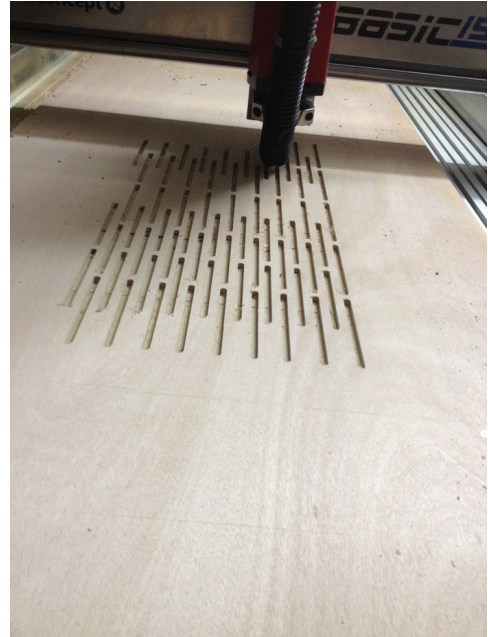


Figure 15. Kerfing a linear pattern in plywood ("Cutting Plywood," Unknown).

robots (Breaz et al., 2017, p. 796). Milling with robots has some advantages over milling with traditional 3-axis CNC machines. A robotic arm has a higher kinematic range which allows the tool head to move and rotate in nearly any direction, depending on its own technological limitations. It can reach places which are difficult or even impossible to be machined on a regular CNC milling machine or by using manual tooling methods. Because of the incredibly complex geometries that can be involved in the machining process, these advanced machines require Computer Aided Manufacturing (CAM) programming for optimal performance (Thomasnet, 2018).

Choosing the right process for manufacturing requires certain decision criteria, with relation to the part to be manufactured. The criteria can be divided into geometric (undercuts), properties (wall thickness, dimensions, weight, shape and complexity etc.), technological (tolerances) and production (processing cost/part) (Breaz et al., 2017).

CNC Milling is not limited to shape flat plates, as with laser cutting. It can handle practically every material that can be drilled or cut, of which the thickness of the material is usually not an issue. The technical limitations of the milling machine and tools determine the maximum dimensions of the material to be shaped. As with drilling and cutting, the proper machine tools need to be selected for each material in order to prevent potential problems during the milling process (Thomasnet, 2018). Due to the diameter of the used tooling bit, the size of the shapes and holes will have a minimum dimension.

2.3. PATTERN DESIGN

2.3.1. INTRODUCTION

As mentioned in the literature study, application of certain types of patterns gives rigid panels flexibility. The linear and meander pattern are the two most outstanding designs in terms of bending capabilities. Both can be used to design flexible freeform elements, but the main focus will be on the design of the meander pattern, as this design allows for more freedom in freeform surface curvatures. Although linear patterns can also be manipulated to obtain more variations in the final surface curvature, the options remain limited due to the linear orientation of the segments. The linear pattern will be examined first, as the meander pattern is based on the basic principles that apply for this pattern. All patterns that are being discussed are 2-dimensional, which means that all applied kerfs perforate the material entirely, resulting in an equal surface pattern on both sides.

2.3.2. LINEAR PATTERN

The linear pattern in Figure 16 is based on the first designed pattern that increases a material's flexibility. It is composed out of a series of linear kerfs that all have the same orientation and are placed in an alternating pattern. The orange colored segments between the so-called junctions are able to twist. The combination of all segments allows the complete surface to obtain a certain curvature. The alternating pattern of the kerfs is the most efficient way to achieve the highest flexibility. This approach ensures an equal length of the two inline segments, the connected length between two junctions. An equal length of these segments allows for the same angle of displacement for each segment. The distance between two adjacent segments, the kerf width, is important for the maximum twist of the individual segments. When they are too close together, the

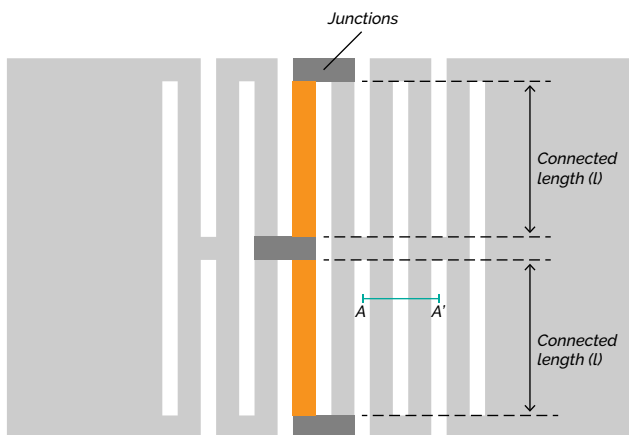


Figure 16. Connected lengths of a linear pattern.

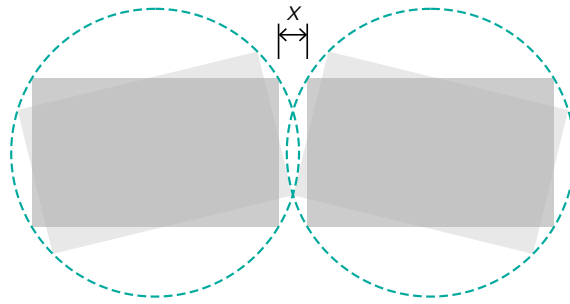


Figure 17. Cross-section A-A'. The kerf width determines possible rotation of segments.

twisting segments obstruct each other and limit their possible rotation, and thus the overall flexibility of the panel (Figure 17).

For linear patterns, the attainable surface curvature is dependent on the orientation of the kerfs. The local surface curvature at any given point would be perpendicular to the orientation of the segments in that region, because of the rotation of the segments. The pattern in Figure 18a would only be able to curve into the direction perpendicular to direction of the kerfs. Figure 18b and c show some examples of linear patterns that have been altered to manipulate the local surface curvatures and create a variable surface curvature across the surface.

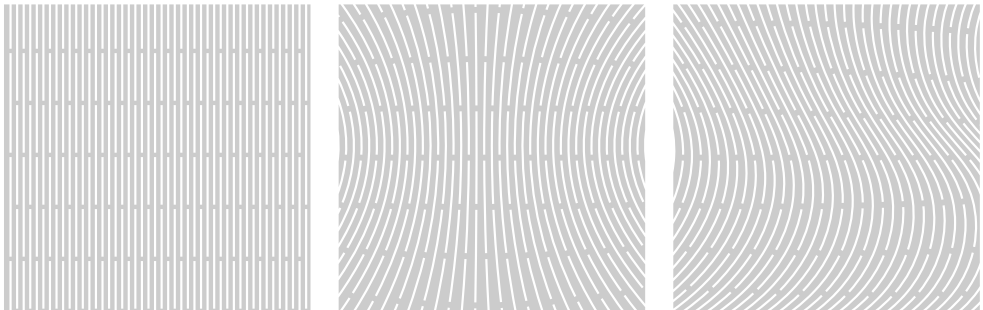


Figure 18. Linear patterns: A standard parallel orientation (a) and linear patterns with manipulated orientation (b & c).

2.3.3. MEANDER PATTERN

The meander pattern as shown in Figure 19 is based on the original meander pattern discovered by Ivanišević, but has been given some extra parameters to manipulate the final pattern.

The repetitive element in this pattern is a [4,2] meander with 4 iterations. Each single unit covers 4 grid cells and divides the surface into 36 interconnected segments for every complete unit, as shown in Figure 20. The number of segments is dependent on the

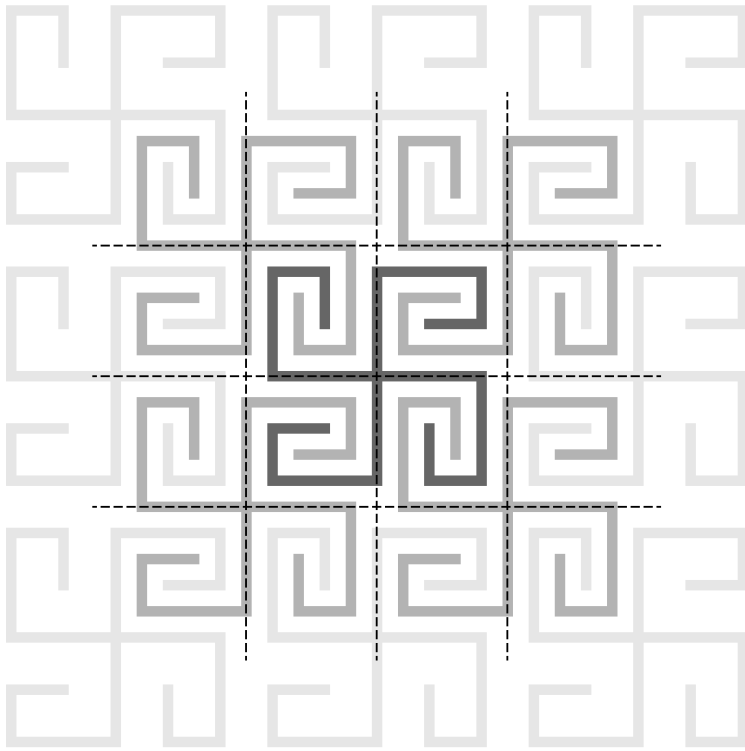


Figure 19. A [4,2] meander unit is repeated to create the final pattern, where each branch interlocks with a branch of a different spiral tree.

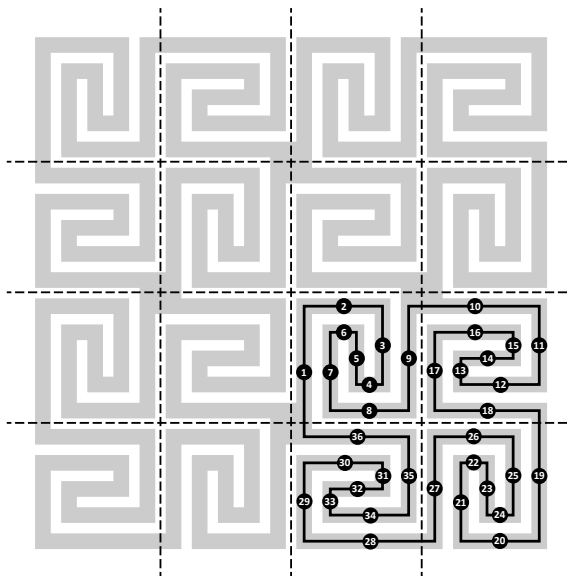


Figure 20. The subtracted meander pattern divides the surface into multiple interconnected segments, which are subjected to bending and/or torsion.

number of iterations for each branch. Every extra iteration adds 2 additional segments for each set of interconnecting branches in a single cell.

2.3.4. PARAMETERS

A panel with relief cuts obtains its flexibility mainly through the segments that are subjected to torsion. To adjust this flexibility in a controllable manner, it is important to know which factors are of influence and how they are mutually related. The scheme in Figure 21 shows the relations between the different pattern and material parameters for a surface applied with a meander pattern.

The resulting surface curvature is obtained by a combination of torsion and bending in each of the segments. Whether a segment is being subjected to torsion or bending depends on the direction of the applied loads and thus the orientation of the surface curvature. The amount of torsion and bending with a certain load case is dependent on the material properties and dimensions of the individual segments. The width and length of these segments are in turn being determined by the main pattern variables: (a) the size of a single unit, (b) the number of iterations and (c) the kerf width (Figure 22).

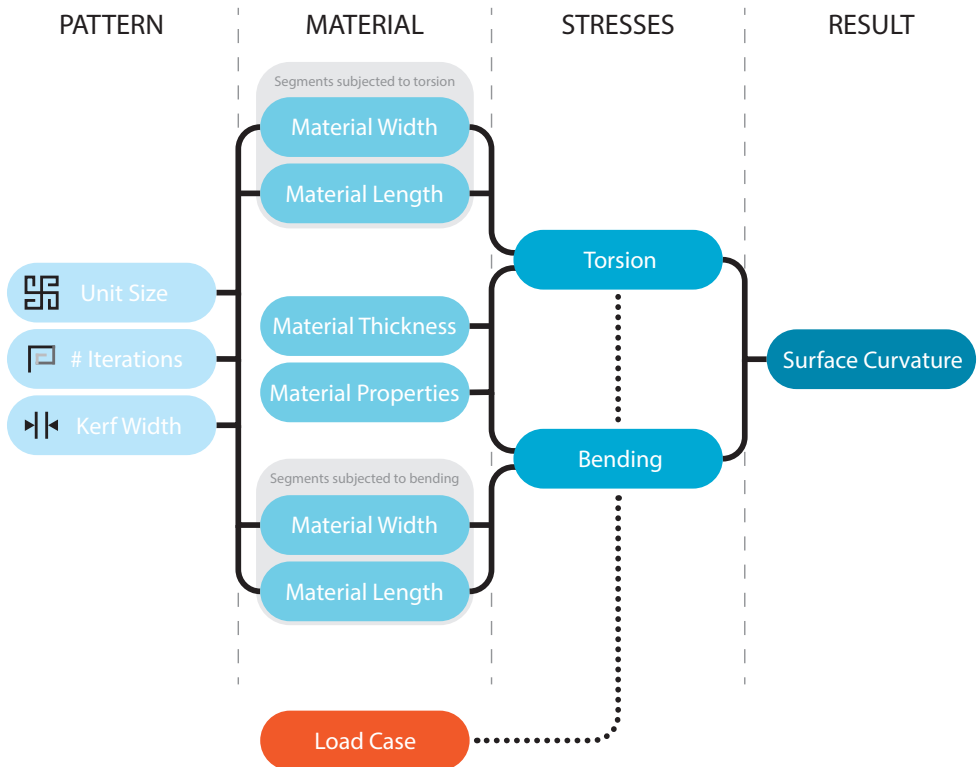


Figure 21. Relations between the different pattern and material parameters for a meander pattern.

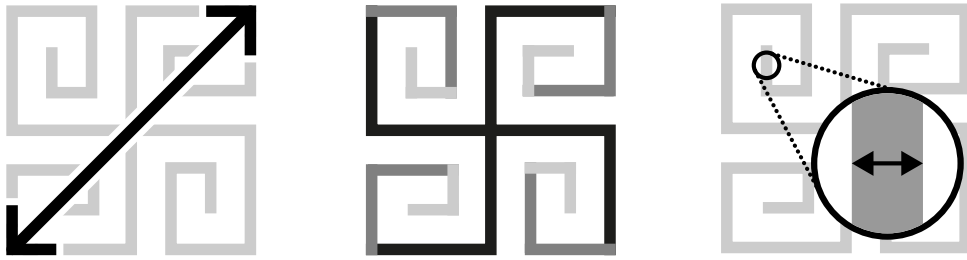


Figure 22. The three main pattern variables: Unit size (a), number of iterations (b) and kerf width (c).

The properties of the material are excluded from this research as the focus is on the influence of the pattern and not the type of material.

In a meander pattern, the single unit refers to the specific element that is being repeated to create the final pattern, which is in this case a [4,2] meander (Figure 19). Each of the four spiral branches is interlocked with one other spiral branch of another 4-branched spiral tree. The amount of iterations for a spiral branch determines the number of segments the remaining surface will be divided into, and consequently their minimal dimensions in length and width.

Basically, the kerfs are being applied on a straight line, which is only one-dimensional. But these kerfs do not necessarily have to be stated as one-dimensional, therefore the width of the kerf is the third pattern variable, making the kerfs two-dimensional. In other words, if the kerf width increases, the material width of the adjacent segments decreases, if the unit size and number of iterations remain equal. A larger kerf width simply means that more material is removed, resulting in segments that have a smaller width.

Flexibility

The created segments take together all the stresses, causing a particular individual deformation. The deformations result collectively in the final surface curvature of the panel. More segments means more available torsion and thus a smaller attainable curvature radius. In other words, the flexibility increases when there are more segments in the same area (Figure 23b), to absorb torsional stresses. More segments in the same area also means that the width of the segments will be smaller, which decreases their stiffness and consequently increases the possible angle of twist.

A second approach to manipulate the flexibility is to change the width of the kerfs (Figure 23c). The number of segments remains equal for the same area, but a larger kerf width results in narrower material segments, that can easier be twisted. With this approach, the stiffness of the panel will be decreased because more material is being subtracted.

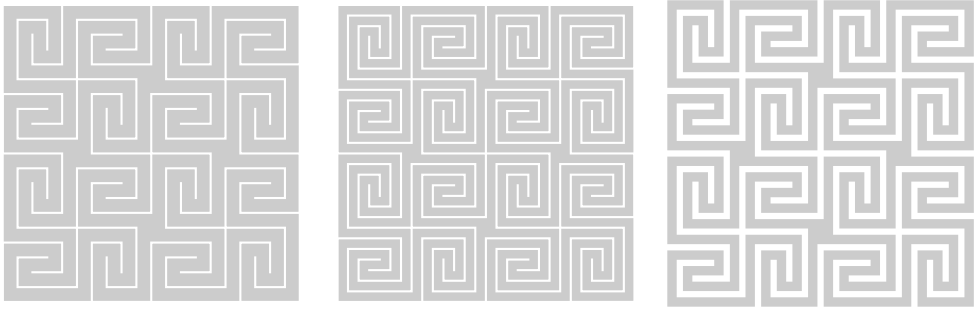


Figure 23. Flexibility can be increased by a higher number of iterations (b) or a larger kerf width (c).

The size of a single meander unit determines the scale of the meander pattern, and in terms of flexibility, it scales up the curvature in both directions (measured in absolute units). The unit size is directly related to the combined width of the kerfs and the segments, and is included in that part of the analysis. The thickness of the material is mentioned as a material parameter, because it has a significant impact on the stiffness and is therefore included in the analyses on flexibility.

The expected changes in stiffness by changing the mentioned pattern and material parameters are visualized in Figure 24. A larger segment height (material thickness) or segment width increases the stiffness of the panel, where a higher number of segments decreases the stiffness. The relationship between the stiffness and the pattern parameters may be different from the linear relationship as shown in the diagrams. Analyses on flexibility by means of physical and digital models will give more accurate results about this relationship, explained in paragraph 2.5.

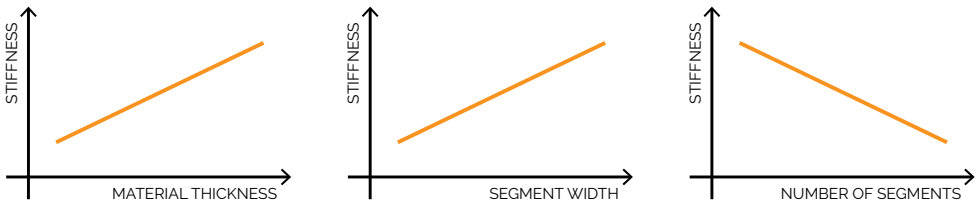


Figure 24. Expectations for changes in stiffness when manipulating the segment parameters.

Local flexibility

The basic meander pattern is based on a square grid, which gives all meanders the same dimensions and gives the panel the same level of flexibility in both directions. One way to manipulate the unit dimensions and level of flexibility in a specific direction is to adjust the grid, like shown in Figure 25. A distorted grid in Figure 25b results in meander pattern with a certain randomness. But the grid orientation can also be manipulated in a controlled way, to adjust the pattern and thus the flexibility in a specific direction (Figure 25c).

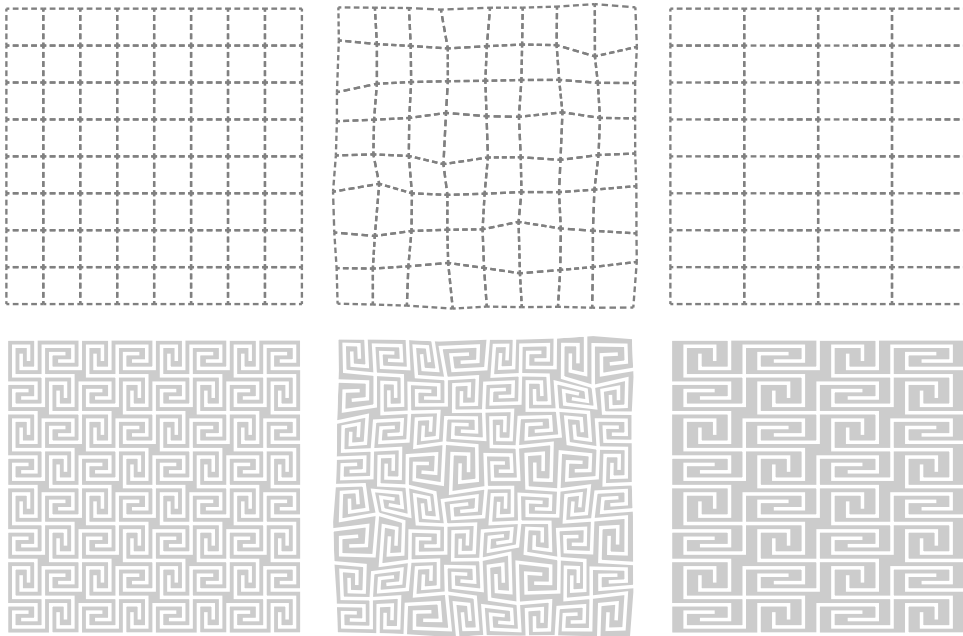


Figure 25. Grid distortion by randomizing or stretching.

Two other methods as described in the previous paragraph can also be used to adjust the flexibility of a panel locally. These are based on the other two pattern parameters: number of iterations and the kerf width. In Figure 26, the local kerf width has been determined by means of an attractor, which can be a point, curve or any other shape. The value for this parameter on a given point on the surface is determined by the distance from that point to the attractor. The configuration of the current parametric model that created this pattern does only allow for changes down to the level of individual branches. That means that inside a single branch, all iterations have the same kerf width and cannot be distinct.

A third approach to manipulate local flexibility is to change the local number of iterations. They can only be changed up to the level of a single grid cell, containing two interlocking spiral branches. Because the branches are interlocked, they cannot have a different number of iterations. In Figure 27, the number of iterations has been determined by the distance to an attractor point. At (a) the number of iterations is higher closer to the attractor point, dividing the surface into more segments and decreasing the local stiffness. For figure (b), the principle is inverted.

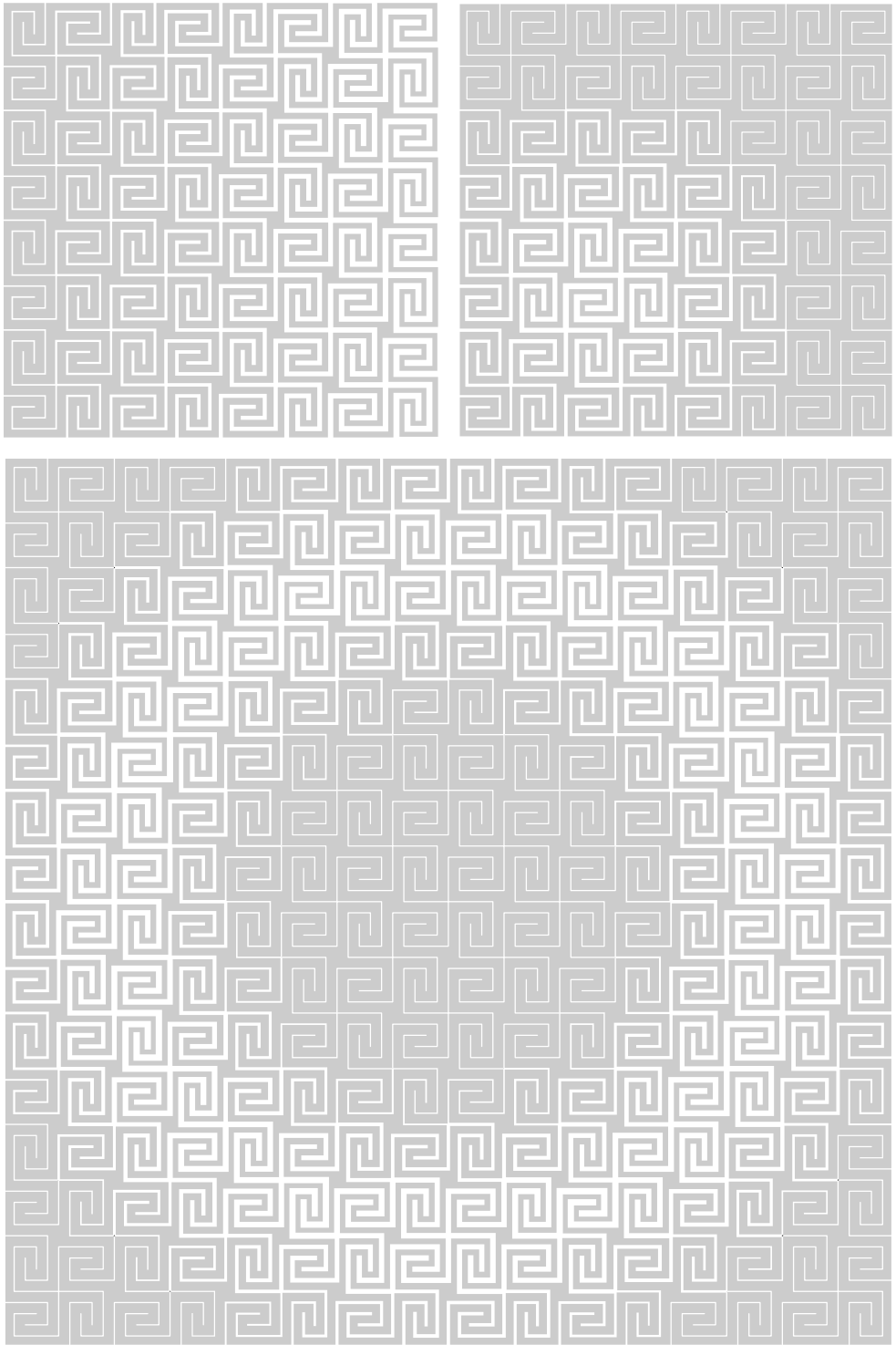


Figure 26. Variable kerf width based on a line attractor (a), point attractor (b) or shape attractor (c).

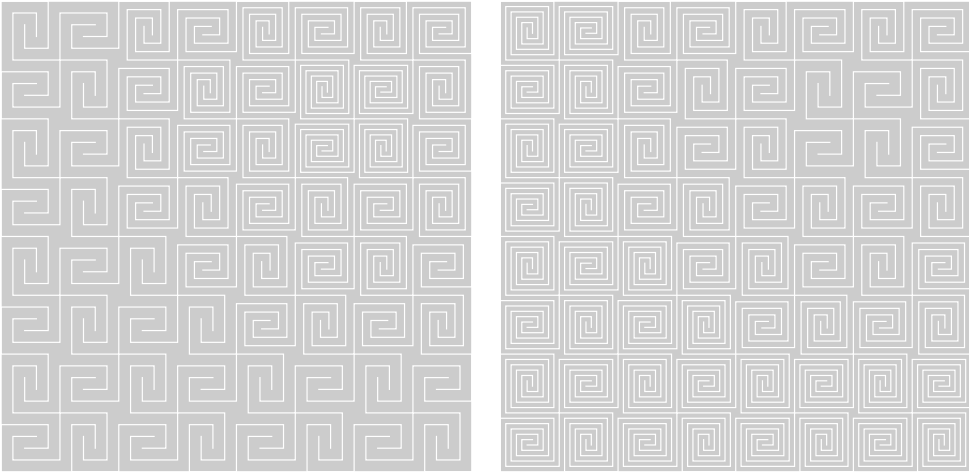


Figure 27. Local flexibility obtained by varying number of iterations based on a point attractor. Regular (a) and inverted (b).

2.4. PARAMETRIC MODEL

2.4.1. INTRODUCTION

The pattern design is made in Rhinoceros®, a computer-aided design (CAD) application for 3D modeling, and the plug-in Grasshopper®, a visual scripting language for the parametric design environment. A parametric model is made of a set of parameters forming the input for the constructed algorithm. The result of this algorithm is in this case a two-dimensional meander pattern that can be adjusted by changing the input values. It only allows for [4,2] meanders, a spiral tree with 4 branches and 2 interlocking spirals.

2.4.2. PARAMETERS

The pattern parameters as described in "2.3. Pattern design": the size of a meander unit, the number of iterations and the kerf width form the base input for the parametric model. Together with additional constraints regarding local adjustments and surface dimensions, the final pattern will be created as a line drawing ready to be exported for the cutting machines. The width of the kerfs determines the offset for the outline of the meanders which together form the complete drawing of the final pattern.

Figure 28 shows the pattern parameters as input for the Grasshopper model, of which the size and number of units is divided into X and Y direction. Within the model, the option is given to define the pattern based on the unit size in combination with the width of the kerfs or the segments. By choosing the width of the kerfs, the segment dimensions will be generated automatically based on the given value. A restriction has

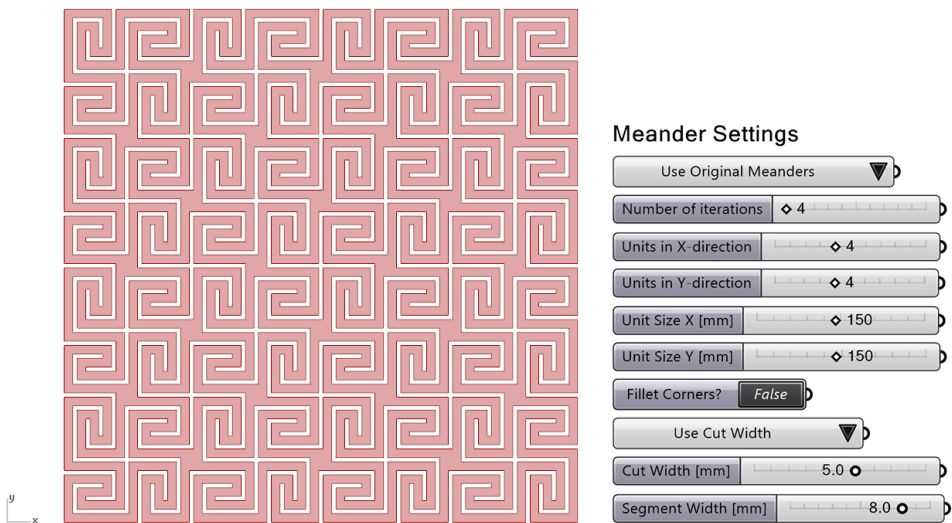


Figure 28. Parametric model from Grasshopper based on the pattern parameters.

been added to maintain a predefined minimum segment width. With the second option, the kerfs will be generated automatically based on the given value for the width of the segments.

2.4.3. ALGORITHM

The meander pattern is constructed of repeating elements. Within this model, this element is just one branch of the spiral tree that forms the pattern by means of rotation and translation. Using the spiral branch as repeating element and not the whole spiral tree gives an advantage for local kerfing adjustments in the pattern. This way the value of the kerf width can be determined for each individual branch, allowing adjustments on a smaller scale.

The first input for the creation of the branch is the number of iterations. It determines the coordinates of each corner point of the branch, which has a certain translation based on the coordinates of the starting point of the branch and the given number of iterations. A polyline connects the points at the generated coordinates and forms a single branch.

The next step is to define a grid, of which the given size of a single meander unit determines the dimensions of the grid cells. Each cell will contain two interlocking branches, which are projected onto the grid in a checkerboard pattern, where they have been rotated 90 degrees for every other cell (Figure 29). This results in a pattern that contains [4,2] meanders.

At the third step in the process, the given value for the kerf width will determine the offset from the spiral branches. This offset can be uniform for all branches, but might also be given a variable value in order to adjust local areas in the pattern. The created outlines are merged with the constructed edge of the surface and form the final pattern.

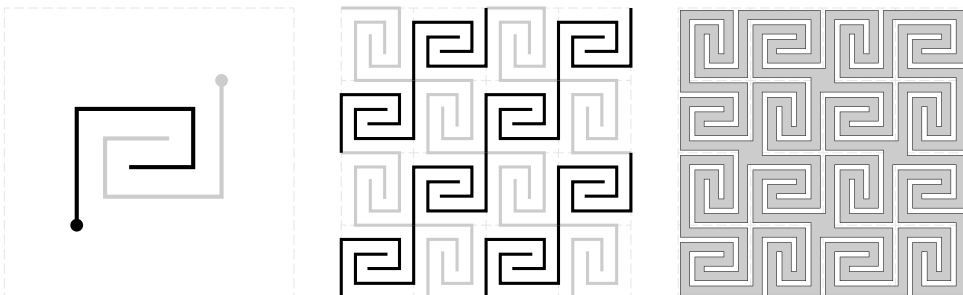


Figure 29. The three main steps in the process: Interlocking branches (a) are projected onto the grid (b) and given an offset to be merged together (c).

A meander pattern with local adjustments for the number of iterations requires a different approach. Then the first step will be to determine the number of iterations at each grid cell manually or by means of attractor points. The cells are divided into different groups, based on the number of iterations. In the following step a set of interlocking branches with the right number of iterations should be projected onto the right grid cells. This also happens with the same checkerboard pattern, where they are rotated 90 degrees for every other cell. The third step is equal to the one described above.

Figure 30 shows the algorithm, simplified in a flowchart. On the left side is the main process to create the entire pattern. On the right side, an option is included to distort the grid and therefore to distort the pattern.

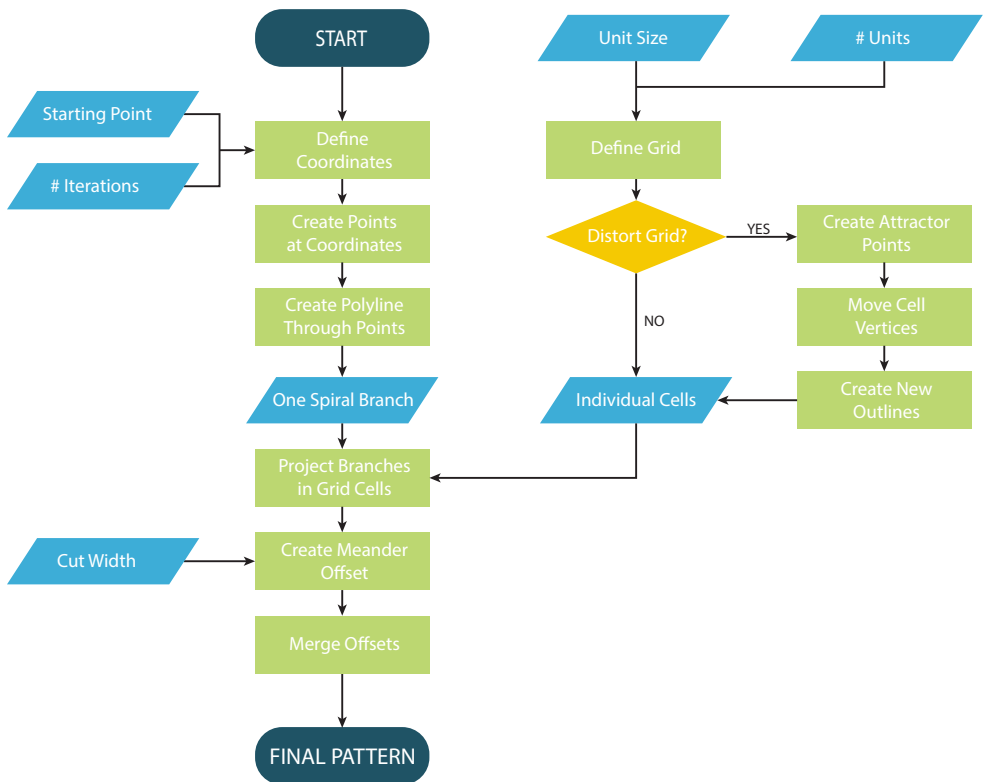


Figure 30. Flowchart of the meander pattern algorithm in Grasshopper.

2.5. ANALYSES ON FLEXIBILITY

2.5.1. INTRODUCTION

The measurements described in this chapter are focused on the behavior of panels with applications of different patterns. These are done by means of both physical and digital models.

Small scale prototypes were used to analyze the behavior of the panels in practice and see how the different pattern variables influence the flexibility of a physical model. The majority of these models is made of MDF and a few from plywood and cardboard. The main reason to choose MDF above plywood for these small scale prototypes, is the cost of the material. However, MDF is an isotropic material and comes in variable thicknesses, which makes it well suited for these measurements and a suitable alternative for plywood.

Next, the same patterns were analyzed with simulation tools inside Karamba® , a plugin for Grasshopper® . This tool is able to provide accurate structural analyses and visualizes the stresses and deformations directly on the model. The analyze-component that has been used is still work in progress, which means that the simulation results may not be entirely accurate. This component is however the only one available in Karamba® that allows for large deformation analyses. Without a proper alternative, the output of this component is compared with the physical models and only used to make assumptions on the flexible behavior. A detailed structural analysis is not part of this research.

2.5.2. OBSERVATIONS

A special bending-tool has been designed to test the flexibility of the small scale models, see Figure 31. The tool has two parallel beams at a variable distance, that support the model placed in between. It allows for bending about a single axis with high precision, by moving the support beams closer to each other. This increases the applied bending moment on the model, resulting in a larger deformation. The position of the model can be fixed by securing the movable support to the base plate. A fixed position of the model makes it easier to observe the deformations in the individual segments of the model.

What is immediately noticeable when bending a meander pattern, is that part of the segments protrude the curved surface (Figure 32). Looking more closely reveals that these areas are protruding as a result of the unnoticeable bending in the segments perpendicular to the rotation axis. A larger bending moment with greater deformation does however exhibit a small inflection in these segments, but it is clearly not substantial for the final surface curvature.

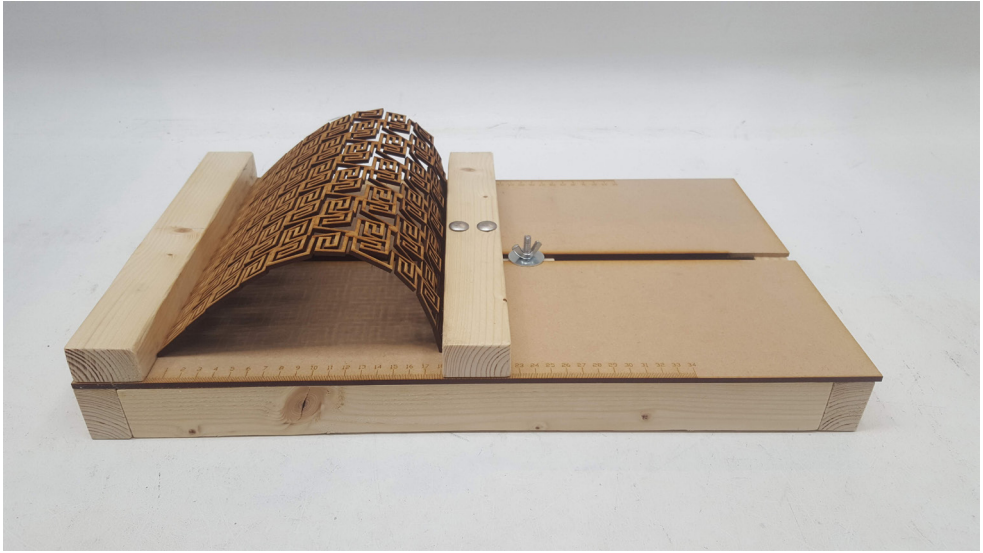


Figure 31. Bending tool to examine the bending behavior of different patterns. Here a non-uniform pattern is displayed, as shown in Figure 26a.



Figure 32. Close-up from protruding segments.

Assuming that the segments subjected to bending do not deflect, the amount of torsion must be the most significant factor for the attainable surface curvature. The diagram in Figure 33 shows the principle of the bending behavior of a meander pattern. The colored regions resemble the segments without noticeable deflection which get their angular displacement by the torsional segments in y -direction.

The protruding segments are located at the regions with the least amount of torsional segments, like region B-C in Figure 33.

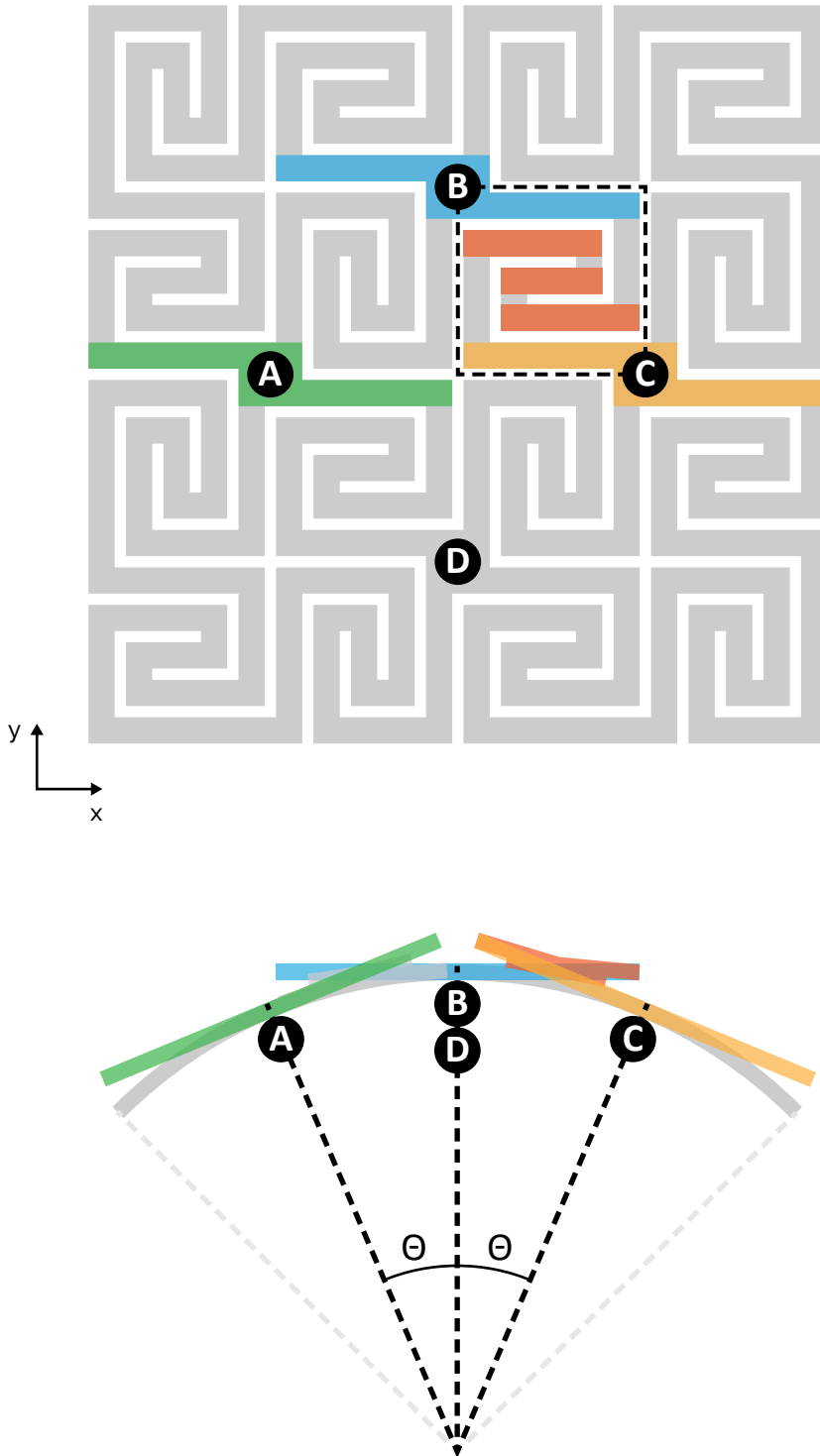


Figure 33. Angle of displacement between the colored regions.

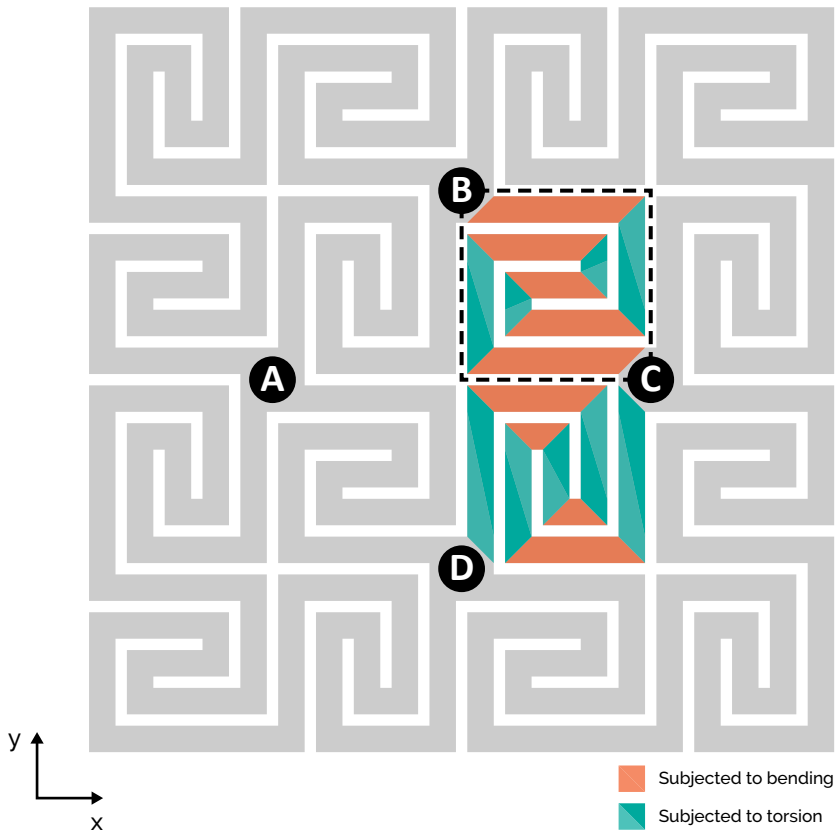


Figure 34. Segments subjected to bending (red) and torsion (green) when a bending moment is applied about the y-axis.

As described in "2.3.3. Meander pattern", every individual cell contains a certain amount of segments, dependent on the number of iterations. These segments are important for the flexibility of the panel, as the surface curvature will mainly be realized through the segments subjected to torsion. For simplicity of the calculations, only one bending moment will be applied on the panel, about the y-axis. This means that all segments parallel and perpendicular to the y-axis are respectively subjected to torsion and bending .

If the panel in Figure 33a is bent about the y-axis, there will be an angular displacement between the given points. As can be seen from the side view (Figure 33b), point B and D are located in the same plane, which means that both will have the same angular displacement relative to point C. The forces due to the applied bending moment get absorbed by each of the individual segments as bending or torsional stresses.

The number of segments connecting point B to C is equal to the number of segments between point C and D, but with a different orientation. Whereas the segments in region B-C are merely orientated in the x-direction, the orientation in region C-D is

in the y-direction. Stated that the angular displacement is the same, means that the stresses are distributed differently amongst the segments (Figure 34). Red indicates the segments subjected to bending, green indicates the ones subjected to torsion.

One of the observations was that torsion is the main factor and bending is of minor importance. In other words, the angular displacements are mainly caused by the segments subjected to torsion. Region B-C contains less twisting segments than region C-D, but has to obtain the same angular displacement. That means that the torsional stresses are likely higher in region B-C.

This may indicate that if the maximum curvature of the panel gets exceeded, it will likely break at one of these segments. The segments with the highest torsional stresses therefore determine the attainable curvature of the panel.

Segments

The amount of segments in a single grid cell (S) can be calculated with the number of iterations (a) in the following equation:

$$S_{cell} = 2a + 1$$

The total length (L_S) of these segments in one cell is dependent on the number of iterations and the size of a single meander unit (U). As a meander unit covers 4 grid cells, this number has to be divided by 2 to get the dimension for a single cell. The width of the kerfs are not of influence on the length of the segments, because the length is measured at the centerline of the segments, which remains equal with any given kerf width.

$$L_S = \frac{U}{2(a + 1)} \cdot ((a + 1)^2 - 1)$$

This equation is only applicable for meander patterns based on a grid with square cells, meaning that the size of a single meander unit is equal in both x and y direction. Each cell has the same dimensions, but every other cell has its interconnected segments rotated by 90 degrees.

2.5.3. SIMULATIONS

The flexible behavior of the panel has been visualized with simulation tools inside Karamba®, a parametric structural engineering tool. In the latest software version of Karamba® (1.3.0), there is just one analyze component that allows for large deformations. However, this component is still work in progress, which means that the results may not be accurate enough to be used for a detailed structural analysis. But as it gives the most relevant results, this component is still being used for the analyses.

Analysis Phase 1

The first model that has been analyzed was a flat surface, applied with the original [4,2] meander pattern. Because the panel is constructed out of a flat surface, it seemed reasonable to convert the model into a shell structure, with a cross-section of constant height. The model was supported along two opposite sides and has been exposed to a negative uniformly distributed load. The resulting deformation is shown in Figure 35. At first, the deformations of the interconnected segments seem to match with the observations of the physical model: protruding segments and a surface curvature of parabolic shape. The relative stresses on the top and bottom surface due to the bending moments, are visualized by the colors red (compression) and blue (tension). However, torsion is not visible in the resulting model, while this appeared to be an important aspect for the deformation of the panel. The surface curvature in this model is only caused by bending deformations, which makes this model not useful for further elaboration, as it does not match the behavior of the physical models.

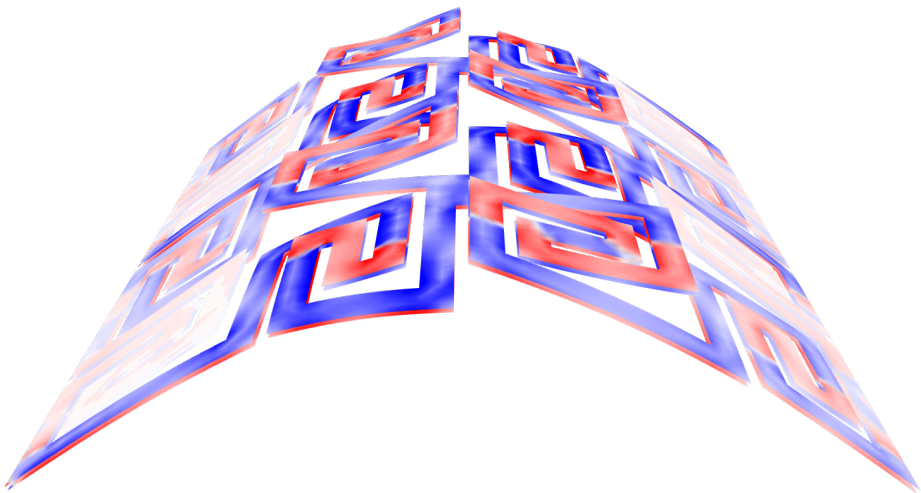


Figure 35. Deformation of a shell structure with axial stresses, due to a bending moment.

Analysis Phase 2

The second approach was to consider the individual segments in the panel as small beams, instead of the entire surface as a shell. A beam is created from the given centerlines of the segments (Figure 36). Lines that meet at a common point are connected to each other. The dimensions for these elements are determined by their length and a rectangular cross-section. The connected beams have their endpoints at common points, which explains the jagged appearance of the pattern outline in Figure 36c .

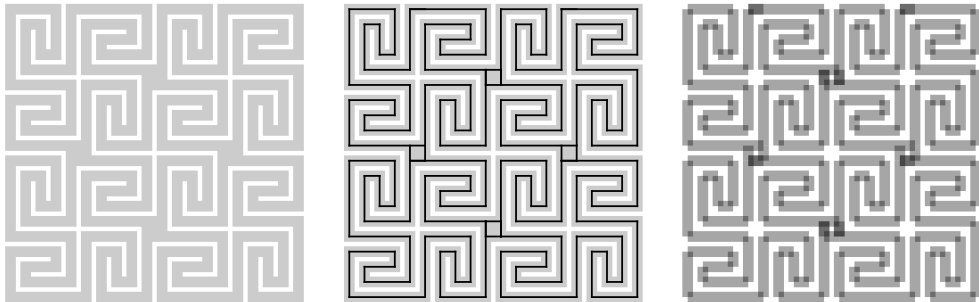


Figure 36. Conversion of a panel into a Karamba model. A regular meander pattern (a), centerlines of all segments (b) and beams created from the centerlines (c).

The configuration of the Karamba simulation can roughly be divided into 4 steps: input, model assembly, algorithm and output (Figure 37). The first step is to specify the various inputs. The centerlines of the pattern are converted into beams, which are interconnected at common points. These elements are supported at given points, located along these lines. A given cross-section determines the dimensions of the beam elements. Material properties can be added to give the model more accurate results in terms of bending behavior. Finally, a load case is required to generate a deformation that can be analyzed.

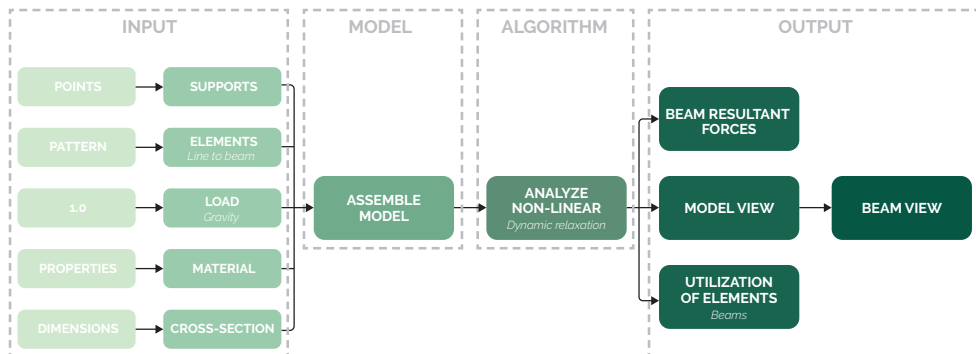


Figure 37. Karamba flowchart for the constructed algorithm.

In the second step, all different inputs are combined into one component to assemble the model. Next, the assembled model will be analyzed with a specific algorithm, which is in this case a Analyze Non-Linear component, able to analyze large deformations. The output from this algorithm component forms the last step in the process. The analysis provides the stresses and utilization for each element and gives a visual representation of the deformed model.

The dimensions of the panel for the second approach are increased, so that the behavior of the individual segments is better visible in different areas of the model. The green arrows in Figure 38 indicate the fixed translations for each support, meaning that they are not able to move along these particular axes. None of the supports have a fixed rotation, they can rotate freely about any axis.

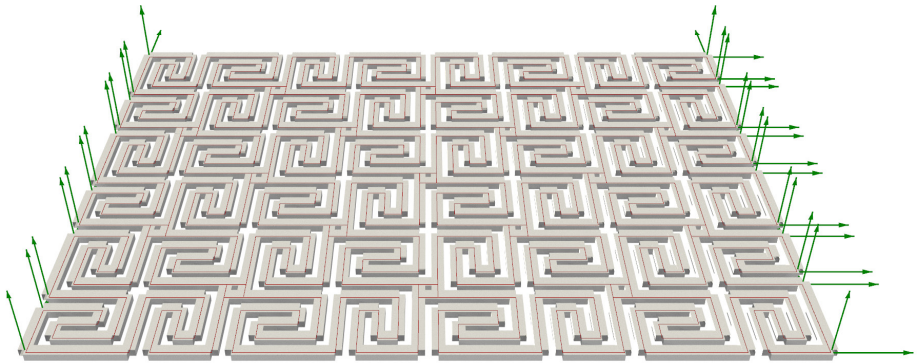


Figure 38. The model is supported on two opposite sides, with green arrows indicating the fixed translation along that particular axis.

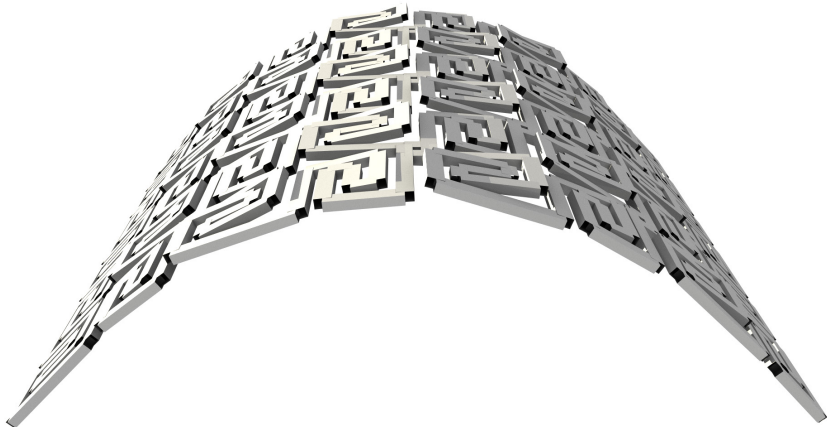


Figure 39. Deformation of the model, built up of interconnected beams.

Again, the model has been supported along two opposite edges and is exposed to a uniformly distributed negative load, to match the appearance of the tested physical models. The resulting deformation of this beam structure is more in line with reality. It has the characteristic of protruding segments and more importantly: bending is hardly noticeable, indicating that the deformations are mainly caused by torsion. The angle of displacement is still difficult to notice for the individual segments, but together, the small angles are able to cause a significant deformation for the entire panel (Figure 39).

In Figure 40, The uniformly distributed load has been increased gradually, to visualize the behavior of the model with different load cases. The applied loads are a couple of times higher than the actual gravitation load on earth, ranging from 0 to 14 times the actual gravitation load, in steps of 2. Here is clearly visible that a higher load case causes a greater deformation with further protruding segments. The protrusion is the greatest at the region with the highest bending moment, and thus the smallest curvature radius.

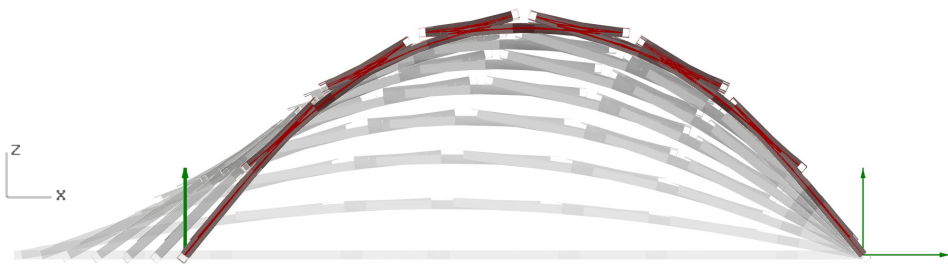


Figure 40. Model with gradually increased uniformly distributed load.

The applied load also comes with axial stresses and bending moments in the material. Figure 41 shows the axial stresses for each segment, on the top and bottom surface. The red color marks a negative stress level, indicating compressive stress. The blue color marks a positive stress level, indicating stress from tension. A darker color in the central region means higher axial stresses, related to the segments near the supports. It is also noticeable that these stresses are only visible on the segments that are subjected to bending.

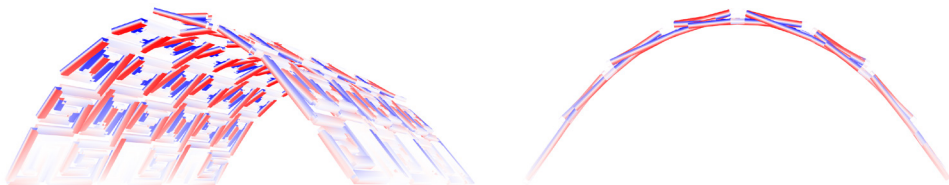


Figure 41. Axial stresses on the top and bottom surface.

The bending moments (M_x) about the local x-axis (torsional moments) are being displayed in Figure 42. Figure 43 shows the bending moments (M_y) about the local y-axis. The height of the colored planes indicates the relative bending moment for each segment and follows the bending moment diagram for the whole surface.

The direction of the colored planes has to do with the orientation of the local axes of each element, which is rotated for adjacent segments. The absolute value for the bending moment is the same, but applies on the opposite direction. That means that the blue segments are twisted in the opposite direction relative to the red ones. And consequently, the yellow segments are bent in the opposite direction relative to the green ones.

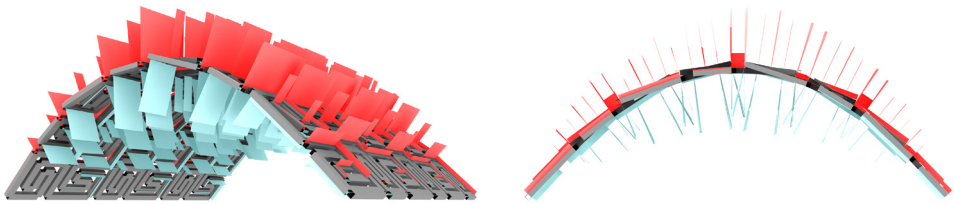


Figure 42. Bending moments (M_x) about the local x-axis (torsional moment).

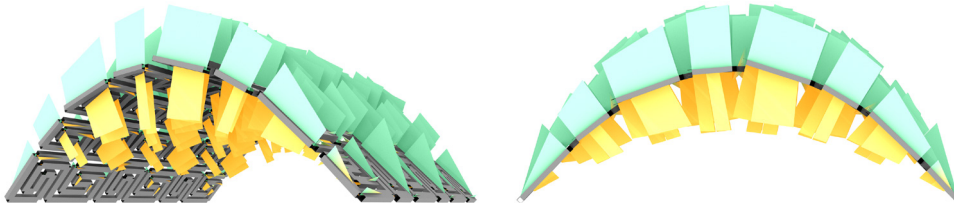


Figure 43. Bending moments (M_y) about the local y-axis.

Analysis Phase 3

During phase 3, the simulations are focused on the effect of several parameters on the maximum displacement. Two of the three parameters mentioned in "2.3.4. Parameters", were chosen to be analyzed, combined with the segment thickness. They either relate to the pattern or the material. The surface curvature is mainly obtained by the combined torsional deformations of all segments. The parameters that directly affect these segments are:

1. The **number of iterations**, defining the number of segments
2. The **kerf width**, defining the width of the segments
3. The **thickness of the material**, defining the height of the segments

The unit size remains constant for these simulations, as it only scales the entire pattern and is directly related to the width of both the material and kerfs. The material properties that have been used apply to plywood and also remain constant during all simulations (Table 1).

Material properties of plywood

Young's Modulus	500	kN/cm ²
Shear Modulus	250	kN/cm ²
Yield Strength	4.0	kN/cm ²
Specific Weight	800	kg/m ³

Table 1. Material properties of plywood

The base model that is used for the simulations, is constructed of an array of eight [4,2] meander units with each a size of 150 mm (Figure 44). With 4 iterations, the length of the segments falls in the range of 15 to 75 mm.

The total length of eight units makes a span of 1,20 m, which is supported on two sides like shown in the diagram in Figure 45. For support A, translation is only possible in x-direction. Support B is completely fixed and has no possible translation at all. Both supports allow rotation in all directions.



Figure 44. Base model, used for finding the maximum displacement

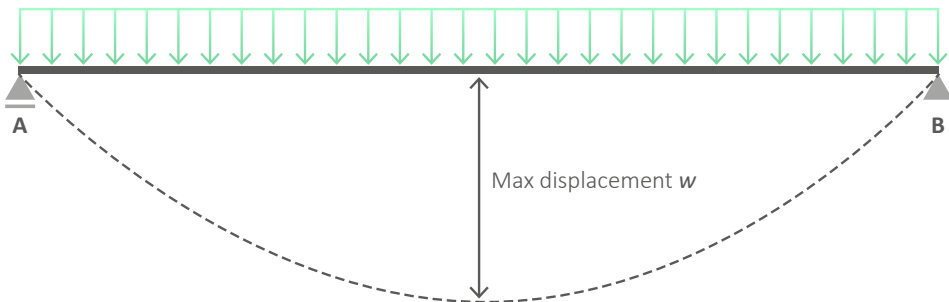


Figure 45. Load diagram of the supported model.

The uniformly distributed load is defined by the weight of the panel itself. That means that this value will be slightly different for every other combination of the above mentioned parameters, as they all affect the dimensions of the segments and thus the weight of the panel. The load causes a deformation for the panel with a maximum displacement w at the point with the highest bending moment. Due to potential large deformations, support A is able to move freely towards support B.

Figure 46 shows the resulting deformation of the model by its own weight and the relative bending moments (M_y) about the local y -axis. The visible deformation is proportionate with the length of the span. The maximum displacement w for this setup is calculated at 257 mm, with the following combination of parameters:

Pattern parameters	
Unit size	150 mm
Number of iterations	4
Segment width	10 mm
Segment height	6 mm

Table 2. Pattern parameters for used.

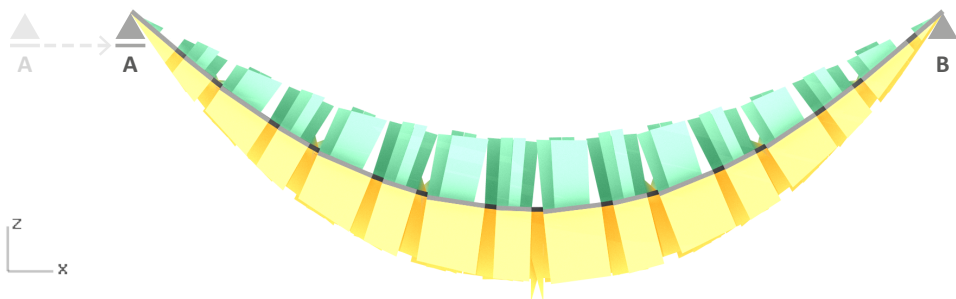
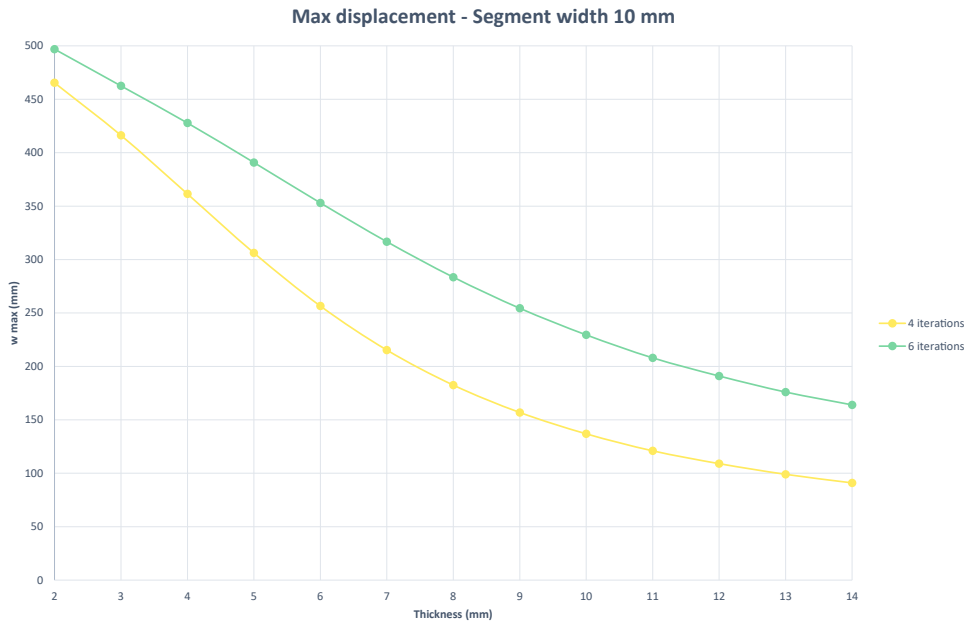


Figure 46. Maximum displacement of 257 mm for the model supported on both ends, with a span of 1.20 m.

The relative bending moment M_y about the local y -axis has been visualized by the green and yellow colored planes.

The graph in Graph 1 shows the relationship between the thickness of the material and the maximum displacement. The thickness of the panel is given on the x -axis, the maximum displacement on the y -axis. The yellow and green line display the model with a number of respectively 4 and 6 iterations, and a constant segment width of 10 mm. Due to a different number of iterations and an equal unit size of 150 mm, the kerf width is different for both models. A model with segments of 10 mm in width means a kerf width of approximately 0.7 mm for 6 iterations, against 5 mm for 4 iterations.



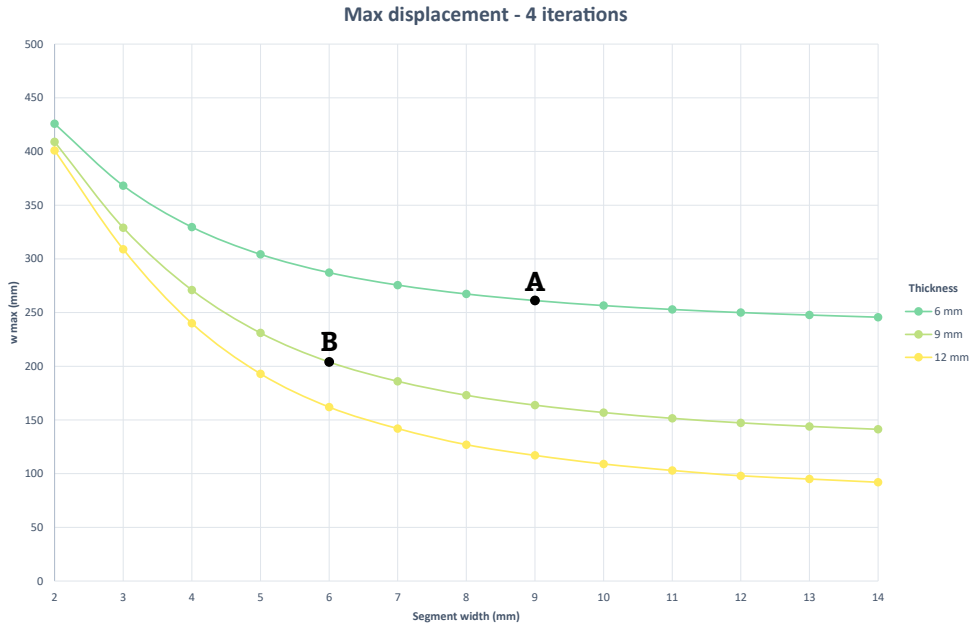
Graph 1. Maximum displacement with constant segment width of 10 mm.

It is immediately visible that a model with 6 iterations results in a higher maximum displacement than with 4 iterations, with equal dimensions for the segments of both models. More iterations means there are more segments that all together are able to achieve a larger displacement.

An increased thickness of the panel does not only increase the height of the segments, but also the total weight of the panel. A larger weight would cause a higher bending moment, resulting in a larger displacement. However, the graph shows a resulting displacement which is less for a higher thickness. That means that the height of the segments has a larger influence on the stiffness of the panel than the increased bending moment. As the thickness of the panel increases, the graph for the maximum displacement seems to level off.

Graph 2 shows the maximum displacement for the model with a variable segment width. All three simulated types have 4 iterations and a thickness of respectively 6, 9 and 12 mm. As expected, the model with a lower thickness results in a higher maximum displacement, at the same segment width. The relative distance between the three thicknesses remains constant but shows a non-linear development along the graph.

When looked at a single segment subjected to torsion, the dimensions of the height and width could be interchanged and still have the same angle of displacement. A rectangular shape upright or laying still has the same cross-sectional area and would therefore have the same angle of displacement. When the maximum displacement



Graph 2. Maximum displacement for a pattern with 4 iterations.

of the model is entirely caused by the segments subjected to torsion, it would have the same value for height 6 and width 9 (point A), and height 9 and width 6 (point B). As this is obviously not the case, torsion could not be the only aspect. The maximum displacement at point B is less which indicates an increased stiffness of the panel, due to the higher thickness. This means that besides torsion, bending is also involved in the displacement.

A [4,2] meander pattern with a unit size of 150 mm and 4 iterations has a distance of 15 mm between the centerlines of the segments. This is equal to the combined width of a single segment and one kerf. The maximum width of a segment is therefore set at 14 mm corresponding with a kerf width of 1 mm.

Besides the pattern parameters and the thickness of the panel, the length of the span is also an important factor for the maximum displacement.

The equation for the maximum displacement for a basic beam supported on both ends with a uniformly distributed load, contains the quantity length of span to the power of 4. That means that the maximum displacement will increase by a factor of 16 for only two times the distance.

$$w_{max} = \frac{5}{384} \frac{ql^4}{EI}$$

This equation is not directly applicable on the model in this situation, as additional aspects are involved, related to the pattern parameters. That the length of the span has a significant impact on the deformation of this model as well, can be seen in the maximum displacement for the model with half the span (Figure 47). Where a span of 1,20 m resulted in a maximum displacement of 257 mm, does a span of 0,60 m result in a maximum displacement of no more than 21 mm. The factor of 16 is not noticeable with these values, due to the additional aspects that affect the displacement, but the span certainly has a significant impact.

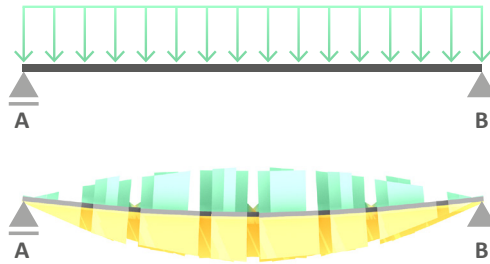


Figure 47. Maximum displacement of 21 mm for the model supported at both ends, with a span of 0,60m.

The used model in Figure 48 is equal to the one shown in Figure 44, but has an additional support at the center. The maximum displacement is reduced significantly to a value of approximately 10 mm. The bending moment diagram related to the basic setup of a uniformly distributed load on a beam with three supports, matches the relative bending moment visualized by the colored planes.

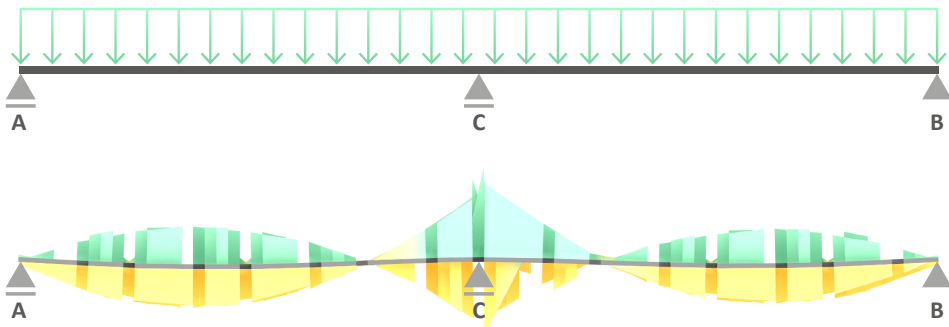


Figure 48. Maximum displacement of 10 mm for the model supported at both ends and in the middle, with a total span of 1,20 m.

The supports as shown in Figure 48 would in practice be the mounting points for a suspended cable system, to attach the panel to the ceiling. For the deflection of the panel it would not make a difference, as the same principle applies. The simulation shows that a surface curvature can be obtained easily, by removing one of the supports by loosening the cable (Figure 49). Changing the length of the support cables individually allows for a variety of surface curvatures. This causes a different force-flow through the cable system, as the weight of the panel is distributed over all supports, depending on the defined length for each cable. Construction calculations are not part of this research and therefore not further elaborated.

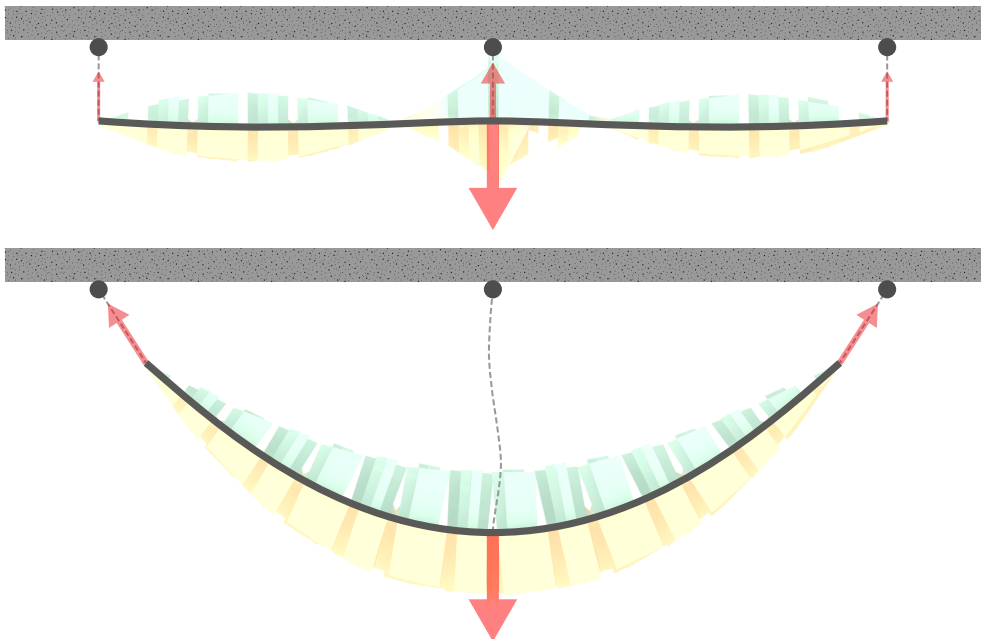


Figure 49. Loosening one of the cables causes large deformations of the panel and a different force-flow.

2.6. CONCLUSIONS

2.6.1. SIMULATIONS

The simulations that have been done with the plugin Karamba confirmed the theoretical assumptions based on the literature study and the observations with physical models. Larger dimensions for the width and height of the segments result in an increased stiffness of the panel, of which the height is of greater influence. This result indicates that the flexibility is affected not only by torsion but also by bending. The exact share of both aspects to the final curvature could not be determined, as the simulations only showed the bending moments for each segment, but not their individual angle of displacement.

A higher number of iterations is accompanied by a higher number of segments, which should result in a higher flexibility. The simulation confirmed this theory by showing an increased maximum displacement for the higher number of iterations.

Simulations have been done with a gravity load, which gives a different load case for each unique set of parameters. When compared to the model with 4 iterations, the same model with 6 iterations has a higher number of segments, which means more weight and thus a larger bending moment. In other words, the higher maximum displacement is the result of a larger number of segments in combination with a larger bending moment. The larger bending moment only applies when the dimensions of the segments in both models are equal.

The simulations only apply for the wooden surface. In practice a layer of flexible sound-absorbing foam will be added to the wooden surface, which might slightly influence the overall flexibility of the panel.

The results of the simulation can have some flaws and errors, caused by the following aspects:

- Inaccurate or incorrect values for the material properties might give different outcomes during the simulation.
- The used analyze-component within Karamba is still tagged as work in progress, which means that the results might be not entirely accurate.

2.6.2. FINAL REMARKS

The corresponding sub-question that has been asked at the beginning of this chapter can now be answered.

How does pattern kerfing influence the attainable curvature of a panel?

A meander pattern can be defined by the three main pattern parameters: the size of a meander unit, the number of iterations and the kerf width. The pattern divides

the surface into multiple interconnected segments, which are able to enhance the attainable surface curvature by means of torsion and bending of the segments. The individual dimensions of these segments are based on the pattern parameters and determine the flexibility of the panel.

The flexibility of a panel can be adjusted locally, by changing the amount of iterations or the width of the kerfs in specific areas. For the simulations only uniform patterns have been analyzed, the effect of local adjustments was not examined. Physical and theoretical models have shown that local flexibility is possible, but need further elaboration.

3. ACOUSTICS

3.1. INTRODUCTION

In general, acoustics used for sound improvement can be divided in two categories: soundproofing and treatment. Soundproofing is meant to reduce unwanted noise and treatment is to improve the quality of the sound related to the purpose of the room. With soundproofing, the noise that has to be reduced can derive from both inside and outside the room. Sound reduction from outside is usually obtained with insulation by mass or cavity. Sound treatment contains absorbing and/or reflecting elements inside the room, which will be further discussed in this chapter.

Depending on the situation, the purpose of a building or room determines the main requirements for the acoustic design. The acoustic applications in private dwellings for example, would be different from the ones in industrial or commercial buildings with usually a higher sound intensity. Specific buildings like a theatre or concert hall require an even more sophisticated architectural design for acoustics.

This chapter will first explain the basic principles of acoustics based on a literature study. The following subject will be about the acoustic design in which different acoustic parameters are explained and three different scenarios are given for distinct compositions of the designed acoustic panel.

The corresponding sub-questions that will be answered in this chapter, are:

How does kerfing influence the acoustic performance of a panel?

and

What effect has a curved surface of a panel on its acoustic performance?

Both questions will be further examined in paragraph 3.4 , where actual measurements give more information and insight on the influence of the patterns and the curvature on the acoustic performance.

3.2. LITERATURE STUDY

3.2.1. PRINCIPLES

The physics of sound can be described by three characteristics: Sound level (or energy, strength, loudness), frequency (or tone, wavelength) and propagation (or path, elapsed time) (Ermann, 2014).

Figure 50 shows the relation between sound level and sound pressure, at a single frequency. A greater amplitude of the soundwave means a higher sound level and a higher sound pressure.

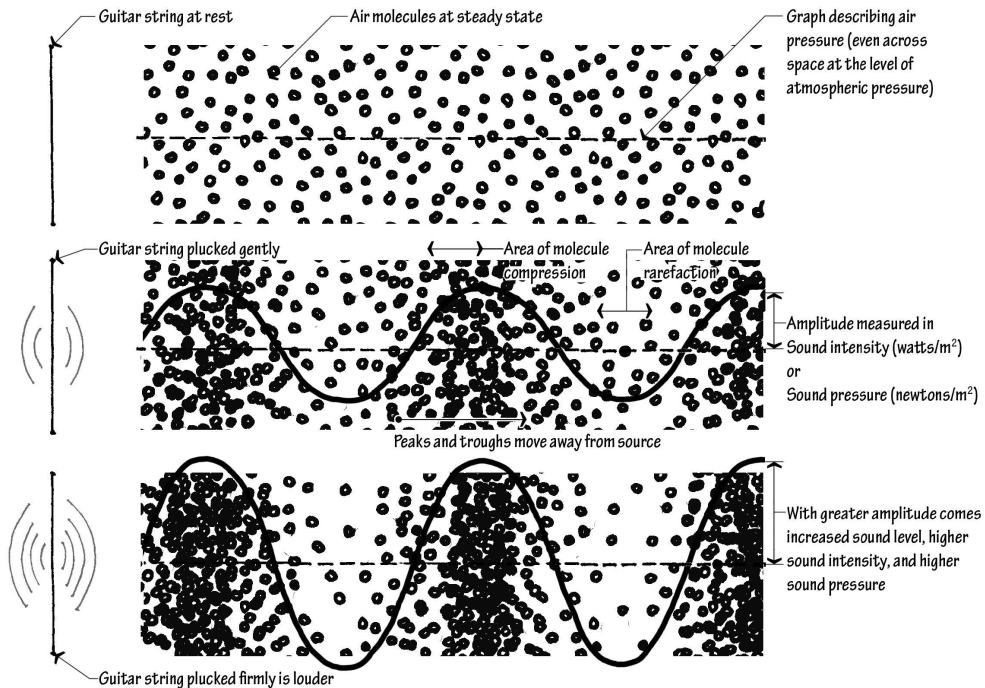


Figure 50. Relation between sound level and sound pressure, at a single frequency (Ermann, 2014, p. 3).

Sound level

The strength of sound at the source is described by the sound power (W) and is measured in Watts. To measure how much sound arrives at the receiver, two different methods can be used. Sound intensity (I) is measured as the sound power at the source divided by the area over which the source energy has spread, expressed in Watts/ m^2 . Secondly, sound pressure (p) is measured as the amplitude of the sound wave, measured in Newtons/ m^2 or Pascal (Pa) (Ermann, 2014).

The values for the sound intensity or sound pressure are inconveniently small as expressed in the given units, and usually cover a range of several orders of magnitude. The sound pressure at the threshold of pain is a million times greater than at the hearing threshold. Therefore, the logarithmic scale of the decibel unit (dB) is used to compress these sound pressures into values which are easier to use. Table 3 shows the perception of different sound levels.

The sound pressure level (L_p) in decibels can be calculated with the following equation, with p_{eff} as the effective sound pressure and p_0 as the sound pressure at the hearing threshold, with a value of $2 \cdot (10)^{-5}$ Pa:

$$L_p = 10 \log \left[\frac{p_{eff}^2}{p_0^2} \right]$$

THRESHOLD OF FEELINGS		THRESHOLD OF AUDABILITY	
		Sound Pressure (Pa)	Sound Pressure Level (dB)
DEAFENING	Jet Takeoff	20	120
	Artillery		
	Elevated Train		
VERY LOUD	Subway	2	110
	Printing Press		100
	Police Whistle		90
LOUD	Vacuum Cleaner	0,2	80
	Street Noise		70
	Noisy Office		60
MODERATE	Large Store	0,02	50
	Conversation		
	Average Office		
FAINT	Private Office	0,002	40
	Quiet Conversation		
	Studio (Speech)		
VERY FAINT	Rustle of leaves	0,0002	20
	Whisper		
	Soundproof Room		
		0,00002	0

Table 3. Typical A-Weighted Sound Levels (Adapted from Acoustical Surfaces Inc. (2018)).

The decibel units cannot simply be added together. They follow a logarithmic scale and need to be converted back to a linear scale, to calculate the total sound pressure level. For instance, combining two vacuum cleaners with equal sound pressure does not double the amount of decibels, it only adds 3 dB to the resulting sound pressure level. The total sound pressure level of multiple sources can be calculated with:

$$L_{p;tot} = 10 \log \left[\sum_{i=1}^n 10^{\left(\frac{L_{p,i}}{10}\right)} \right]$$

For example, the sum of the 3 sound pressure levels: 60 dB, 67 dB and 75 dB can be calculated as:

$$L_{p;tot} = 10 \log \left[10^{\left(\frac{60}{10}\right)} + 10^{\left(\frac{67}{10}\right)} + 10^{\left(\frac{75}{10}\right)} \right] = 75,8 \text{ dB}$$

Sound frequency

The frequency of a sound wave is simply the number of complete vibrations occurring per second (Cavanaugh & Wilkes, 1999) and is being measured in Hertz (Hz).

The audible range of humans lies between 20 Hz to 20.000 Hz. Sounds below 20 Hz are merely experienced as vibrations than as a tone, which are known as infrasonic. Frequencies above 20 kHz fall in the ultrasonic spectrum and are inaudible altogether. The range of human speech is roughly 150 Hz to 6000 Hz.

When a sound consists of only a single frequency, it is called a *pure tone* (Figure 51). Instruments produce sound with a pattern of frequencies, which can be termed as *harmonic sounds*. Most of the everyday sounds, including speech, traffic and audience clapping are called *complex sounds*, with varying levels of sound across the audible frequency spectrum (Ermann, 2014).

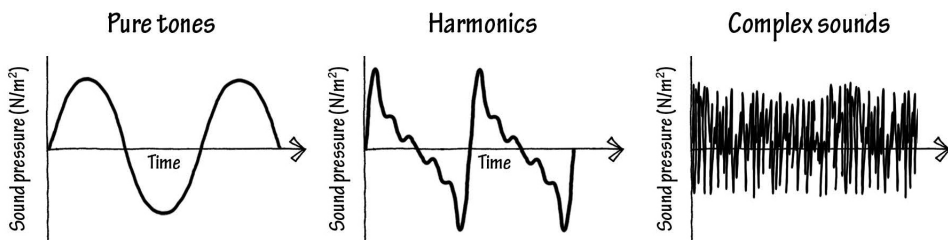


Figure 51. Acoustic Waveform for pure tones, harmonics and complex sounds (adapted from Ermann (2014)).

Sound propagation in air with a temperature of 20 °C has a speed of 343 m/s. The wavelength (λ) of a given frequency can then be calculated by dividing the speed of sound (c) by the frequency (f):

$$\lambda = \frac{c}{f}$$

A visual representation of the wavelength for a given frequency is shown in Figure 52.

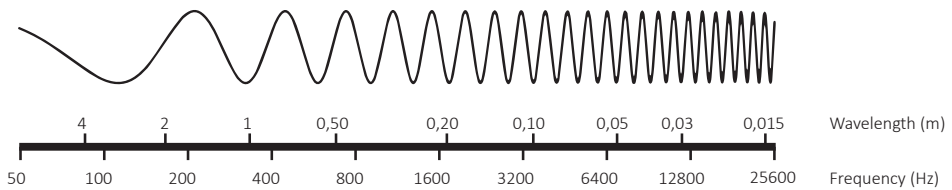


Figure 52. Wavelength vs. frequency.

Sound propagation

In a free field with no nearby reflective surfaces, sound energy generated by an omnidirectional sound source is spread in all directions. The same sound energy is spread over four times the area, resulting in a decay of 6 dB every time the distance is doubled. With indoor sound propagation, the room boundaries or other objects placed inside will influence the propagation. Sound energy hitting a surface will be reflected back and continues its path, until all sound has decayed.

Each material has its own acoustic properties behaving differently on sound, so that they will transmit, absorb or reflect sound waves (Figure 53). Reflected sound can either be redirected by flat surfaces (specular reflection) or scattered by a diffusing surface (Cox & D'Antonio, 2009).

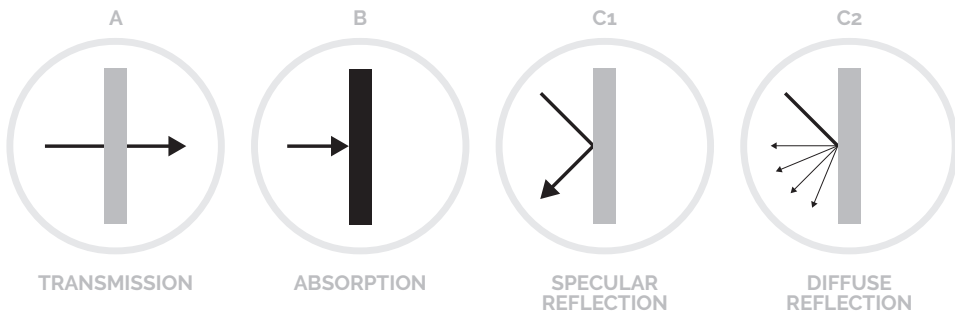


Figure 53. Incident sound will be distributed into transmission, absorption or reflection.

The sum of these three aspects is equal to the incident sound, conform the law of Conservation of Energy. The energy distribution between transmission, absorption and reflection is dependent on the surface's acoustic properties. All sound energy is ultimately converted into heat energy. This may occur within the transmission medium itself or through interactions at boundaries with other materials (Godbold, 2008).

Acoustic materials

Any material is able to absorb a part of the incident sound, but not all of them can be stated as 'acoustic materials'. This term is mainly used for those materials that have been produced for an acoustic purpose with high values of absorption and consequently low values of reflection. There are plenty of sound-absorbing materials, that provide absorption properties which are dependent upon frequency, composition, thickness, surface finish and method of mounting (Arenas & Crocker, 2010, p. 12).

To describe the sound absorbing quality of a surface and to quantify the proportion of incident sound energy that gets absorbed, we use the absorption coefficient (a), a number between zero and one (Ermann, 2014, p. 27). A value of zero means that no absorption occurs at all, where an absorption coefficient of one means that all sound energy gets absorbed by the material. Depending on the measured frequency, the absorption coefficient can be different.

Reverberation time

The sound absorption can either be measured, or calculated by measuring the reverberation time (T_R). The reverberation time is the time for sound to decrease by 60 dB after the source is silenced. The sound absorption coefficient can be calculated with the following equation:

$$T_R = \frac{0,161V}{\sum S_i a_i}$$

where V is the volume of the room and a_i is the absorption coefficient associated with given surface area S_i .

In practice the reverberation time is a well-known aspect used to describe the acoustic quality of a room. Too much reverberance causes speech to lose intelligibility because important details (consonants) are masked by louder, lingering speech sounds (vowels) (Dunn et al., 2015). To improve the speech intelligibility, the reverberation time can be reduced by decreasing the room volume or by increasing the amount of absorption.

Sound absorption can occur by several types of absorbing materials. According to their physical composition we can distinguish porous absorbers, resonant absorbers and

membrane absorbers. Porous absorbers are materials where sound propagates through a network of interconnected pores, where losses occur due to friction and thermal conductivity. Resonant absorbers involve a mass vibrating against a spring where the mass is the air inside the opening of the perforated sheet. For a membrane absorber, the sheet of the material itself acts as the vibrating mass. The spring is in both cases provided by air enclosed in the cavity (Cox & D'Antonio, 2009). The designed acoustic panel is a combination of porous and resonant absorbers which are further explained below.

3.2.2. POROUS ABSORPTION

Well-known porous absorbers that are often used to treat acoustic problems are carpets, curtains, acoustic tiles, cotton and mineral wools. These materials have in common that sound propagation occurs in a network of interconnected pores, in such a way that viscous and thermal effects cause acoustic energy to be dissipated (Cox & D'Antonio, 2009). Incident sound energy is converted into heat energy by the frictional and viscous resistance inside these pores and by vibration of the small fibers. Absorption is most effective when the pores are interconnected and form an open pore structure instead of a closed structure. A schematic representation of the difference between an closed and open pore structure is given in Figure 54.



Figure 54. Schematic representation of closed (top) and open (bottom) pore structures (adapted from Cremer and Muller (1982)).

The characteristics of sound absorption are highly diverse with varying frequencies. Sounds with a low frequency are in general hard to absorb because of their long wavelength. The thickness of the absorbent material does have a high influence on the frequencies that will get absorbed. As the thickness increases, the amount of absorption in the lower frequencies usually also increases.

Beside the thickness of the absorbent material, the placement in the room relative to the structure, is also important to gain significant absorption. The layer of particles adjacent to the boundary surface has zero velocity, while the particles a finite distance away oscillate freely (Godbold, 2008). This distance is called the viscous boundary layer, illustrated in Figure 55. Placing the absorbent material close to the boundary will generate insignificant absorption, so it needs to be placed somewhere where the particle velocity is high (Cox & D'Antonio, 2009).

Another important aspect is that the amount of absorbed energy by a porous material varies with the angle of incidence and the density of the absorbent (Cox & D'Antonio, 2009). When the density is too high, the absorbent will reflect the sound from its surface and reduces the absorption. Consequently, a too high angle of incidence causes the sound to reflect as well, so the absorption reduces.

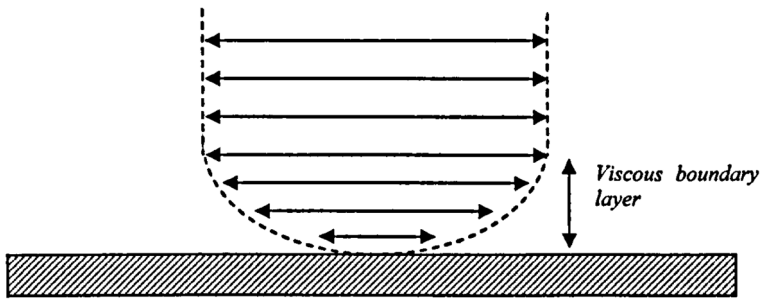


Figure 55. Oscillatory viscous flow over a surface (Godbold, 2008, p. 15).

Covers

Porous absorbers are often soft materials and therefore vulnerable when placed close to spaces with high risk of impact damage. Surfaces close to eating or preparation areas for example, need to be robust and washable. A soft absorbent material mounted on such a place would be unsuitable. In this scenario, placement would be better higher up on the wall or on the ceiling.

Absorbent materials are often wrapped in cloth for protection and aesthetical reasons. Cloth wrapping usually has little effect on the obtained absorption, as it still allows sound to enter the porous absorbent. But if glue is used to fix the cloth to the absorbent, care must be taken to ensure that it does not prevent sound entering the porous material, reducing the high frequency absorption (Cox & D'Antonio, 2009).

When mechanical protection is required, the absorbent can be covered by perforated panels to protect the material against abrasion and impact damage.

3.2.3. RESONANT ABSORBERS

A porous absorber, covered by a perforated panel, that is placed at a certain distance from the construction is called a resonant absorber. Placing such devices at the boundary of a room is usually more effective than application of porous material alone.

The mechanism of a resonant absorber involves a mass vibrating against a spring. The Helmholtz absorber, named after the German physician and physicist Hermann von Helmholtz, is one common form of this device where the mass is a plug of air in the opening of the perforated sheet and the spring is provided by the air enclosed in the cavity (Cox & D'Antonio, 2009). Figure 56 shows the typical constructions for a Helmholtz absorber. By changing the vibrating mass and the stiffness of the air spring, the resonant frequency of the device can be tuned, and it is at the resonant frequency that absorption is at its maximum (Cox & D'Antonio, 2009).

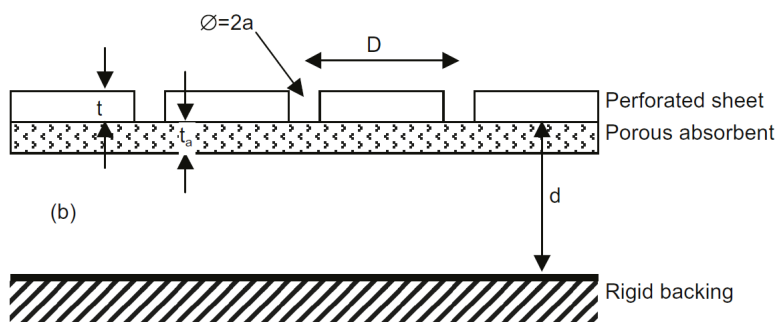


Figure 56. Typical construction for a Helmholtz absorber (Cox & D'Antonio, 2009, p. 197).

Damping provides the absorption of sound energy, usually combined with a layer of porous absorber directly behind the perforated sheet. The absorption characteristics of these resonant devices are a peak of absorption. The problem here is the difficulty to achieve wide band absorption in one device. Changes in the spacing of the openings, the opening diameter and the rear air cavity depth make it possible to obtain absorption over a wider variety of frequencies (Cox & D'Antonio, 2009). When the open area provided by the perforations is greater than about 20%, the expected absorption is entirely controlled by the properties of the porous absorber, and the panel has no effect (Bies & Hansen, 2003, p. 306). That means that any value above 20% would not influence the amount of absorption (and thus reflection). However, Cox and D'Antonio (2009, p. 160) state that for hybrid diffuser-absorbers, having both absorbing and diffusing abilities, even a 50% open area perforated sheet can have significant effect on the absorption. The effect of these factors will be examined during the measurements as described in the next chapter.

3.2.4. ARCHITECTURAL ACOUSTICS

For any situation, architectural acoustics involves two main considerations: (1) the acoustic quality of the room, which is dependent on its sound absorption and reverberation properties, and (2) the insulation of sound to prevent transmission from outside (Roohnia, 2016, p. 9). Too much reverberance and background noise have a negative effect on the speech intelligibility. The focus lies on the first consideration, as background noise is treated in a different way and not part of this research.

Absorption versus diffuse reflection

Naturally, the focus of attention for noise control lies on absorption to remove sound energy. However, in architectural acoustics both absorbers and diffusers play an important role to prevent acoustic distortion. Whether absorbers or diffusers are better depends on other acoustic factors, if a decrease in reverberation and/or sound level is desirable (Cox & D'Antonio, 2009).

A diffuser scatters the sound in multiple directions to reduce the distortion, without removing sound energy from the room. This is preferable when the reverberation time and sound energy should be maintained. For good intelligibility, a balance between absorption and diffusion is required. A very absorbent room is not suitable to be used for a listening room, as most of the sound arriving at the receiver will only come directly from the source and not from reflections. When there is hardly any reflection, the room turns out to be rather 'dead' and uncomfortable for a listening room. Studies have been done to define the best acoustic parameters like the reverberation time, but finding the perfect balance between absorbers and diffusers remains to a certain extent a subjective business.

To manage low frequencies, both absorbers and diffusers require a substantial depth to work. In practice depths of acoustic treatments are often limited, but the speed of sound in porous materials is lower than in air, meaning that an absorber can work to a lower frequency than a diffuser of the same thickness (Cox & D'Antonio, 2009). Combining the two in a hybrid structure or resonant absorber is therefore an appropriate and favored solution. The advantage of diffusers is that they are usually more robust than absorbers. This robustness gives a better protection against environmental impacts. Fibrous materials are more vulnerable and often do not endure well the effects of wind, rain or other impacts. Over time the pores can get clogged or damaged, decreasing its absorbing qualities. A robust cover will be a suitable solution to prevent these issues.

Variable acoustics

The acoustic design of a room is ideally made to match the acoustic requirements for the purpose of the room. In most cases, the applied acoustic elements are fixed, mainly because there is no need to change the acoustic performance in the room. For multi-purpose rooms, the desired acoustic performance might be distinct for different

activities. A design with variable acoustics could improve the acoustic performance for each scenario in the room. Varying amounts of reflective or absorptive surfaces are able to change an important aspect for room acoustics: the reverberation time. For most situations, listeners can detect a change in reverberation greater than or equal to 0,1 s (Unknown, 2010). This makes good acoustic design a substantial aspect of architectural design.

The reverberation time of a room can be reduced by decreasing the volume of a room and/or increasing the amount of absorption (De Vries, 2001). Next, several examples show how variable acoustics have been applied to acquire an adaptive acoustic design.

Variable absorption

Different architectural and mechanical solutions are developed to manipulate the variable acoustics. Hanging curtains are a simple but effective solution for changing the amount of absorption. They can be opened or closed depending on the desired amount of absorption. Movable panels on the wall or ceiling, having a reflective and absorptive surface, is a mechanical solution that for example is applied in the IRCAM institute for Research and Coordination in Acoustics and Music (Figure 57). The space is surrounded by a series of alternating panels. Each panel contains three rotating prismatic modules, having a direct reflective, diffuse reflective and absorbent surface. The modules can be positioned in the right position, to optimize the reverberation time in the room. The variable absorption can even be adjusted during a live performance to maintain the optimal conditions, with the audience still present.

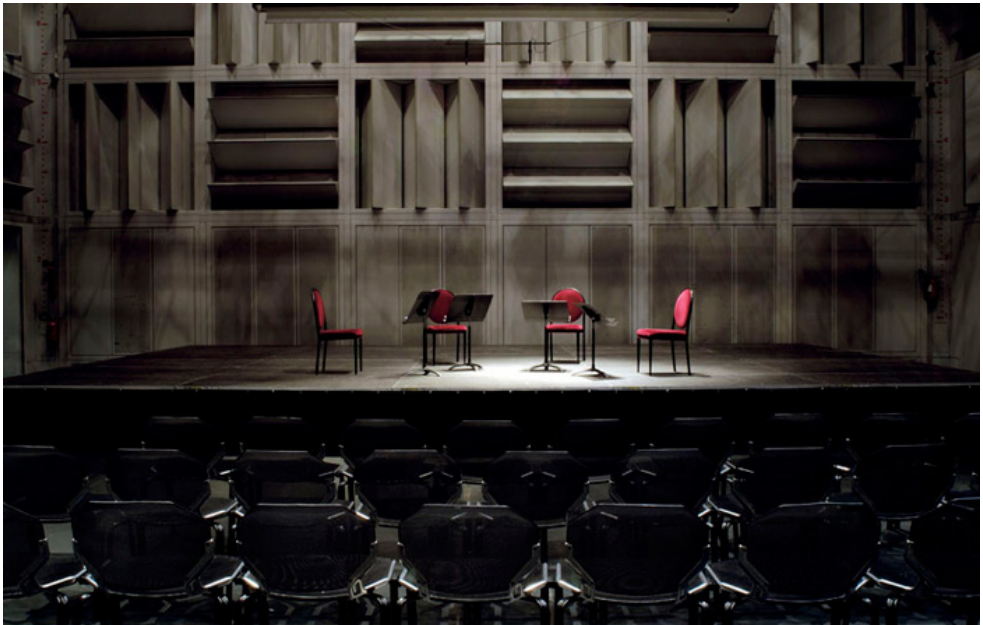


Figure 57. Variable room acoustics in l'Espace de Projection, IRCAM, Paris (Panier des Touches, 2014).

Variable room volume

Another way to adjust the reverberation time is to change the volume of the room. Although this technique is not suitable for every situation due to space limitations, there are some examples of auditoriums or concert halls where the volume can be varied. One of them is the Jones Hall in Houston, Texas (Figure 58). It has a unique ceiling of hundreds of hexagonal segments that can be raised or lowered to change the volume of the hall. The E. J. Thomas Performing Arts Hall in Akron, Ohio, also has a movable ceiling to regulate the volume and acoustics of the space (Figure 59). The ceiling can close off the balconies creating a one, two or three level auditorium.

The ratio between the room volume and the area covered by the audience and performers is an important aspect for the achievable reverberation time (Dunn et al., 2015, p. 328). Both factors are also included in the equation for the reverberation time, where the area covered by the audience is considered a surface with a certain absorption coefficient.

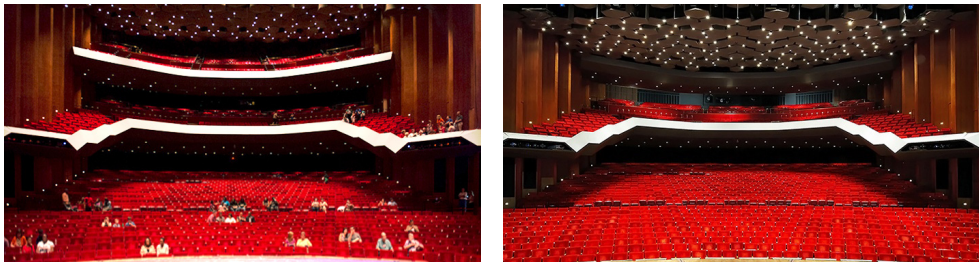


Figure 58. Jones Hall, Houston, Texas (adapted from Arie, 2013; Downtown Houston, 2010).



Figure 59. E. J. Thomas Hall, Akron, Ohio (Dionne, 2012).

Electronic acoustics

Besides the physical solutions to change the amount of absorption and room volume, more recent technical developments allow a different way to improve the acoustic quality of a room. Variable acoustics can also be conducted with electronic resources to simulate specific values for the reverberation time and sound level, without changing the room volume. Modern music halls are often made completely 'dead', with as much absorption as possible. With this approach, an electronic system can control the acoustic performance of the entire space by simulating the reverberation time and sound levels with multiple speakers located across the space.

Management

Most of the movable ceilings or other elements remain unchanged, because the perceptual effect of such changes is hardly noticeable or because people do not know the optimal position for a certain performance (De Vries, 2001). The same issue is also applicable to the electronic systems which have an even larger number of variations in settings. So it is not only about the actual facilities but also management of these facilities. Variable acoustics are therefore merely applied in larger spaces like auditoria or concert halls where acoustic experts are responsible for the variable acoustic systems.

3.2.5. CLASSROOM SCENARIO

Education institutions are of all times and will continue to play a dominant role in the future. But times change, and so do the traditional formats of classrooms and the way learning spaces are used.

Technologies have found their way into the learning environment. Interactive or conventional whiteboards mounted on the wall behind the speaker, projectors hanging from the ceiling and the ability to make use of a wireless network have been implemented. But these alterations have rarely altered the dynamics of the design (JISC, n.d.).

The role of academic teachers is gradually moving, from the front of the class to the side along the students, while the student is expected to combine the role of being a reflective absorber with that of active participant (AMA Alexi Marmot Associates in association with haa design, 2006). As more and alternative forms of teaching are being implemented, changes in learning spaces also demand changes in their acoustical performance (Pääkkönen et al., 2015). Several studies have proven that the acoustics in classrooms and lecture halls are important to students' learning and wellbeing (Scannell et al., 2016). A classroom with well-designed acoustics will enhance the speech intelligibility inside the room, which will result in an improvement of learning and students' behavior (Madbouly et al., 2016). Puglisi et al. (2015) states that a good acoustic environment will primarily be achieved by minimization of the contributions of

noise from both external and internal sources and that good communication is ensured when the relevant parameters for room acoustics and intelligibility are in the acceptable ranges for teaching and learning purposes.

Methods

When a sound is produced inside a room, it gets reflected off all surfaces in the room. The material and finish of the surface determine the amount of reflected sound. The harder a surface is the more sound will be reflected back into the room. The combination of direct sound with sound reflections as indirect sound determines how students in a classroom will hear the teacher.

There are different guidelines for different types of spaces. The most widely used acoustic measure in classrooms is the measurement of the Reverberation time (Sala & Rantala, 2016). The recommended reverberation time for traditional classrooms falls between 0,5 and 0,9 s (Pääkkönen et al., 2015).

"Good architectural acoustic design requires the right room volume, the right room shape and surface treatments, utilizing an appropriate combination and placement of absorbers, diffusers and flat surfaces." (Cox & D'Antonio, 2009)

Changes in the form of teaching means there will be multiple scenarios in a learning environment. Each available scenario has presumably varying requirements regarding the acoustic performance in the room. In order to obtain the most efficient learning space in each scenario, the room acoustics should be flexible and controllable. In paragraph 3.5 Acoustic Design , three scenarios will be given with a conceptual acoustic design. Later on they are elaborated on in relation to the results of the measurements.

3.3. ACOUSTIC DESIGN

3.3.1. INTRODUCTION

The literature study described current applications of variable acoustic designs. The focus of this research is on the design of a responsive surface, in order to create a new type of acoustic panel with adjustable surface curvature. The pattern design determines the flexibility of the panel, but it has also an effect on the acoustic performance. Where the presence of material is important for the level of flexibility, for the acoustic performance it is all about the absence of it. Openings in the panel allow sound waves to pass through, into the sound absorbing material behind the front surface.

3.3.2. ACOUSTIC PARAMETERS

The patterns which are elaborated on in chapter 2 are now being examined in terms of acoustics, combined with porous absorbent material. The flexible wooden surface holds and protects the porous absorbent and is the aesthetic appearance of the panel in the room. It is assumed that the sound absorption of the wooden material is zero, meaning that all sound absorption is caused by the absorbent material behind the surface. Sound waves hitting the wooden surface will be reflected back into the room.

Multiple aspects are of influence on the acoustic performance, in terms of absorption and reflection. The aspects that directly relate to the absorbing material itself are excluded for this research, such as its porosity and thickness. One type of absorbent material has been chosen, that is suitable for application in a flexible acoustic panel. The four aspects that will be elaborated on are related to the applied pattern and the configuration of the entire panel (Figure 60). The main pattern parameter besides the type of pattern, is the ratio between the open and closed surface, which is determined by the width of the kerfs. The flexibility of the panel allows for a certain surface curvature, causing more randomized incident sound waves and redirecting their reflection. A variable surface curvature also creates a fluctuating distance between the panel and the rigid backing. This air cavity is expected to affect the amount of absorption for specific frequencies.

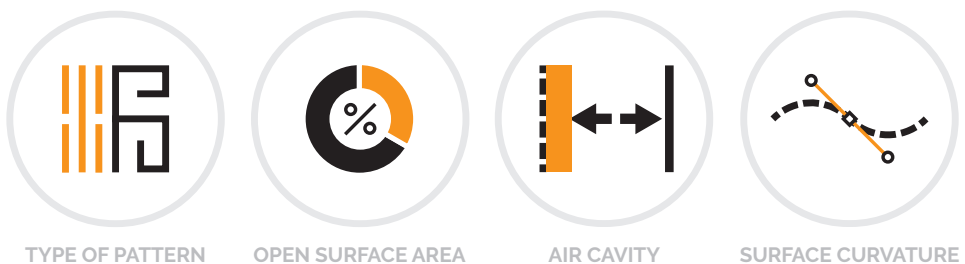


Figure 60. Acoustic parameters: Type of pattern (a), open surface area (b), air cavity (c) and surface curvature (d).

3.3.3. SPACE DEFINITION

The acoustic parameters allow for varying acoustic performance of the panel. The type of pattern and open surface area are static properties that are directly related to the panel itself. The thickness of the air cavity and the surface curvature are variables that indicate their position in the room that are able to be adjusted. Based on actual classroom situations, three scenarios have been defined to illustrate different compositions of the adaptable acoustic panels. To attain optimal acoustic conditions inside the classroom, the panel composition should be different for each scenario. Of the factors that determine the quality of the speech intelligibility, the reverberation will be examined, by means of the combination of acoustic reflection and absorption in the room. These aspects are affected by the surface curvature of the acoustic panels and their physical position in the room, in relation to a rigid backing. Figure 61 illustrates the conceptual compositions for (1) a traditional lecture setup with a single speaker, (2) a round-table group discussion and (3) working in small groups. These compositions only cover situations with acoustic panels that are placed continuously on the ceiling.

At the first composition, the acoustic panels have been placed almost parallel to the ceiling but with a slight parabolic curve towards the back. The acoustic panels act as a suspended ceiling, which decreases the room volume. In combination with the addition of sound absorption, the reverberation time will be reduced, resulting in better speech intelligibility. The placement of the panels distributes the sound reflections across the room with a focus on the central area where the audience is seated, so that direct sound and early reflections improve the speech intelligibility. The dotted line indicates sound propagation with reduced sound energy due to the part that has been absorbed by the acoustic panels.

The second scenario is a round-table group discussion where the conversations happen within a larger group of people, facing each other while seated in a circle. The distance for sound to cover is larger in comparison with the small groups of the second scenario. Together with direct sound, the early reflections are helpful for a comprehensible conversation. The acoustic panels are positioned in a parabolic shape, causing the majority of the reflected sound to be directed towards the opposite side of the group. In the center, the panels are placed close to the ceiling to minimize the depth of the air cavity and increase the amount of reflection in that particular area. This is based on the principle that the particle velocity is low close to the room boundaries, reducing the amount of sound absorption and consequently cause an increased amount of reflection. Closer to the sides, the parabolic shape creates a larger distance between the panel and the ceiling, which increases the amount of absorption and consequently reduces the reverberation time in order to improve the speech intelligibility in the room.

When the scenario involves working in small groups, it is desired that the sound levels of other groups should be kept low in order to reduce unwanted noise and to improve

the comprehension of the group conversation. In the ideal situation, the sound produced by a group should be partly absorbed and reflected back to the source instead of towards other groups. Due to the concave shape of the panels above each group, sound reflections will be redirected back while the convex part distributes the reflections in a diffuse pattern, reducing distinct echoes and reflections. The varying distance between the panels and the ceiling allows for an averaged sound absorption of multiple sound frequencies.

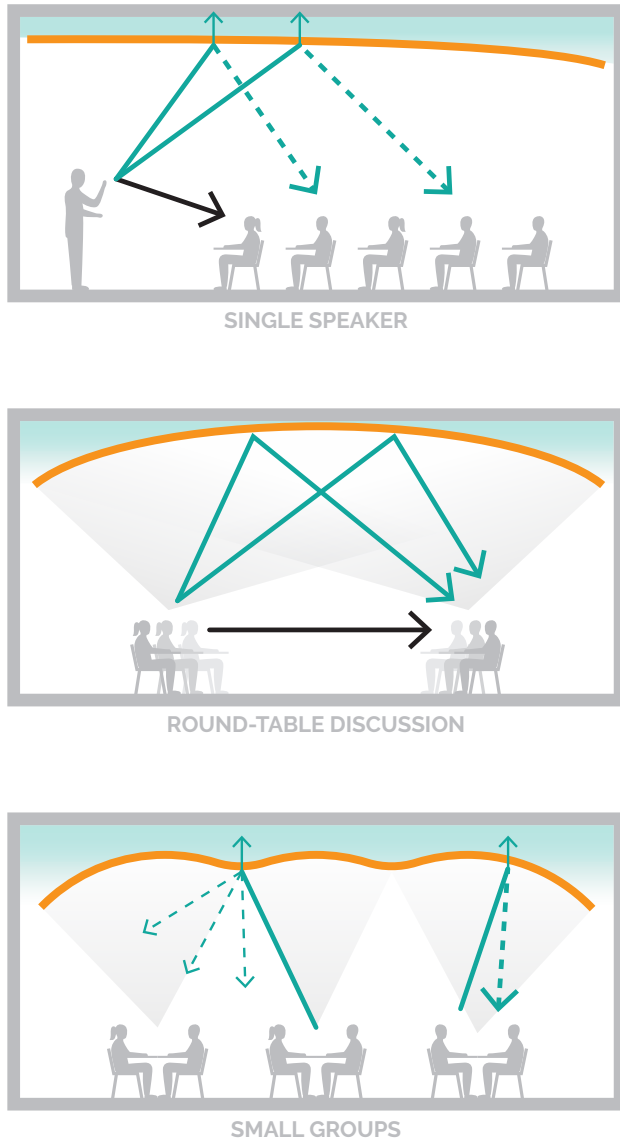


Figure 61. Three different scenarios: Classroom with a single speaker (a), classroom with round-table discussion (b) and classroom with small groups (c).

3.4. MEASUREMENTS

3.4.1. INTRODUCTION

With the given acoustic parameters of pattern design, open/closed surface ratio, the distance of the air cavity and the surface curvature, various patterns have been created for acoustic measurements. Measurements are important to verify theoretical assumptions and to define the acoustic performance of the concept model. Two types of measurements are chosen to be done during this research: Impedance Tube and Impulse Response. A more detailed description for each type is given at the related paragraphs.

The first type of measurement is primarily done to determine the effect of each parameter on the acoustic performance. It only requires small scale models which makes it suitable for analyzing multiple configurations. The output of measurements with the Impedance Tube are the coefficients of absorption and reflection.

An Impulse Response measurement requires a larger acoustic sample to determine its acoustic performance in a certain space, which is usually measured in a reverberation room. By measuring the reverberation time with different configurations, the absorption coefficient of the acoustic panel can be calculated.

The next step is to compare the results of both measurements and define the acoustic performance of the concept model.

3.4.2. IMPEDANCE TUBE

With an impedance tube, we can measure the absorption coefficient and reflection coefficient of small samples of acoustic absorbing materials. The two-microphone Impedance Measurement Tube Type 4206 is used (Figure 62), which covers the frequency range from 50 Hz to 6400 Hz. This range should be measured with two different settings (Figure 63). The large tube setting with an interior diameter of 100 mm, covers 50 Hz to 1600 Hz, the small tube setting with an interior diameter of 29 mm is for measurements between 500 Hz and 6400 Hz. The size of the measurement steps are respectively 2 and 8 Hz for the large and small sample. With an impedance tube, the measured values for sound absorption and sound reflection are only for normal incidence. This technique is not suitable for measuring samples with oblique incidence but the advantage is that it only requires small samples of the absorbing material.

A speaker produces a stationary random signal which travels down the tube and reflects from the test sample. The two microphones placed on the side of the tube, close to the sample, measure the pressure difference between the incident and reflected waves. If the sample absorbs a part of the incident sound energy, the amplitudes of the reflected waves will be different, causing a difference in pressure. The ratio between the pressure



Figure 62. Setup for Impedance Tube measurement.

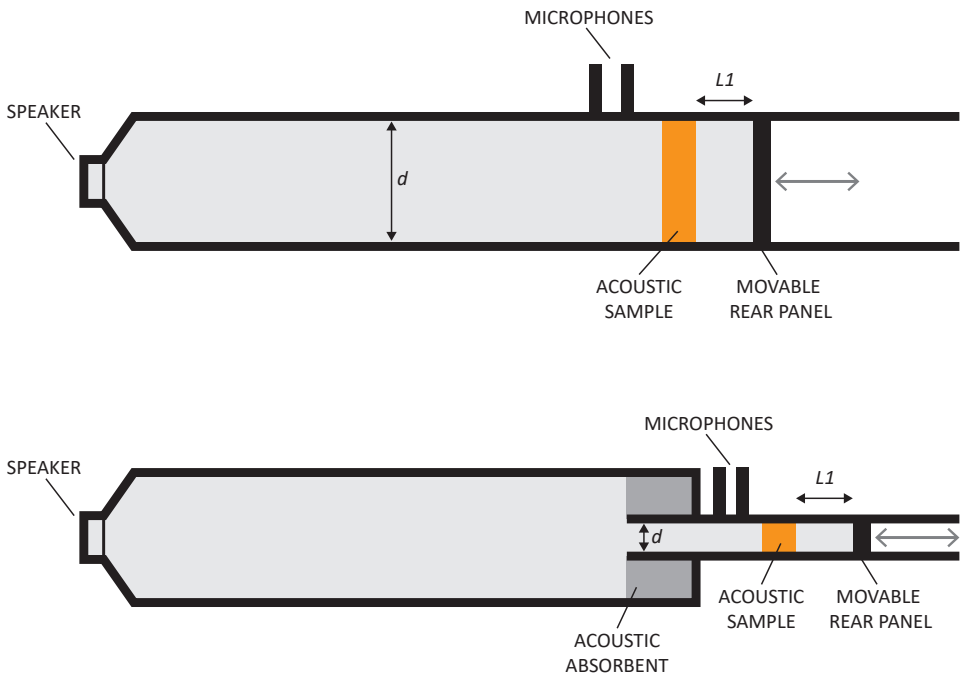


Figure 63. Setup of Impedance Tube. Top: Large tube setting for measurements from 50 to 1600 Hz. Bottom: Small tube setting for measurements from 500 to 6400 Hz.

produced by the speaker and the pressure received at the microphones determines the absorption and reflection coefficient of the sample. Due to the rigid backing and the entirely closed tube, the amount of sound transmission is neglected as it is practically zero. Thus the sum of the coefficients for absorption and reflection is assumed to be 1.

$$a + r = 1$$

Equipment

In order to do these measurements, the following equipment is required. The model names indicate the exact equipment that was used for these particular measurements. The technical details of this project setup can be found in Appendix A.1 and A.2.

- Impedance Measurement Tube (Type 4206)
- Function/Waveform Generator
- Audio amplifier
- Frequency Analyzer
- Microphones
- Calibrator
- Calibrator samples
- Laptop with software LabShop
- Acoustic samples

Depending on the frequency range that needs to be measured, either the large tube with an interior diameter of 100 mm or the small tube with an interior diameter of 29 mm should be used.

Acoustic samples

The measured acoustic samples all have the same setup: A wooden surface, a layer of foam and a variable depth of the air cavity behind the sample. The front surface is a circular piece of 4 mm MDF with a certain pattern applied by means of laser cutting. It covers the sound absorbing layer of polyether foam, which is placed directly behind it. The layer has a thickness of 2 cm and a specific weight of 25 kg/m³. The movable rear panel can be moved up to 20 cm, creating an air cavity behind the sample.

The variety of patterns that are used during the measurements are shown in Figure 64. The diameter of the samples is a few millimeters larger than the interior diameter of the tube. This way, the samples can be placed directly at the end of the tube and clamped down by the cap to maintain a stationary position during the measurements. One of the samples has an oval shape without a border, which has been bent and tightened (Figure 65) to fit perfectly into the tube. The intention of the curved sample is to relate the results of normal incidence to oblique incidence on a curved surface area.

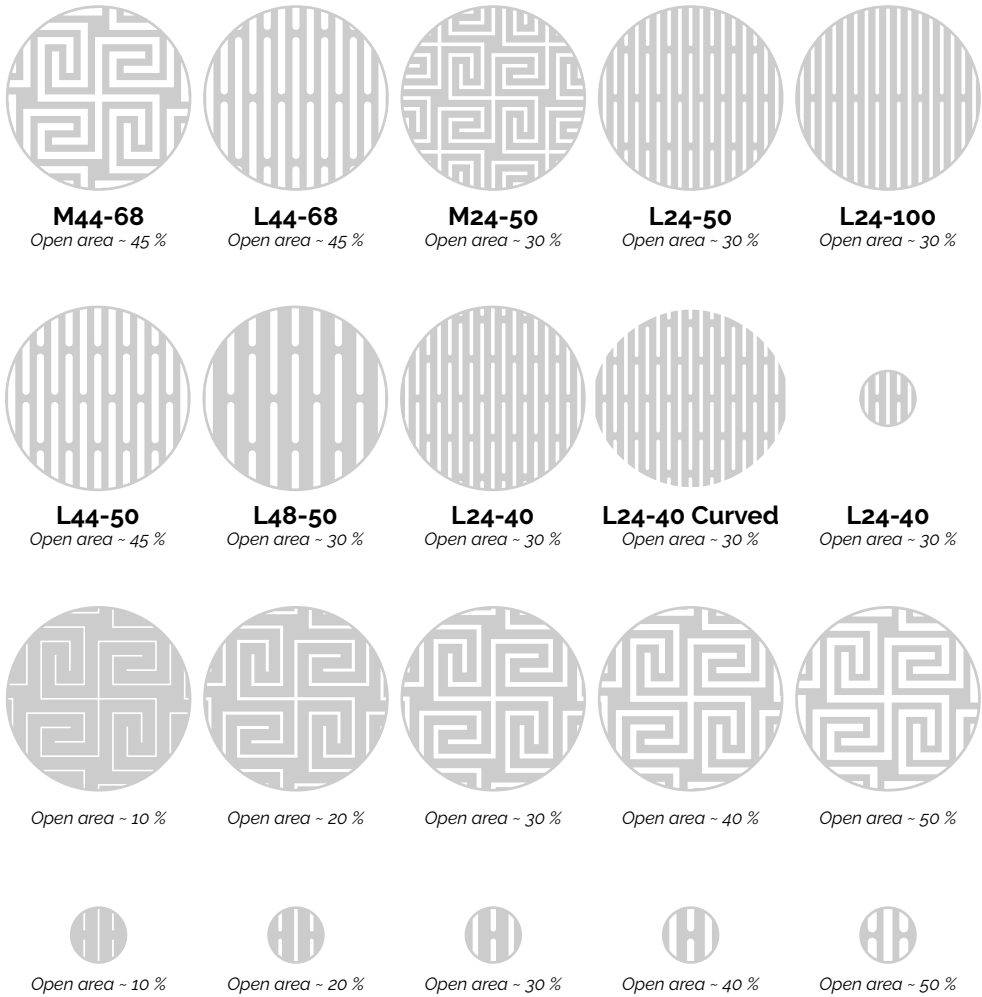


Figure 64. Acoustic samples with different pattern parameters.



Figure 65. Sample with surface curvature (L24-40 Curved).

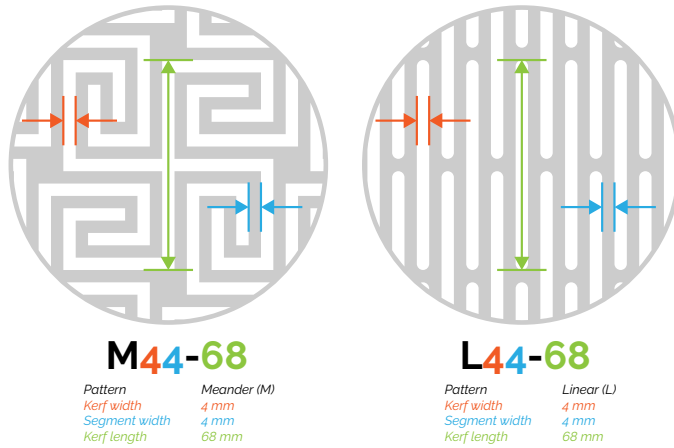


Figure 66. The given codename for each sample is composed of the dimensions of the kerfs and segments.

The codename of each sample is composed of the different pattern parameters. The first letter indicates the type of pattern, which is in this case a linear (L) or meander (M) pattern. The numbers relate to the dimensions of the kerfs and the segments (Figure 66). The kerf length is based on the centerline of the pattern. The wavelength of soundwaves at a frequency of 6400 Hz is still over 5 cm, which means that the thickness of the surface is too small to have significant impact on interference with incident soundwaves and is therefore not taken into account during the measurements.

Although the majority of the samples has a linear pattern, the first measurements have shown that the results are interchangeable with meander patterns with the same open surface area. The linear patterns were used for practical reasons. The possible effect of kerf width and length could be measured separately, which was not possible with a meander pattern. Secondly, a meander pattern on a small sample was not recognizable as such, which led to the use of a linear pattern. It was in this case also more suitable to create a curved sample from a linear pattern at this sample scale level.

Methodology

Before the impedance tube can be used to do the measurements, the microphones have to be calibrated in order to give more accurate results. Once the calibration is completed, the sample has to be placed in the impedance tube with a cap clamped down tight to close the tube. The moveable rear panel can then be placed in the desired position to get the right thickness of the layer of air.

This measurement will be performed with a series of acoustic samples, with various pattern parameters. All samples will be measured four times, each time with a different depth of the air cavity. It is important to record the type of setup for every individual measurement, so that all data will be manageable afterwards. A single measurement

will take up to 30 seconds, before showing the results on the screen. Once all measurements are completed, all data can be exported as an excel file for further processing.

Results

In this chapter, only the relevant results and comparisons are mentioned. The results of individual samples are included in Appendix A.3.

The measurements give more insight into the influence of several factors on the absorption coefficient. The factors that are included are: type of pattern, kerf width, kerf length and open surface area.

The following comparisons have been made:

- Linear pattern versus meander pattern
- Variable kerf width and variable open surface area
- Variable kerf width and equal open surface area
- Flat sample versus curved sample
- Large sample versus small sample
- Various open surface areas
- Average absorption coefficient

There are several remarks to be mentioned that apply to the graphs and results of all measurements:

- All measurements have been performed with the same sound absorption material placed directly behind the wooden surface, 2 cm polyether foam.
- Not all graphs are shown in the same scale. See the note at each graph whether a logarithmic or linear scale has been applied. The used scale has been chosen merely to visualize the most important aspects of the specific graph.
- The measured absorption coefficients up to approximately 100 Hz are not reliable because of the long wavelengths in the lower frequencies. These values are therefore excluded from further elaboration on the results.

Possible causes for errors in the results of this measurement:

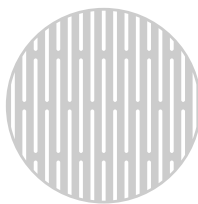
- Inaccurate placement of the movable rear panel may affect the measured values.
- Unwanted noise from outside the tube can cause interference.

Linear versus Meander - L24-50 vs M24-50

The first comparison is done between a linear and meander pattern with similar pattern parameters: a kerf width of 2 mm, a segment width of 4 mm, a kerf length of 50 mm and an open surface area of approximately 30%. The main difference is the orientation of the individual kerfs which are respectively in a linear and meander pattern.

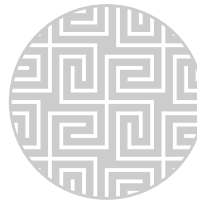
The results show that this orientation is hardly affecting the amount of absorption, as there is no significant difference between the measured absorption coefficients. What does have significant impact is the thickness of the air cavity behind the sample. A larger air cavity increases the sound absorption for the lower frequencies and comes with multiple crests that are closer together. The crests for the different measured air cavities have a similar value of absorption, but at different frequencies.

At 270 Hz, there is a small trough visible that occurs at all of the graphs. This frequency relates to a wavelength of approximately 127 cm, which is roughly twice the length of the Impedance Tube. This trough is probably the effect of a standing wave between the surface of the sample and the speaker at the end of the tube.



L24-50

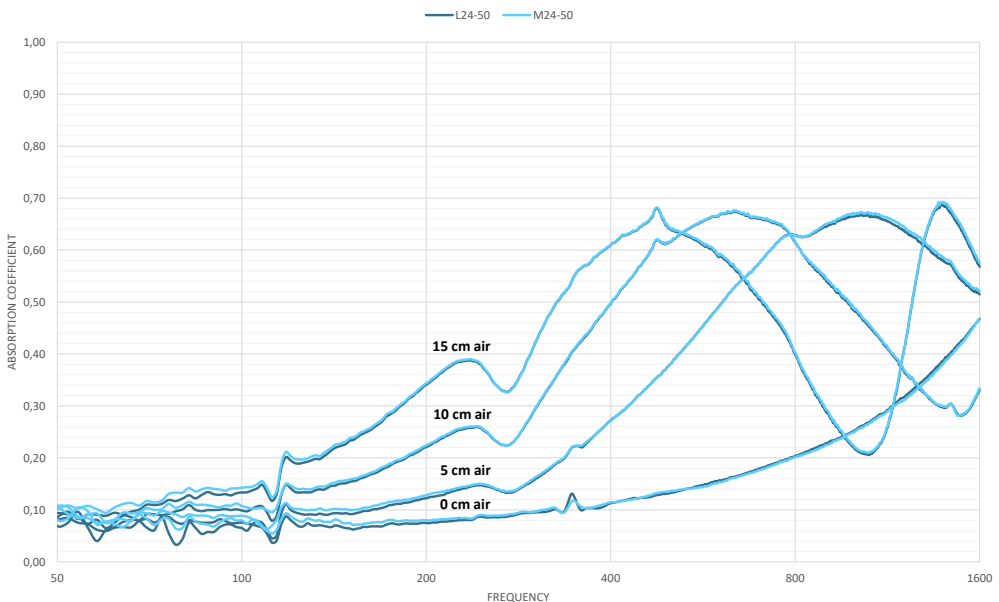
Kerf width 2 mm
Segment width 4 mm
Kerf length 50 mm
Open area 30 %



M24-50

Kerf width 2 mm
Segment width 4 mm
Kerf length 50 mm
Open area 30 %

ABSORPTION COEFFICIENT: L24-50 (31,1%) & M24-50 (30,5%)

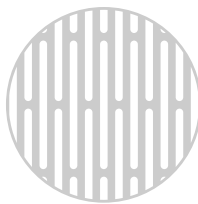


Graph 3. Absorption coefficient for L24-50 and M24-50. (Note: graph is in logarithmic scale)

Linear versus Meander - L44-68 vs M44-68

The second comparison is again between a linear and meander pattern, but with a difference in the pattern parameters. Both patterns have similar pattern parameters: a kerf width of 4 mm, a segment width of 4 mm, a kerf length of 68 mm and an open surface area of approximately 45%. The main difference between these samples and the previous ones is the doubling of the kerf width. The number 68 might seem like a random number, but it is directly related to the width of the kerfs and segments of the meander pattern. The width of the segments has not been changed and remains 4 mm, but by increasing the kerf width from 2 to 4 mm, the length of the kerfs automatically increases to a value which is in this case 68 mm.

The crests and troughs occur at the same spots and there is hardly any difference between the absorption coefficients of the two patterns. This confirms the outcome of the former comparison that the pattern and orientation of the kerfs has no significant influence on the sound absorbing qualities. The drop at 270 Hz is also visible in this graph, which indicates the standing wave between the surface of the sample and the speaker at the end of the tube.



Kerf width 4 mm
Segment width 4 mm
Kerf length 68 mm
Open area 45 %

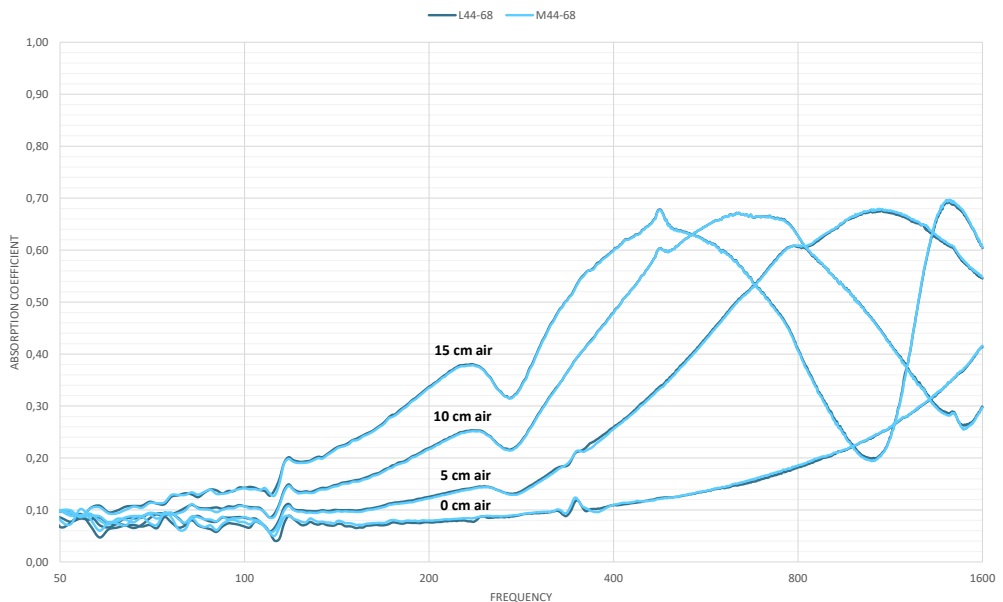
L44-68



Kerf width 4 mm
Segment width 4 mm
Kerf length 68 mm
Open area 45 %

M44-68

ABSORPTION COEFFICIENT: L44-68 (46,5%) & M44-68 (46,6%)

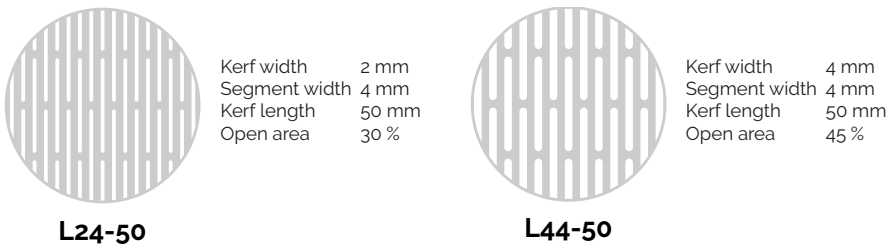


Graph 4. Absorption coefficient for L44-68 and M44-68. (Note: graph is in logarithmic scale)

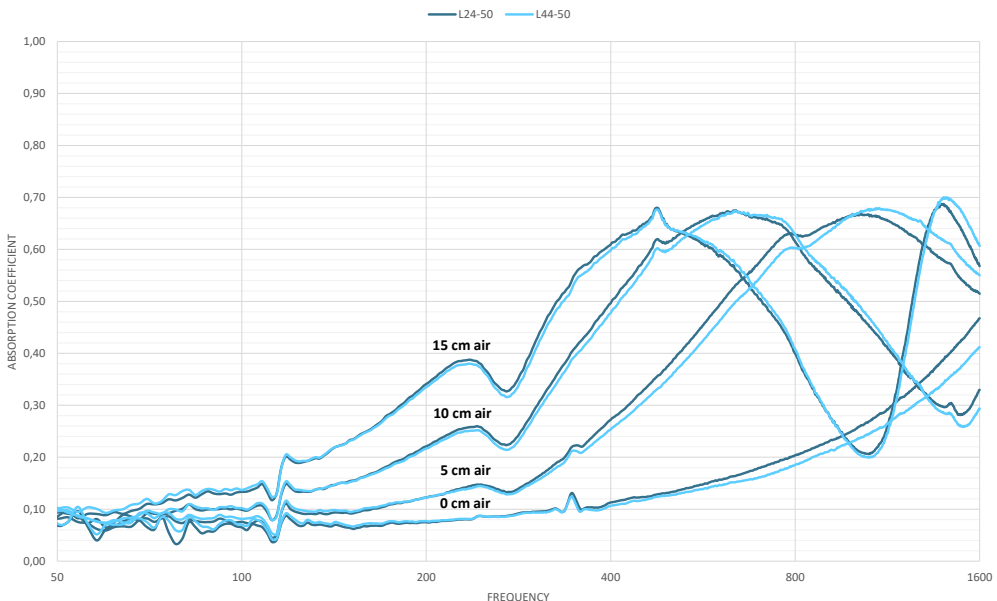
Variable kerf width – L24-50 versus L44-50

This comparison is to examine how the width of the kerfs affects the sound absorbing qualities. With the L44-50 the kerf width of the pattern has been doubled relative to the L24-50. The dimensions of the segments remain unchanged, which gives the second pattern an open surface area of approximately 45% compared to 30% of the first pattern.

In the lower frequencies, the absorption coefficient seems rather similar. Closer to 1600 Hz, the amplitude of the crests and troughs of the L44-50 is a marginally larger and slightly shifted. The difference is however still small, which makes it hard to say that the kerf width has a significant effect on the absorption within this frequency range. The slight shift of the graphs is more likely to be affected by the difference in open surface area, which is not equal for both samples.



ABSORPTION COEFFICIENT: L24-50 (31,1%) & L44-50 (46,5%)

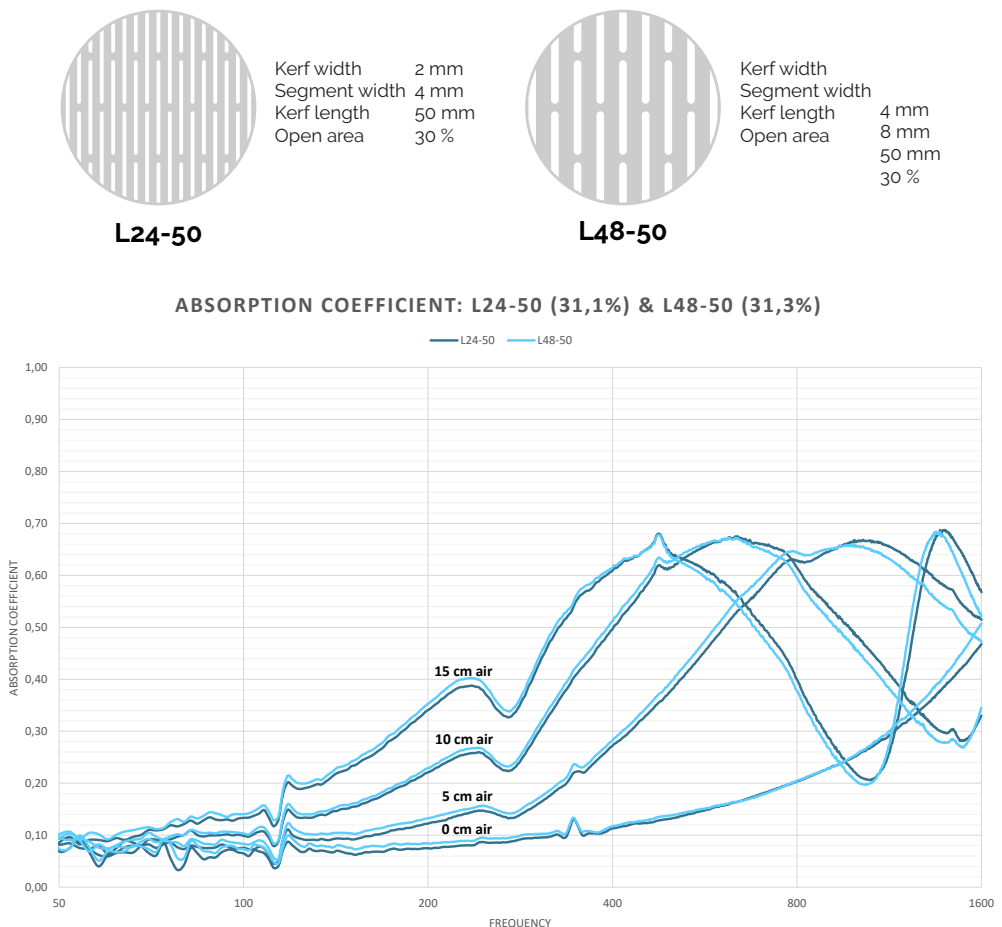


Graph 5. Absorption coefficient for L24-50 and L44-50. (Note: graph is in logarithmic scale)

Variable kerf width, same open surface area - L24-50 versus L48-50

The comparison between the L24-50 and L48-50 is to discover the influence of doubling the kerf width, and maintaining the same open surface area. This has been done by doubling both the width of the kerfs and the segments. This results in an open surface area of approximately 30%.

The absorption coefficients of both samples are similar, but the graph of the L48-50 seems to be slightly shifted towards the left. The differences are however small, which means that just an increase of the kerf width and equal open surface area, have no significant effect on the sound absorption up to the measured 1600 Hz. The difference may however be larger with higher frequencies.

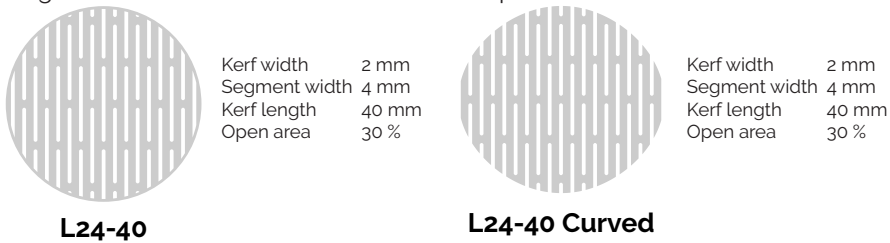


Graph 6. Absorption coefficient for L24-50 and L48-50. (Note: graph is in logarithmic scale)

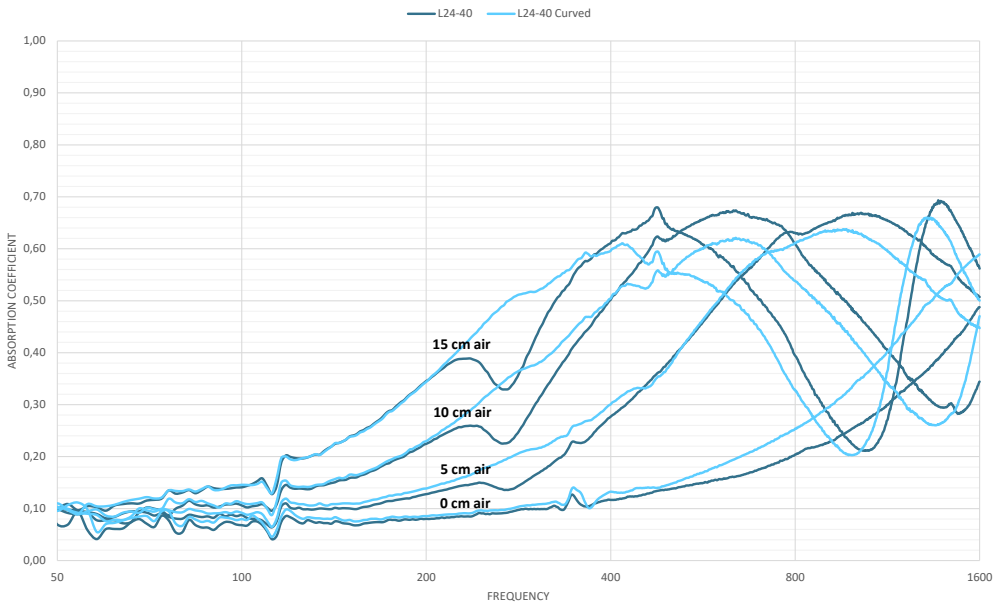
Flat versus curved sample – L24-40 versus L24-40 Curved

Measurements done with the Impedance Tube are meant for samples that have a flat surface. The results of these measurements are only based on normal incidence. To find out how a surface curvature affects the absorption coefficient, a specific sample has been constructed which has been bent and tightened to fit exactly into the tube. The sample with a surface curvature is a better representation of the final flexible acoustic panel which has a surface curvature as well. It would therefore give more accurate results that match with a real situation, where incident soundwaves are also by random incidence. The kerf length of 40 has been chosen to obtain the possible curvature of the sample. A flat sample with the same pattern parameters has been measured as a comparison. The absorption coefficients are expected to be smaller for the curved sample because the orientation of the openings is different and not facing directly towards the sound source.

In the measured frequency range, the crests are indeed smaller for the curved sample, but the maximum sound absorption is still relatively high. Another difference is the absence of the troughs around 270 Hz. This confirms the theory of the standing wave between the flat surface of the sample and the speaker at the end of the tube, as a standing wave cannot occur with the curved sample due to its curved surface.



ABSORPTION COEFFICIENT: L24-40 (30,2%) & L24-40 CURVED (29,6%)



Graph 7. Absorption coefficient for L24-40 large and curved. (Note: graph is in logarithmic scale)

Small sample - L24-40

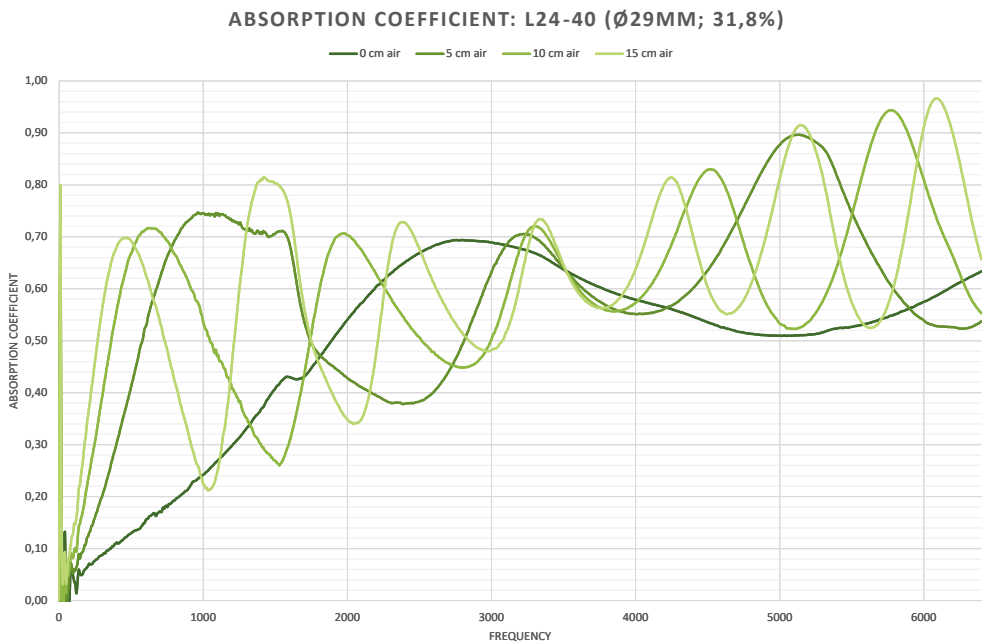
The setup for measuring small samples with a diameter of 29 mm is able to measure up to a frequency of 6400 Hz. It is expected that the absorption coefficient will be larger at higher frequencies because of the smaller wavelengths. As can be seen in the graph below, this is indeed the case. Higher absorption values are reached at the higher frequencies, but the graphs amplitude seems to increase as well causing a bigger difference between the highs and the lows.

Varying the depth of the air cavity changes the crest frequencies and the distance between them. Increasing the depth of the air cavity results in a reduced crest distance. This distance presumably matches twice the depth of the air cavity and thickness of the foam layer combined. In the case of the 15 cm air cavity, the crest distance is about 950 Hz, which corresponds to a wavelength of 36 cm. This does roughly match with twice the depth of the air cavity and thickness of the foam layer combined: $17 + 17 = 34$ cm. This same principle also applies to the other graphs. The difference between the two values might be caused by inaccurate placement of the moveable rear panel or deviations with the sample itself.

Another aspect that stands out from this graph, is that all graphs with any depth of air cavity go through the same point around 3500 Hz. The wavelength that belongs to this frequency is 9,8 cm, which is probably related to the depth of the measured air cavities, all with a multitude of 5 cm.



Kerf width	2 mm
Segment width	4 mm
Kerf length	38 mm
Open area	30 %

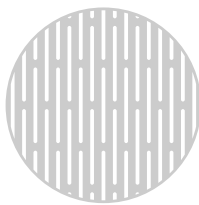


Graph 8. Absorption coefficient for L24-40 small. (Note: graph is in linear scale)

Small and large sample - L24-40 versus L24-40

These two samples have the same width of the kerfs. For the small sample, the distance between the kerfs has been adjusted so that the open surface area would be equal to the large one. The length of the kerfs in the small sample has been set on 40, which is longer than the diameter of the sample itself, meaning that this difference is also neglectable. In other words, the effect of both patterns would theoretically give the same results in terms of absorption coefficients. The measurements however gave some clear differences between the two.

The green colored graphs relate to the small sample, the blue colored graphs to the large sample. The graph of the large sample ends at 1600 Hz, because of the maximum frequency with measurements at this sample diameter. It is clearly visible that the graph of the small sample appear to be smoother than that of the large sample. The bumps in the blue crests are no longer present with the small sample and even so the troughs around 270 Hz. This would indicate that with the small setup, no standing wave occurs at this frequency. This is expected because the small sample is located at a different distance from the speaker than the large sample. Overall, the small sample appears to achieve better results since the crests of the small sample are slightly higher.



L24-40

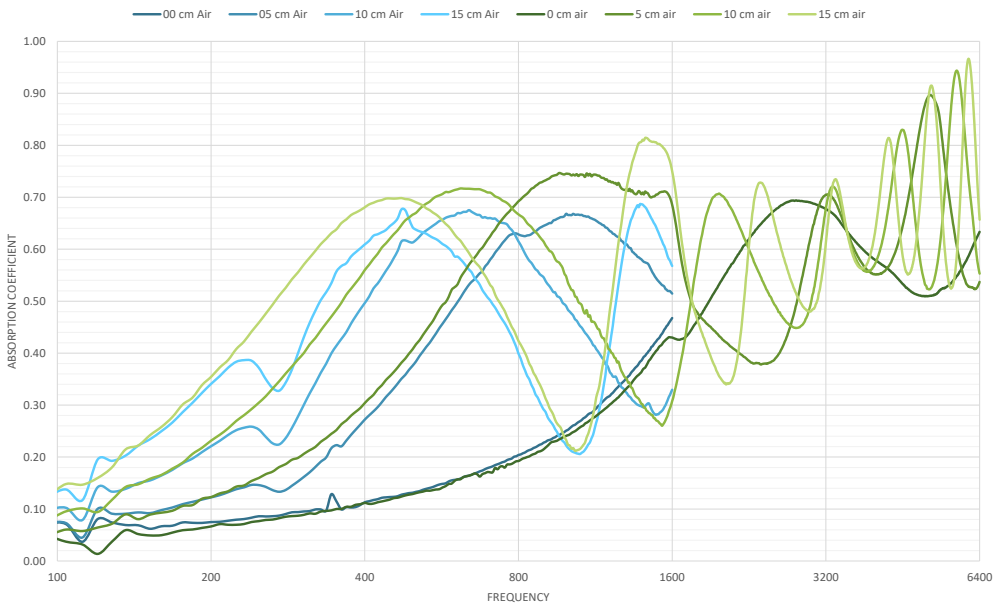
Kerf width 2 mm
Segment width 4 mm
Kerf length 38 mm
Open area 30 %



L24-40

Kerf width 2 mm
Segment width 4 mm
Kerf length 50 mm
Open area 30 %

ABSORPTION COEFFICIENT: L24-40 & L24-40 (~30%)



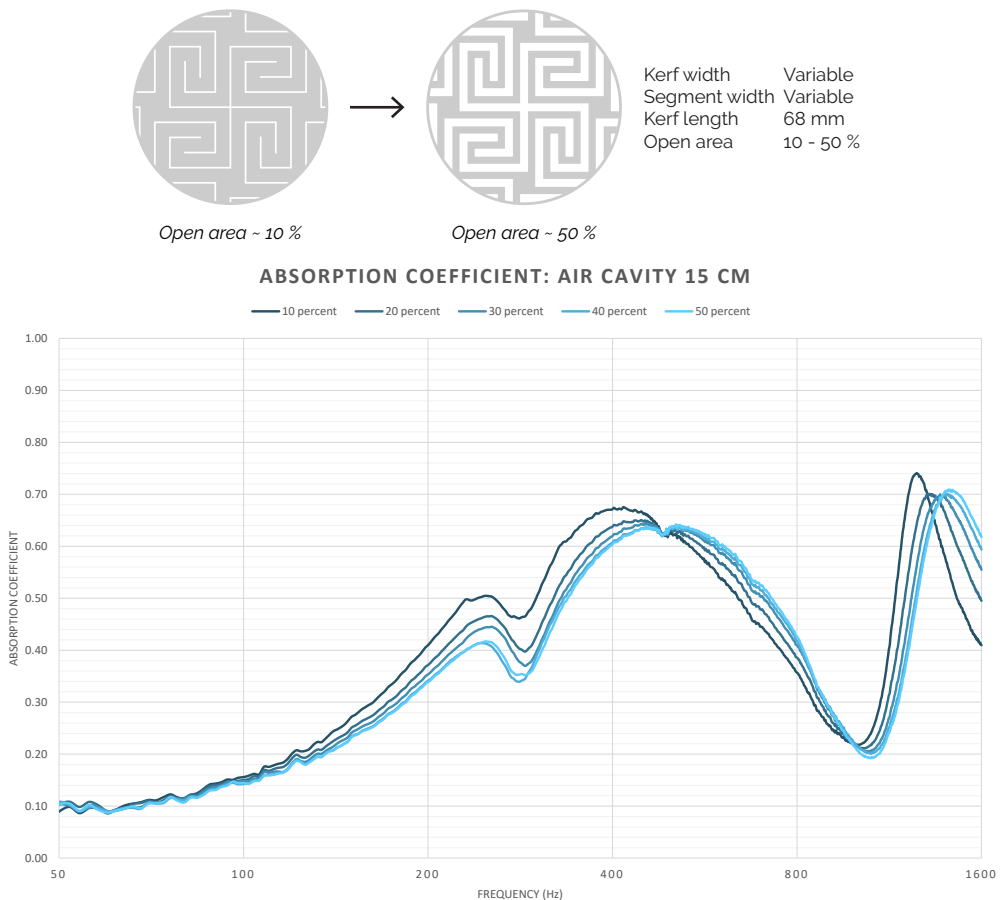
Graph 9. Absorption coefficient for L24-40 large and small. (Note: graph is in logarithmic scale)

Various open surface areas (Large samples)- 10 to 50%

The five samples that are used for this specific measurement are large scale samples with a meander pattern and an open surface area varying from 10 to 50%. The open surface area determines the variable width for the kerfs and the segments. The graph below shows the results measured at a constant air cavity with a depth of 15 cm. The results of the individual samples measured with different depths of air cavity, are located in the appendix.

The difference between the absorption coefficients does not seem to be significant. Especially the samples with a higher open surface area seem to be more alike. This corresponds with the theory that the amount of absorption is not affected by any open surface area above 20%.

It is remarkable that the crests of the 10% sample are slightly higher than the other samples and slightly shifted towards a lower frequency. Due to the small open surface area, the absorption was expected to be less.



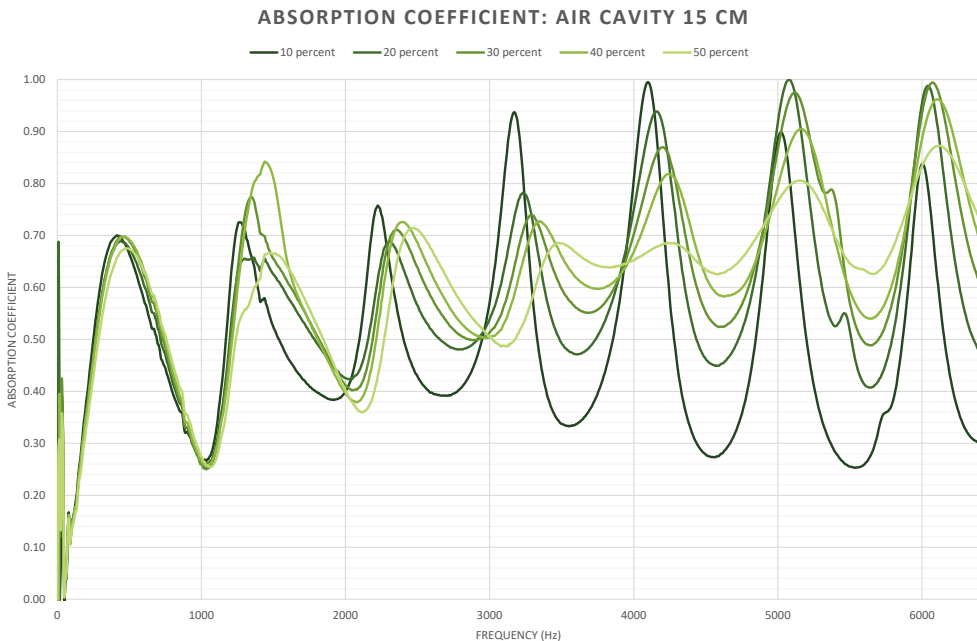
Graph 10. Absorption coefficient for various open surface areas. (Note: graph is in logarithmic scale)

Various open surface areas (Small samples)- 10 to 50%

The five samples that are used for this specific measurement are small scale samples with a meander pattern and an open surface area varying from 10 to 50%. The open surface area determines the variable width for the kerfs and the segments. The graph below shows the results measured at a constant air cavity with a depth of 15 cm.

At the lower frequencies, there is no significant difference in the amount of absorption between the various open surface areas. However, above a frequency of 1600 Hz, the differences appear to be even larger. The crests for each sample are slightly shifted, but are still roughly around the same frequency. The main difference between the samples is the amplitude, which is significantly higher for a smaller open surface area. The crests reach higher absorption coefficients, but the troughs reach even lower. The graphs of the larger open surface areas are smoother and have the highest minima. The cumulative average of all graphs seems to be similar.

Based on these results, the theory that the amount of absorption is not affected by any open surface area above 20% is not correct. For lower frequencies this seems to be true, but for higher frequencies above 1600 Hz the open surface area does matter for the value of the crests and troughs. In practice, the absorption coefficients would be close to the cumulative average due to a varying air cavity. Because this cumulative average is similar for all graphs, it means that a larger open surface area has no significant influence on the average absorption coefficient.



Graph 11. Absorption coefficient for various open surface areas. (Note: graph is in linear scale)

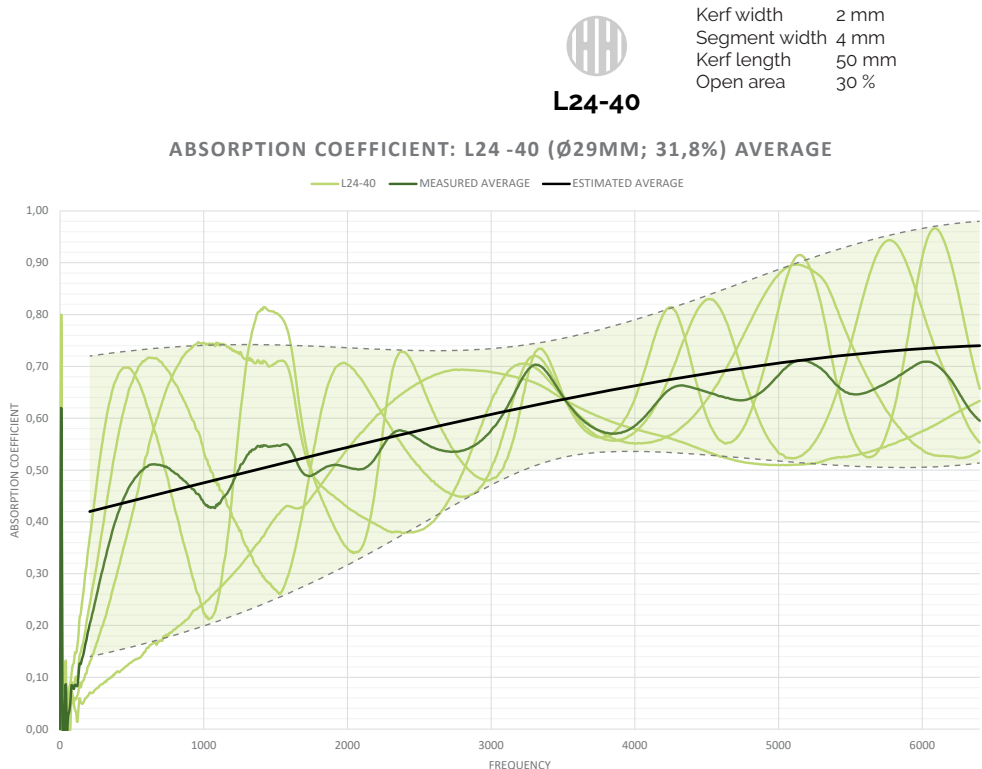
Average absorption coefficient

The small sample L24-40 with an open surface area of approximately 30% is used to define an estimated average, based on the measurements that have been done at various depths for the air cavity. It covers the full frequency range up to 6400 Hz and serves to be a representative estimation for a model with a similar open surface area.

With a constant open surface area, the amplitude of the graphs has a different value at each frequency, but seems to be constant at that specific frequency, not affected by the depth of the air cavity. The variation in the depth of the air cavity only affects the period, the distance between the crests.

Regardless the depth of the air cavity, all crests appear to be lying on the same line, which also applies for the troughs. These boundaries are drawn as dotted lines. The area in between contains all possible absorption coefficients for this sample for any depth of air cavity.

The measured average in dark green is the average of the four measurements with different air cavities. Based on these measurements, an estimated average has been made to include the expected graphs of various depths of air cavity. It crosses the green area directly through the center, being the cumulative average of these graphs. When this gets translated towards a full size physical model, the variable air cavity made by the surface curvature would result in an average absorption graph that lies close to the estimated average.



Graph 12. Average absorption coefficient for L24-40. (Note: graph is in linear scale)

3.4.3. IMPULSE RESPONSE

An Impulse Response (IR) measurement is used to find the reverberation time in a room or enclosed spaces. An omnidirectional speaker emits an exponential time-growing frequency sweep. A microphone receives the direct sound and reflections over time, resulting in a decay slope. Figure 67 shows the paths of direct sound from the source to the microphone, followed by a first order reflection in blue, a second order in green and higher order reflections in gray (Rational Acoustics, 2015).

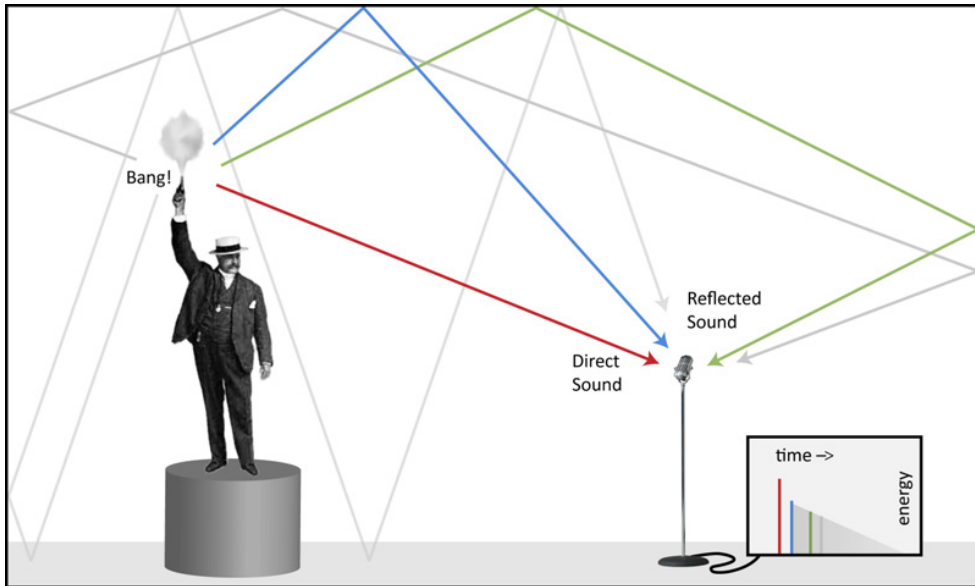


Figure 67. An acoustical Impulse Response (Rational Acoustics, 2015).

For this measurement an acoustic sample will be placed inside the room to measure the difference in reverberation time for the room with and without the sample. The size of the used prototype allows to obtain a surface curvature for the panel which creates presumably a diffuse reflection. It may also influence the absorbing qualities of the panel as incident sound waves reach the panel with random incidence. The goal of this measurement is to determine the absorbing qualities of the panel with random sound incidence. With this measurement, an answer will be given to the sub-question:

What effect has a curved surface of a panel on its acoustic performance?

Limitations in budget and time, leaves room for only one panel to be measured. The chosen pattern parameters are primarily based on the minimum diameter of the available milling bits for the used CNC milling machine. The diameter of the milling bit

determines the width of the kerfs being made in the panel, which is in this case 5 mm. To not overdo the ratio between the open and closed surface area and to maintain a certain stiffness, the material width is set at twice the width of the kerfs. The number of iterations remains 4, resulting in an open surface area of approximately 30% (Table 4).

The acoustic parameters included in the measurements are the reverberation time (T_R) and absorption coefficient (α).

The expected outcome of these measurements is that application of such a panel with adaptable surface curvature decreases the reverberation time in the room. Increasing the amount of absorption is namely one of the possible solutions to decrease the reverberation time. The measured reverberation time is not directly related to the properties of the acoustic panel. The panel is just one of the variables in the equation, with a certain surface area and absorption coefficient. This absorption coefficient is the variable to be determined during these measurements.

A major difference with the measurements done with the impedance tube is the angle of incidence. Where the impedance tube is only able to measure normal incidence, the setup in the reverberation room allows for random incidence including all reflections inside the room. The amount of absorption is presumably affected by the angle of incidence. With oblique incidence, a sound wave is more likely to reflect of the wooden surface than to pass through the openings into the absorbent material. In practice, sound waves usually have random incidence because of all the reflections and movable sound sources, like people. This means that these measurements should give more accurate results in terms of absorbing qualities.

Pattern parameters	
Unit size	150 mm
Number of iterations	4
Kerf width	5 mm
Material width	10 mm
Material Thickness	6 mm
Open surface area	30 %

Table 4. Pattern parameters for used acoustic sample.

Equipment

In order to do these measurements, the following equipment is required. The model names indicate the exact equipment that was used for these particular measurements.

- Laptop with software MatLaus

- Behringer UCA222 Interface
- Audio amplifier
- Omnidirectional speaker
- Microphone
- Microphone stand
- Suitable cables
- Acoustic sample(s)

The software on the laptop controls the electronic equipment (Figure 68). An audio amplifier amplifies the signal coming from the computer and sends it to the omnidirectional speaker, which in turn produces the soundwaves of given frequencies in all directions. The emitted sound is then received by the microphone.

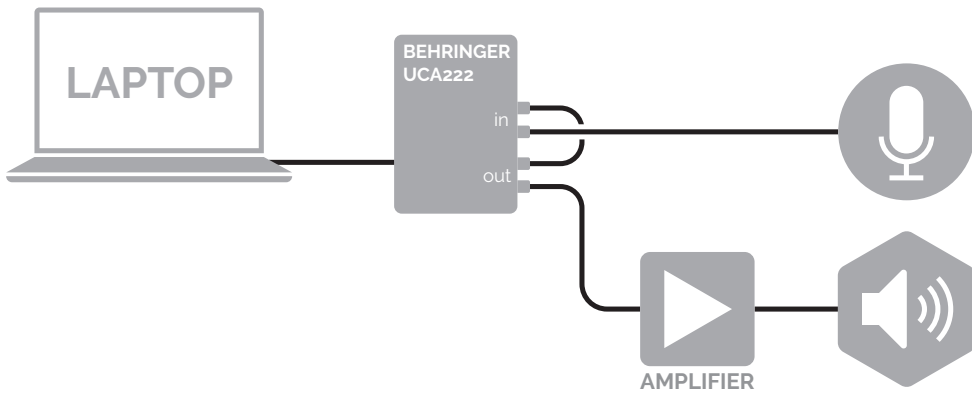


Figure 68. Setup of the equipment for the Impulse Response measurement.

Methodology

The results of the measurements with the impedance tube show that the layer of air behind the panel is an important factor. The distance between the panel and the back wall affects the absorption coefficient for each frequency. The thickness of this layer of air is directly related to the affected wavelengths and thus the frequencies. A varying surface curvature generates a changeable thickness for this layer and will influence the amount of absorption for each frequency.

The used prototype has been positioned with different orientations and varying surface curvatures. For practical reasons, the prototype has been placed in a vertical position against the wall, instead of being hung on the ceiling. This should have little effect on the outcome of the measurement, as the surface area of the sample does not change. However, there is another aspect that does might affect the results. A free standing panel placed at a certain distance from the wall allows soundwaves reflected on the

will be absorbed from the backside of the panel. On the other side, incoming sound waves at the front of the panel may be partly transmitted and reflected at the wall behind, back into the room. To examine this theory, two frames have been constructed: an open frame with open sides and an enclosed box which sides are closed to create a small enclosure behind the panel (Figure 69).

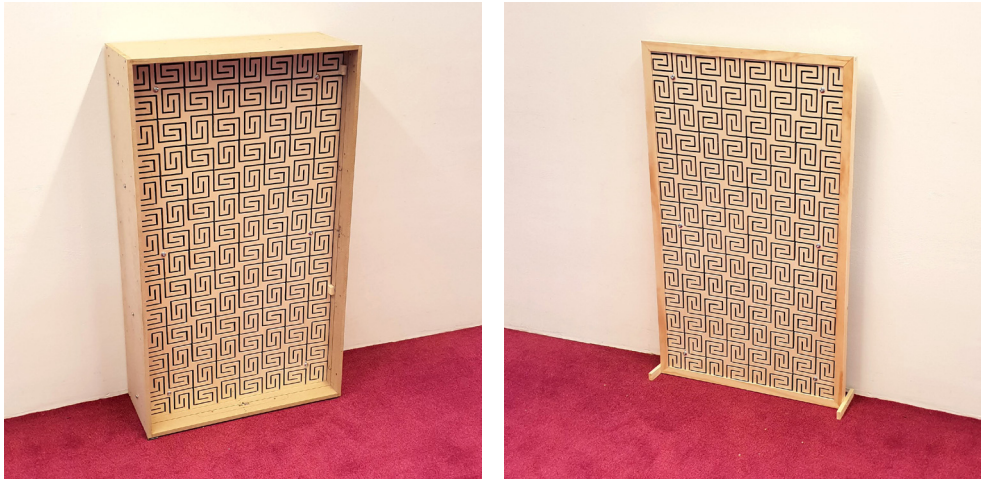


Figure 69. Two different frames have been used for the Impulse Response measurement. An enclosed box (left) and an open frame (right).

It is important to measure the room also without the acoustic panel, to determine the properties of the room itself. The room that has been chosen for the measurement is a small bathroom of just below 3 m². It is located at 01+West.110 at the faculty of Architecture from the University of Technology Delft. This room has been chosen because it was the most suitable location that was available for this type of measurement. To minimize the absorption of elements inside the room, the panels of the suspended ceiling have been removed if possible, to reveal the concrete floor above (see Figure 70). Due to fixed elements such as light sources and ventilation exhausts, not all the panels could be removed. A specific reverberation room located somewhere else on the university campus has not been used due to its larger size in comparison with the size of the sample.

For this small room, two different setups have been measured with interchanged positions of the omnidirectional speaker and the microphone. Figure 71 shows the floorplan with the two different setups of the equipment.



Figure 70. The room that is used to perform the measurement (left) and the removed panels of the suspended ceiling (right).

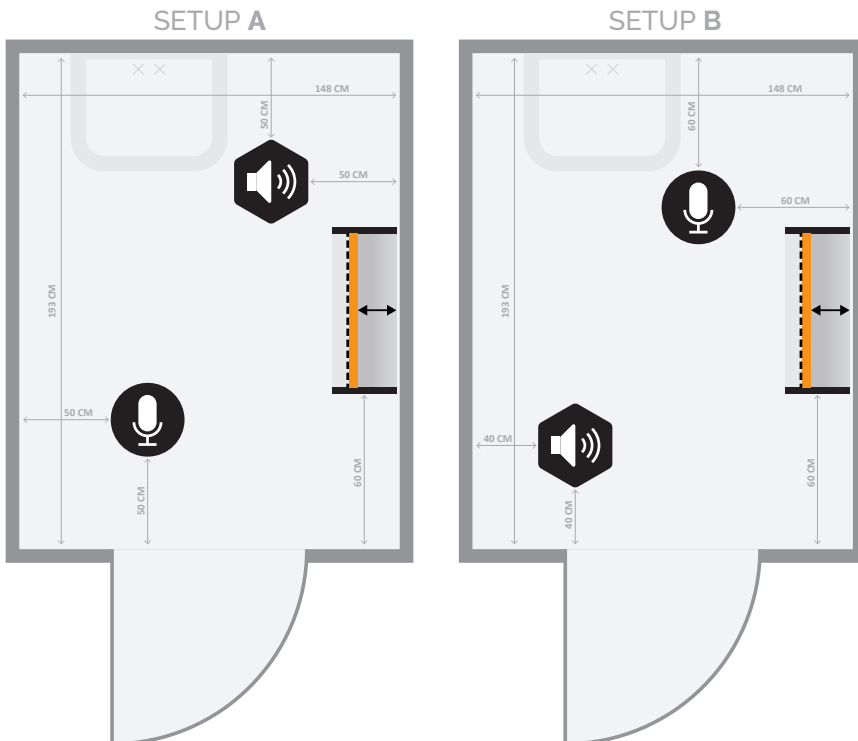


Figure 71. Floorplan of the measurement room with the two different setups.

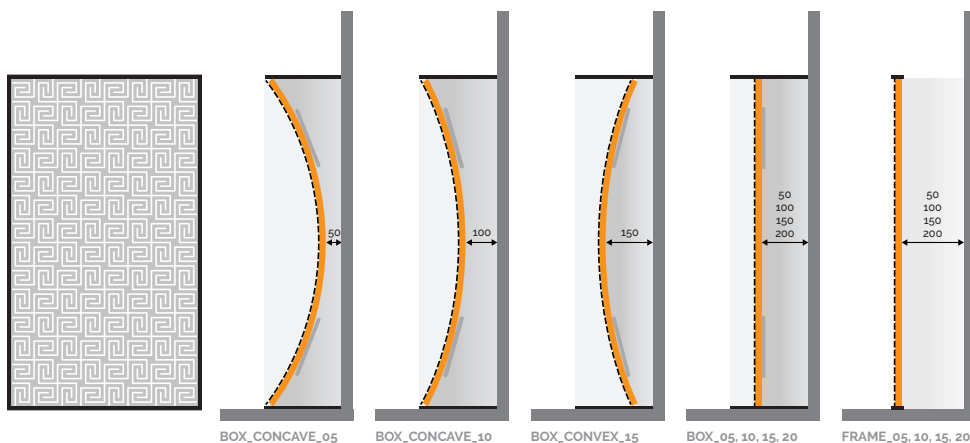


Figure 72. Panel positions, three with a surface curvature, four inside the box and the frame at different air cavity depths.

Figure 72 shows the different positions of the acoustic panel with the given names to identify each position. The sample has been placed inside the frame in a flat and vertical position with at a distance of 50, 100, 150 and 200 mm from the back wall. The same four positions have also been carried out for panel inside the box. The box also held three different positions with both convex and concave surface curvatures.

Results

In order to obtain optimal results, it is useful to remove all elements but the speaker, microphone and the acoustic sample from the room. That includes the removal of the laptop and the person doing the measurements as well. If the process of measuring can be done remotely, there will be no interference of the other equipment or the person in the results of the measurements. The door of the room should obviously be closed during the measurement.

With the impulse response measurement, the reverberation time is the main quantity, which is used to calculate the absorption coefficient. The measurements give more insight into the influence of several factors on the absorption coefficient. The included factors are: depth of the air cavity, surface curvature and open/closed sides. In this chapter, only the relevant results and comparisons are mentioned. Additional graphs can be found in the appendix.

There are several remarks to be mentioned that apply to the graphs and results of all measurements:

- All measurements have been performed with the same sound absorption material placed directly behind the wooden surface, 2 cm polyether foam.
- The data for the reverberation time is measured in octave bands. Their graphs and the resulting absorption coefficients are therefore

visualized as bar charts, related to the different octave bands.

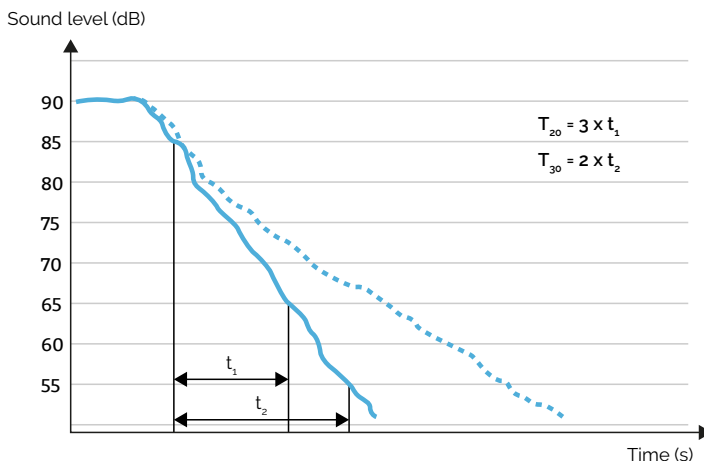
- The results of the 125 Hz octave band are not reliable, because this octave band contains long wavelengths that do not even fit inside the room. The 250 Hz and 500 Hz octave bands are also less reliable because of the same principle.

Possible causes for errors in the results of this measurement:

- The height of the panel placed in a curved position is less than when it is placed in a straight position. This leaves an opening between the top of the panel and the upper edge of the box. Soundwaves are able to move freely through this opening, causing interference with other soundwaves and giving less accurate results.
- A small cavity could appear between the curved wooden surface and the layer of foam behind it. Due to the protruding segments as a result of a surface curvature, this is likely to happen at these specific areas.
- Unwanted sounds from outside the room may interfere with the measurement, as the microphone could detect these signals.

To determine the reverberation time, different parts of the reverberation curve can be used (Graph 13). At T_{20} an interval of 20 dB is used, for T_{30} the interval is 30 dB. When the curve of the decay is straight, the values for all intervals will be the same. However, in reality the curve is rarely straight (dashed line), which means that the results for each interval will be different.

The reverberation time has been measured at different intervals, but for this measurement an interval of 20 dB is used (T_{20}), starting after the sound level has already



Graph 13. The reverberation time can be determined by using different intervals.

decreased by 5 dB. The data at T_{30} and T_{40} show similar development in the resulting graphs. A shorter interval of just 6 dB is expected to be less representative, because it covers a small part of the curve and has to be multiplied by 10 to acquire the resulting reverberation time.

The blue graphs relate to the acoustic panel in straight position inside the box, green for the panel inside the box with a surface curvature and yellow for the panel in straight position placed inside the frame. The red line indicates the base value for the room without the acoustic sample.

Reverberation Time – Setup A and B

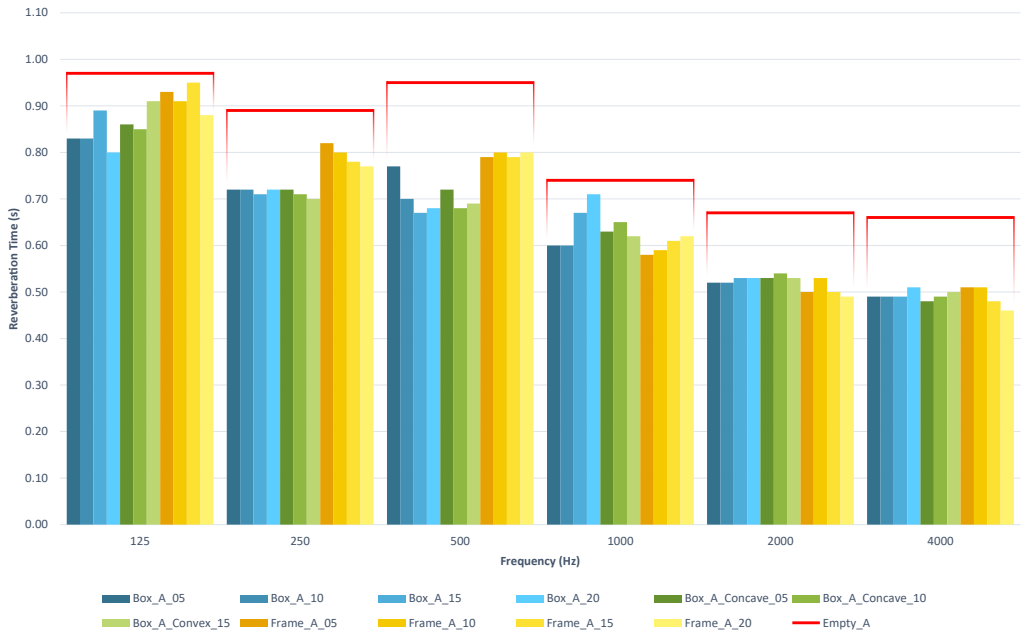
The reverberation time of the empty room is for all measured frequencies at T20 higher than the ones with placement of the acoustic panel. Interesting enough, the reverberation time of the empty room at a frequency of 125 Hz at T30 and T40 is below most of the measured values with the acoustic panel. In theory this could not be possible, as the addition of absorption should lower the reverberation time.

The reverberation time for the empty room is showed as a red line. The bars that indicate the measured values with addition of the acoustic sample lie below this line. This makes sense because addition of absorption should lower the reverberation time. They all show a downward trend at higher frequencies, with no significant differences between the different compositions of the sample, except for the octave bands of 250 and 500 Hz. Here the sample inside the frame seems to be less effective in terms of reverberance reduction, when compared to the box. At higher frequencies, both values are similar and no clear distinction can be made between the two.

The straight and curved surface compositions of the panel inside the box appear to behave in a similar way and do not have significant effects on the reduction of the reverberation time. This also applies for the four compositions of sample inside the frame, of which the results are also alike.

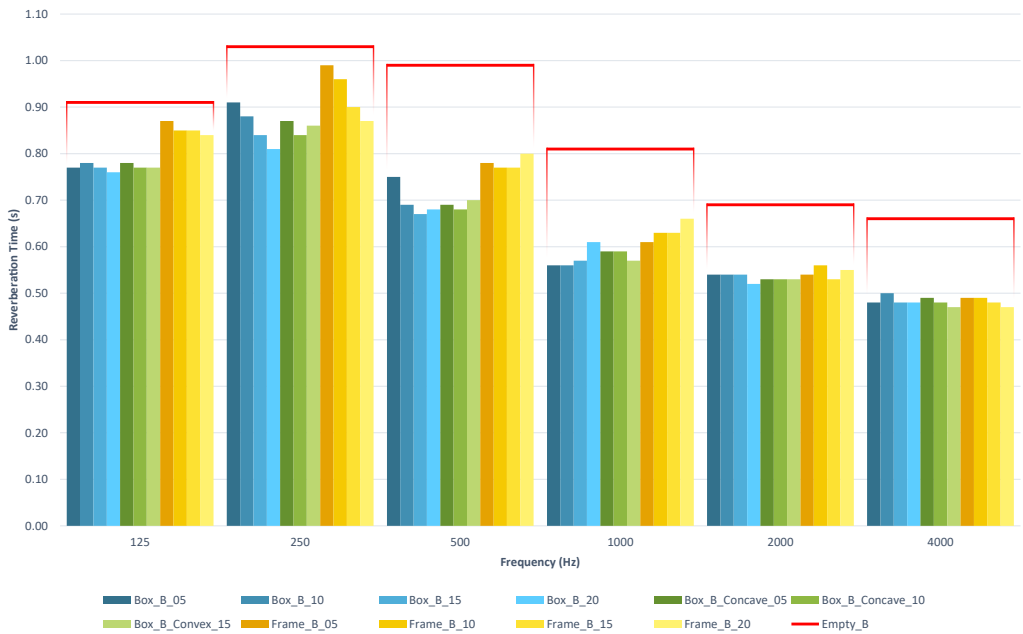
A comparison between the results of setup A and B gives an exceptional insight in one specific part of the graph. Both show the downward trend, but the main difference is visible at the 250 Hz octave band. With setup B there is an increased reverberation time in relation to the adjacent octave bands. This specific octave band contains wavelengths that are equal to the dimensions of the room, causing a standing wave between two opposite walls. Depending on the microphone position and the location of the nodes and antinodes of the standing wave, different reverberation values can be measured.

Reverberation Time - Setup A T_{20}



Graph 14. Reverberation Time for setup A at T_{20}

Reverberation Time - Setup B T_{20}



Graph 15. Reverberation Time for setup B at T_{20}

Absorption Coefficient – Setup A and B

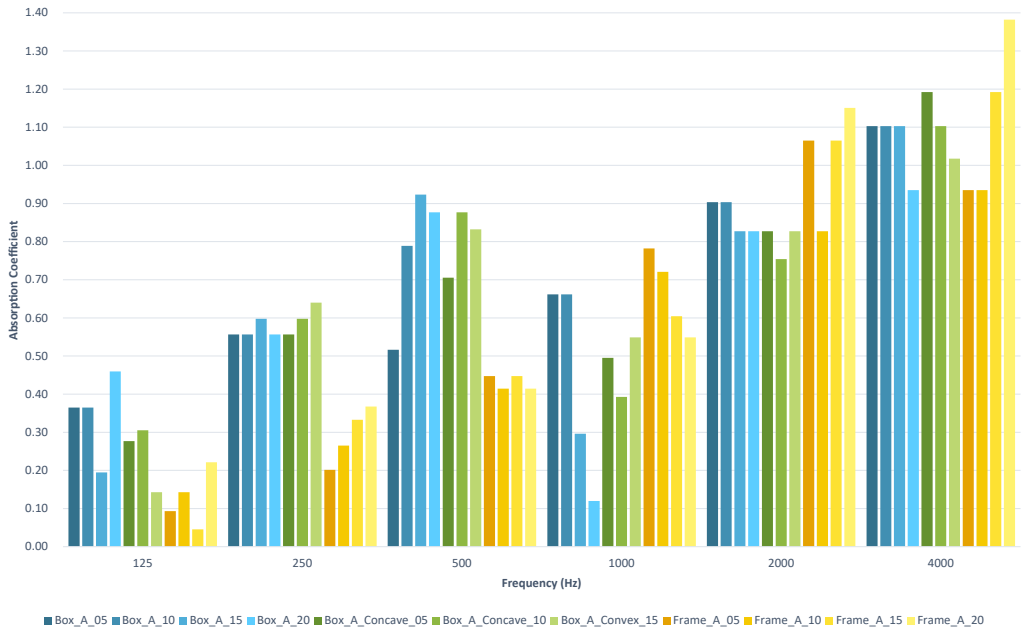
The calculation of the absorption coefficient is based on the measured reverberation times. Lower reverberation times at the higher frequencies relate to higher absorption coefficients, as an upward trend is clearly visible for the absorption coefficient at higher frequencies. The absorption coefficient of the acoustic panel does not only relate to the exact length of the measured reverberation time, it also depends on the relative difference between the measured value with and without the sample. Little to no difference indicates little absorption where a bigger difference indicates that more sound has been absorbed.

Due to these two aspects, the height of the absorption coefficient fluctuates more than the reverberation time, even within one octave band.

It is remarkable that in the higher frequency range, the absorption coefficient reaches values above 1. An absorption coefficient of 1 indicates 100% absorption, which means that higher values would theoretically be impossible. The reason for this is that the thickness of the sample has not been taken into account. The edges of the sample were not included in the surface area calculations, but could have absorbed some of the sound.

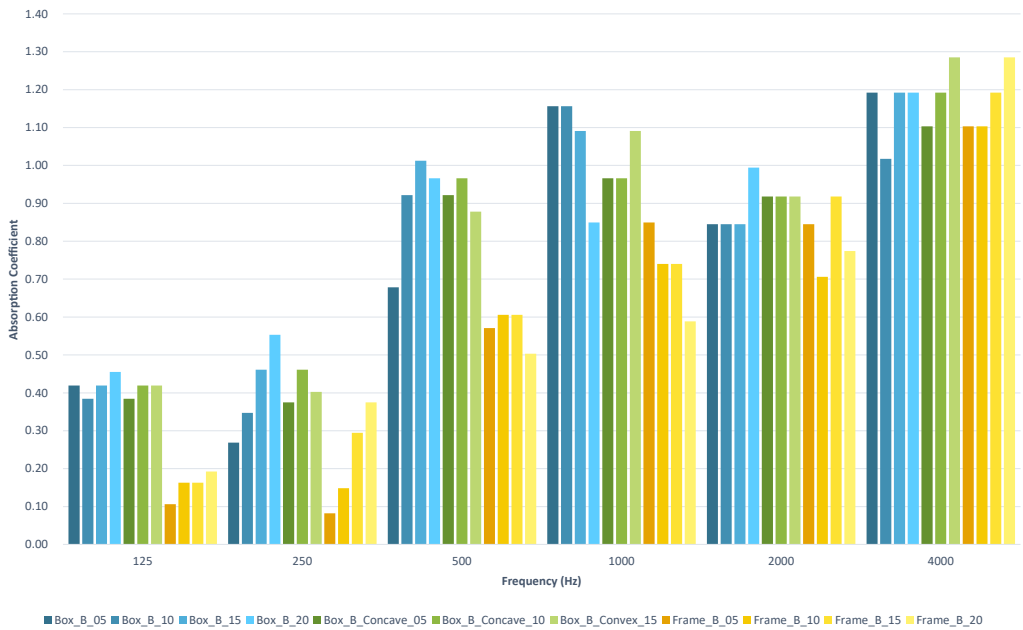
The relative smaller differences in measured reverberation time between the empty room and the frame translates to a lower absorption coefficient. This applies for both setups in the lower frequencies and can be seen by the measured frame. Above the 1000 Hz octave band, the average results of the box and the frame are more similar. The 1000 Hz octave band itself does show a significant different result between setup A and B and can be primarily seen for the box. The amount of absorption appears to be significantly higher at setup B. This variation in absorption is probably caused by the position of the microphone in relation to the box. The space between the box and the corner of the room may have led to interfering reflections, affecting the measured reverberation time and thus the resulting values for the absorption coefficient.

Absorption Coefficient - Setup A T_{20}



Graph 16. Absorption Coefficient for setup A at T_{20}

Absorption Coefficient - Setup B T_{20}



Graph 17. Absorption Coefficient for setup B at T_{20}

3.5. CONCLUSIONS

3.5.1. IMPEDANCE TUBE

There are multiple pattern parameters that can be manipulated to adjust the flexibility of a surface. The combination of a responsive wooden panel with acoustic absorbent changes the boundary conditions of these parameters.

The type of pattern that is applied hardly affects the acoustic performance of the panel for as long the open/closed surface ratio remains unchanged. According to the literature, for any value for the open surface area above 20%, the absorption is entirely controlled by the porous absorbent with no additional effect by the perforated panel. The measurements confirmed this theory only for the lower frequencies. From 1600 Hz and above, higher percentages of the open surface area did affect the amount of absorption. Crests and troughs appear slightly shifted at the same frequency, but with varying amplitude. The cumulative average for these curves seems to be similar, which gives the same average absorption coefficient for any open surface area above 20%. The open/closed surface ratio therefore determines the minimum width of the pattern kerfs.

The results of the impedance tube measurements showed that the depth of the air cavity affects the amount of absorption for each given frequency. It determines the exact position of the crests and troughs of the absorption curve and the distance between them. A larger air cavity relates to a higher amount of crests and troughs, that lie closer together. Because of the variable surface curvature of the panel, the depth of the air cavity will be different at any point of the panel. That means that the amount of absorption for each frequency is also different at these points which makes it difficult to pick a specific frequency range to be absorbed and exclude the other frequencies. The amount of absorption at the troughs is still substantial, especially for the higher frequencies, because regardless the depth of the air cavity, the absorbent has a minimum amount of sound absorption for each frequency. The resulting sound absorption of the panel for each frequency will be an average of the individual values related to the depth of the air cavity.

The results of the Impedance Tube measurements can have some flaws and errors due to the following causes:

- The contact between the wooden surface and the acoustic absorbent may be interrupted by inaccurate placing of the acoustic sample inside the tube.
- The depth of the air cavity might have been slightly different due to inaccurate placement of the movable rear panel.
- Unwanted noise from outside the tube may have caused interference during the measurements.

3.5.2. IMPULSE RESPONSE

Due to the broadband measurement, no detailed information can be given for the individual compositions of the acoustic sample. The measured values relate to octave bands which cover a wide range of frequencies, of which the data has been stacked together into a single value. Therefore only a basic understanding can be derived from this measurement.

Just like the results of the Impedance Tube, the results of the Impulse Response measurement also showed an upward trend for the absorption coefficient towards the higher frequencies. It can be said that this specific composition of acoustic sample is under-performing to absorb the lower frequencies. Increasing the thickness of the absorbent in combination with the air cavity should improve the low frequency absorption. The box and the frame gave different results in the lower frequencies but appeared to behave similar as the frequency increases. Differences between the flat and curved compositions in the box cannot be noticed with the available data, they both have similar results along the measured frequency spectrum.

Especially the results at low frequencies can be taken with a grain of salt. The room that has been used seemed not to be entirely suitable for an Impulse Response measurement. It is too small and allows standing waves to occur inside the room. Ideally, a reverberation room is a large room with a very low absorption coefficient and with geometrical irregularities such as non-parallel walls and diffuser objects to prevent standing waves.

The results of the Impulse Response measurement can have some flaws and errors due to the following causes:

- The suspended ceiling could only be removed for one half. The remaining part may have caused interference and unexpected reflections.
- The wavelengths in the lower frequencies match the dimensions of the room, creating standing waves between opposite walls. Depending on the position of the nodes and antinodes, different reverberation times can be measured for the resonant frequencies at different locations.
- Small scale measurements can give optimistic results, which could be lower in practice, because of other compositions (e.g. panels next to each other instead of single panel).
- Absorption coefficient values greater than 1 arise because of issues with the measurement, such as edge diffraction, which is not included in the calculation of the surface area.
- Reflections of the box (and the sink) related to the position of the microphone may have caused a variation in the measured values.
- Unwanted noise from outside the room may have caused interference during

the measurements, as the microphone could have detected these signals.

Acoustic simulations have not been performed due to the inaccurate results of the Impulse Response measurements and the lack of time.

3.5.3. FINAL REMARKS

At the beginning of this chapter, two sub-questions have been asked that can now be answered.

How does kerfing influence the acoustic performance of a panel?

The acoustic parameters that have been examined and measured are not all of significant influence on the acoustic performance. Kerfing is related to the type of pattern and open surface area, of which only the open surface area showed different results. So kerfing does influence the acoustic performance, but above an open surface area of 20%, there is no significant effect noticeable on the average absorption.

What effect has a curved surface of a panel on its acoustic performance?

The results of the Impulse Response measurement were less accurate than with the Impedance Tube measurement. The data can be taken with a grain of salt, especially at the lower frequencies. Due to the broadband measurement, all data within one octave band has been stacked together. That means that no detailed information can be given on the acoustic performance of individual compositions of the acoustic panel. The effect of a curved surface on the acoustic performance cannot be explicitly mentioned, but it certainly affects the depth of the air cavity. And based on the results of varying air cavities, the effect of a surface curvature is the position of the absorption crests and troughs. The effects on sound reflection are not measured, but it is expected that a surface curvature is able to redirect the reflected sound due to the variable position of the wooden surface.

The idea of the designed acoustic panel is that it has a responsive surface that can be adjusted to meet the desired acoustic performance in the room. The changes in acoustic performance with this concept however appear to be quite limited. The attainable sound absorption for each frequency is mainly dependent on the thickness and type of the used sound absorbing material, which is fixed in advance and cannot be altered once the acoustic panels have been placed. The only thing that can be adjusted real time is the depth of the air cavity by changing the surface curvature, and thus the position of the absorption crests and troughs in the frequency spectrum. Due to the varying air cavity it is expected that application of such acoustic panels will result in an averaged sound absorption coefficient that falls within the frequency range of human speech with an upward trend towards higher frequencies.

4. DESIGN

4.1. INTRODUCTION

The main challenge in the geometric design is to find out the dependencies which influence the final surface curvatures. Using a parametric model provides the opportunity to create relations between operations and or functions, in order to be able to modify the design variables without losing the previous relations or dependencies (Goldberg, 2006). Therefore, a parametric model has been developed in Grasshopper in order to generate pattern variations and to simulate the bending capabilities of a given plate on which these patterns are applied using different geometric parameters.

This chapter combines the principles concluded from the pattern design for flexibility and acoustic performance into a conceptual design. The sub-question that will be answered in this chapter is as follows:

What are the possible uses of responsive surfaces on acoustic performance?

4.2. CONCEPT

The design concept is shown in Figure 73. A series of acoustic panels with adjustable surface curvature is mounted on the ceiling by means of a retractable cable system, that allows the cables to be individually extended and retracted. Changing the vertical position of the individual supports of the panel allows for an adjustable surface curvature, caused by its deformation depending on the stiffness and weight of the panel.

To cover an entire ceiling with these responsive acoustic panels, the surface should be divided into smaller segments, because the dimensions of a single panel are limited due to production, transportation and assembly. Multiple panels are placed next to each other, with a small gap between them to allow free movement when changing shape.

A panel consists of two layers: the layer of kerfed plywood and the porous absorbent for sound absorption. The absorbent material is fastened by means of several eye bolts, that simultaneously act as the supports of the panel.

A single panel is visualized in Figure 74. The chosen dimensions for one panel are approximately 150 by 200 cm, with support positions at every 45 cm in two directions, with a certain offset from the edge. This allows for 20 support points for a single panel. The supports are located at the 'knots' of the pattern, which are the areas where 4 individual segments come together (Figure 75). They have a large enough area of 25 x 25 mm to attach the mounting components.

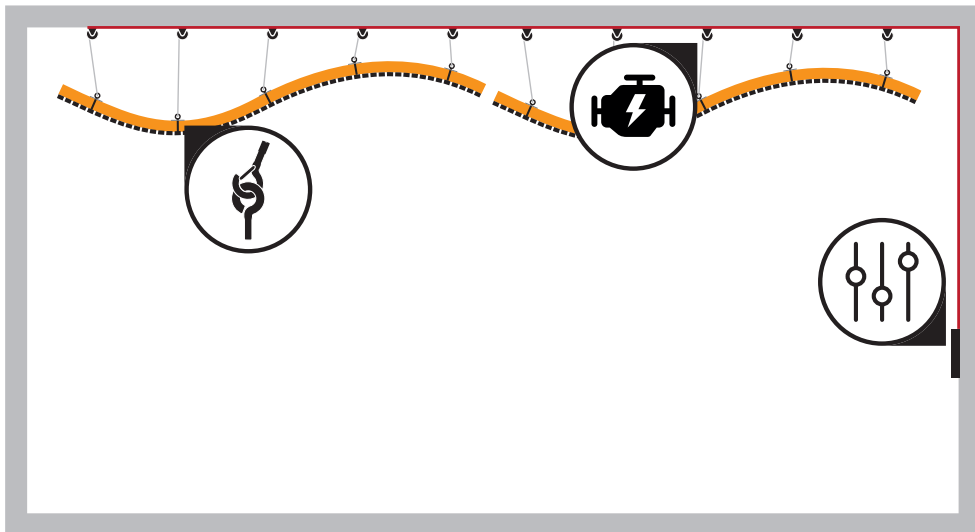


Figure 73. Design concept: Responsive panels mounted on the ceiling with a retractable cable system that is controlled by an automatic system.

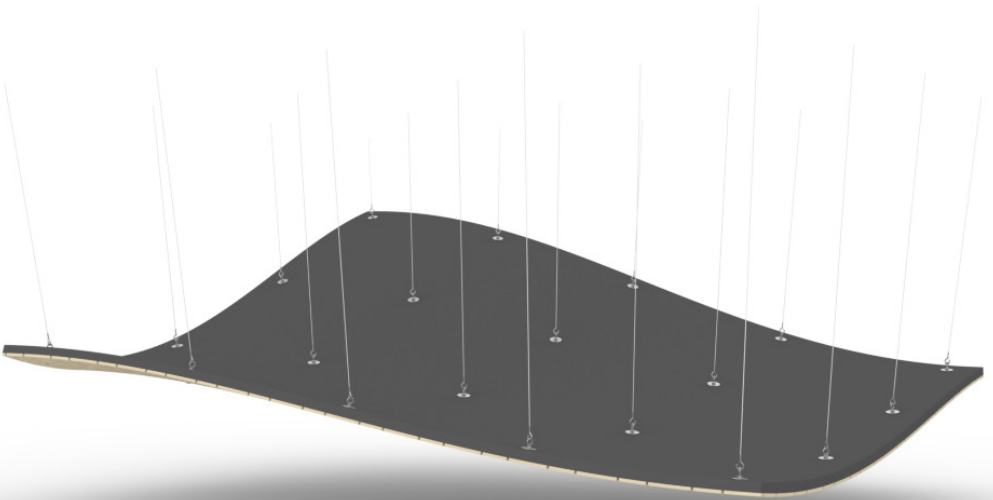
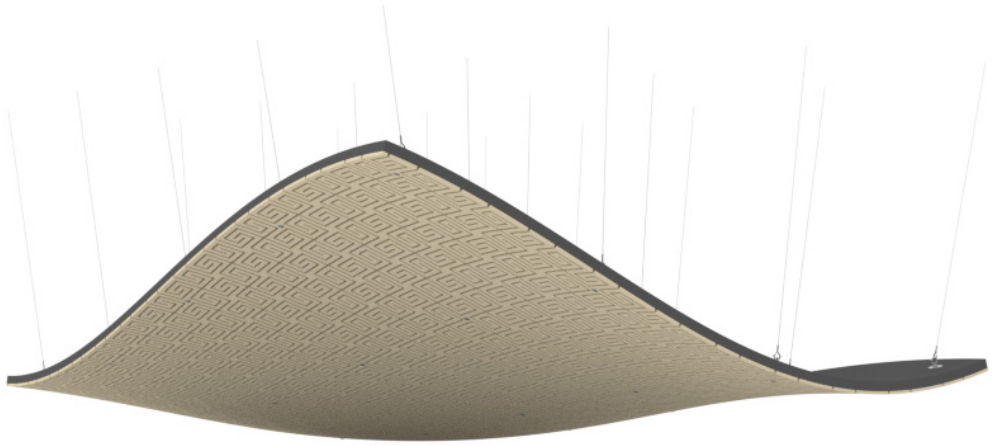


Figure 74. A single panel is attached to 20 cables, which can be individually extended or retracted to deform the panel into a double-curved surface.

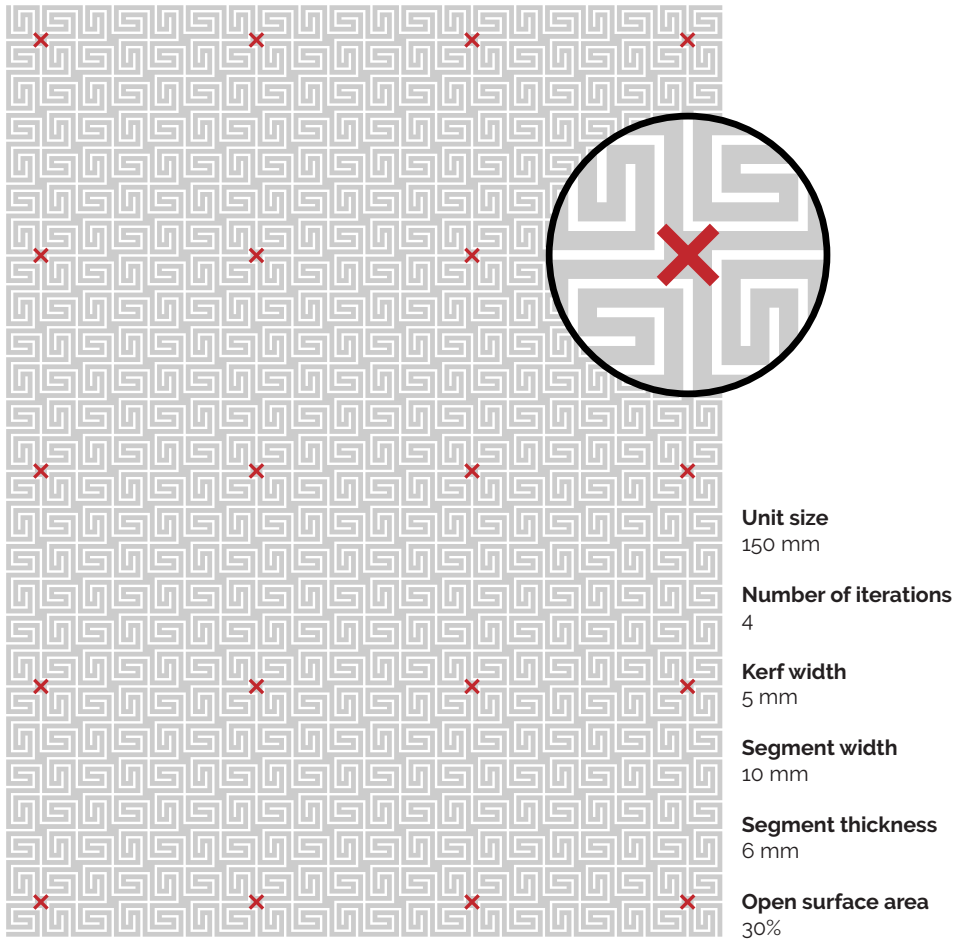


Figure 75. The support locations on the surface and the used pattern parameters.

4.2.1. MATERIAL ASPECTS

The design of an acoustic panel is accompanied by multiple requirements, that are for this research primarily related to performance and manufacturing considerations. A suitable material for this design is wood, because it is a sustainable material with functional, environmental, economic and social advantages. Besides the fact that wood is durable and renewable, three other properties are particularly interesting and beneficial for this design.

Firstly, the structural capabilities of wood, including its bending stiffness, make it possible to use as a common building material. The possibility to customize its bending stiffness with the help of geometric modifications is of particular interest. Geometric modifications can be achieved by subtractive manufacturing methods. These are the processes in which three-dimensional objects are produced by removing parts from a

solid object. When this is done in a systematic way, it is possible to modify the flexibility of the object. Pattern kerfing is a subtractive manufacturing technique which involves a series of cuts and engraves at precise locations in the form of patterns. Eventually, it influences the bending stiffness of the solid plate, and enables the production of curved surfaces out of it, allowing for single or double-curved surfaces depending on the properties of the applied pattern.

Secondly, wood is a suitable material when it comes to acoustics. The dense structure of this material reflects sound, and can easily be made into a surface that guides the sound reflections. Incisions by a kerfing pattern do not only influence the attainable curvature of the surface, but also affect its acoustic performance. The kerfs can be compared with perforations made in traditional wooden acoustic panels, such as Helmholtz absorbers (Figure 56 on page 75), increasing the absorbing qualities. It allows sound waves to pass through the wooden surface and be absorbed by an acoustic absorbent layer due to friction with the material.

Lastly, manufacturing of wood is relatively easy, by both manual and industrial processes, of which laser cutting and CNC milling are the most appropriate techniques.

The acoustic absorbent layer behind the wooden surface determines the acoustic performance of the panel in terms of sound absorption. The layer of absorbent needs to be flexible, able to perform the same deformations as the wooden surface and shape according to its surface curvature. The choice of absorbent material is limited to a layer of 2 cm polyether foam, which meets the requirements of flexibility and allows sufficient sound absorption.

4.2.2. MANUFACTURING

As also shown by Breaz, Bologna and Racz (2017), CNC milling is appropriate for modifying the geometric properties of wooden plates. It allows the transformation of flat wooden plates into three-dimensional curved objects. The prototype of the selected design is produced using 3-axis CNC milling techniques. Although this technique is suitable for the production of such panels, laser cutting would be the preferable approach. It does not give potential damage caused by vibrations and it allows for patterns with more detail and higher accuracy. However, the sides of the cut area have a black appearance due to the burning laser. When this is not desired, either the surface needs a finish layer or has to be produced by means of a milling machine.

4.2.3. ASSEMBLY

Panel

To combine the different components into one panel, a few simple steps are needed. After the pattern has been applied on the plywood surface and the support points are drilled out, each of those points will be filled with a sleeve nut. Then the tailor made layer of absorbent is placed on top of the surface. Eye bolts are pierced through the absorbent and fastened in the sleeve nuts. A washer and nut hold the absorbent in place.

A detailed composition of the support mounted on the panel is shown in Figure 76. An eye bolt holds the layer of foam in place on top of the wooden surface and acts simultaneously as the attachment point for the retractable cable system. The steel cable can be attached using a snap hook to hold and secure the panel.

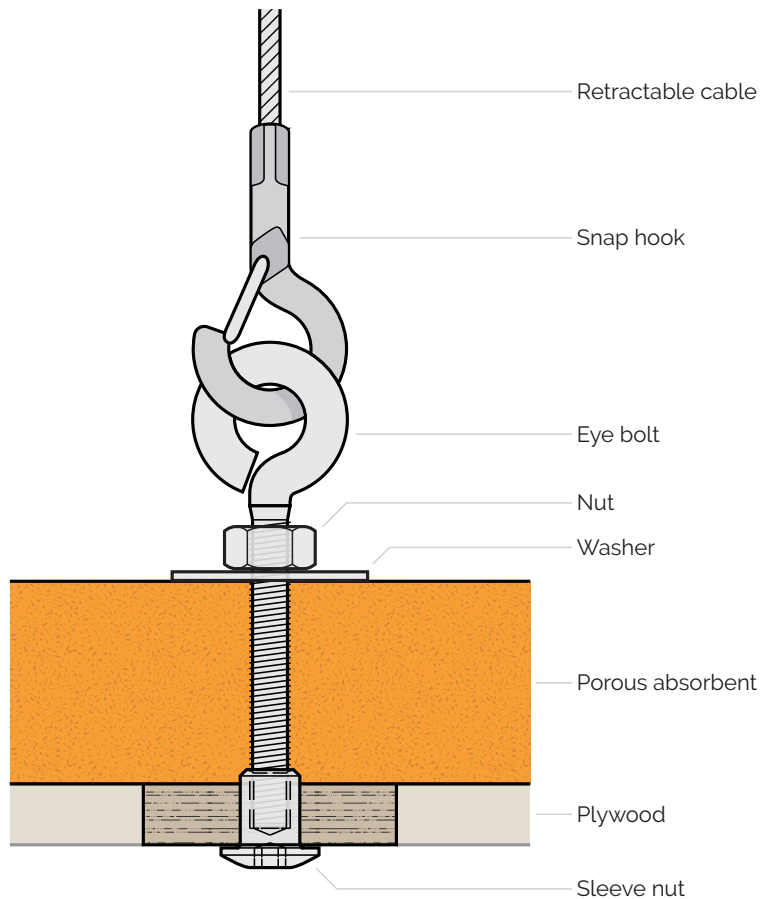


Figure 76. Detail from the support at the acoustic panel.

System control

All supports have a fixed position on the panel, but the deformation of the flexible surface changes their orientation. Due to the fixed mounting points on the ceiling and the variable orientation of the panel supports, the direction and length of the cables will vary, depending on the local surface curvature (Figure 77). The actuators on the ceiling are placed in a grid, which covers the dimensions of the entire panel.

The extension and retraction for the individual cables could be done manually, but an automatic system with motorized retraction is preferable. It can handle pre-installed positions of the panel for different scenarios and allows fast and easy adjustments by the press of a single button.

The entire composition of the panels is included in the parametric model, including the required information for the retractable cable system. The individual lengths of the cables can be distracted from the model for any panel composition. This data is then stored in an Arduino setup that controls the entire system. It transfers the data from the chosen panel composition to the actuators, to find their exact position for the chosen setup. The actuators are small stepper motors, which are placed on the ceiling and control each a single cable. They are low-cost, have high torque and are able to provide low speeds, which makes them perfect for this type of system. A permanent magnet or hybrid stepper would be suitable because it also provides detent torque, which is the amount of torque the motor produces when the windings are not energized (Collins, 2016). In case of a power outage, the motors maintain in their position and prevent the panels from falling down. A position sensor indicates the exact position of the motor in order to maintain the correct cable length for each composition.

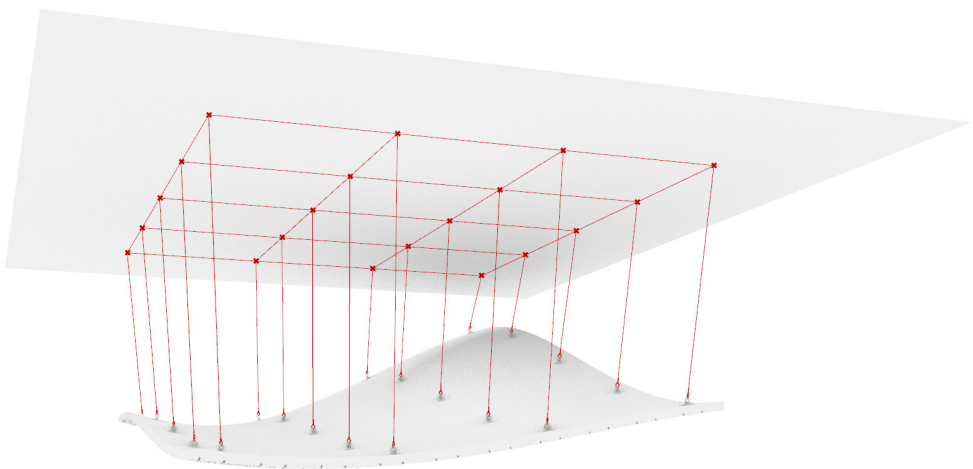


Figure 77. Actuator positions are placed in a grid structure onto the ceiling, above the panel.

Surface

The first step for assembly is to attach the stepper motors onto the ceiling, in combination with the retractable cable system. The position sensors should be calibrated in order to give the correct data to the system.

The second step is to extend the cables in order to attach them to the supports of the panel. After the panel is attached, it can be placed into position by retracting the connected cables. It is preferable to do this for each panel separately to provide enough space around the panel to mount the cables.

The third and final step is to select the required composition of the panels at the control system and the setup has been completed.

Compositions

Based on the three scenarios that are described in "3.3.3. Space definition", three different compositions of the acoustic panels have been defined that are the best for each of the scenarios. Figure 78 shows the compositions of the responsive panels for each scenario. The flat shape on the left is the standard position, from which the other three compositions can be made. Composition 1 is a surface with a full parabolic curvature in x direction and a half parabolic curvature in the y direction. Here the maximum surface height is located above the position of the speaker in the front of the room.

Composition 2 has a full parabolic surface in both x and y direction, to redirect the sound reflections more to the center of the room, which is important for the speech intelligibility during a round-table discussion.

The surface in composition 3 is based on a sinusoidal curvature in both directions to improve the acoustic reflections in the situation of groupwork sessions.

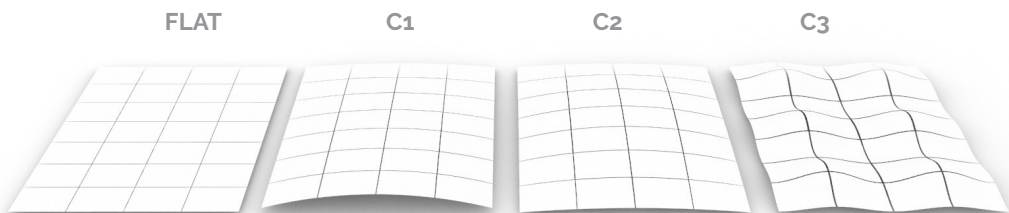


Figure 78. The predefined shapes for the responsive panels, flat and the three compositions for the described scenarios.

4.2.4. TRANSFORMATION

For the responsive panels to change into one of the compositions, each support has a different distance to overcome. Figure 79 shows the principle of the transformation from a flat state to a curved surface. It shows the deformation of the panel with the in between states, based on the vertical support positions which move with an equal retraction speed. When the retraction speed is set to be equal for all actuators, the time for the vertical movement to complete will vary amongst the support points. That means that the panel deformation continues after the first movements are finished until the last point has been put in the right position.

Figure 80 shows the direct transformation from a parabolic surface to a sinusoidal surface with the inbetween states. The red color indicates the maximum Gaussian curvature of the surface, light blue the minimum. A direct transformation does not involve extra deformation and tension in the surface, which means that switching states can be done directly, it is not necessary to return to the standard flat position first.

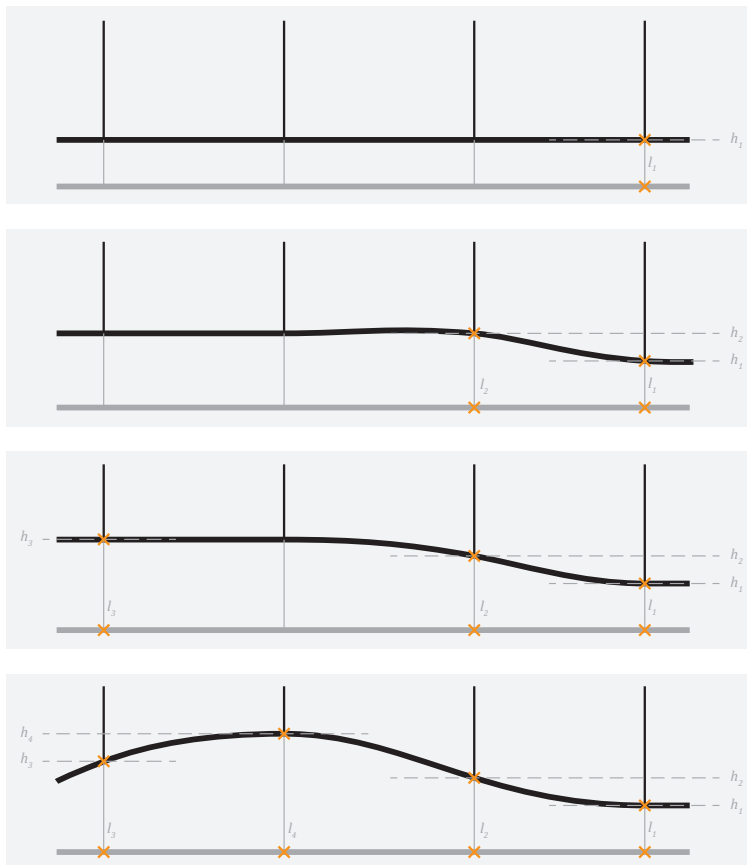
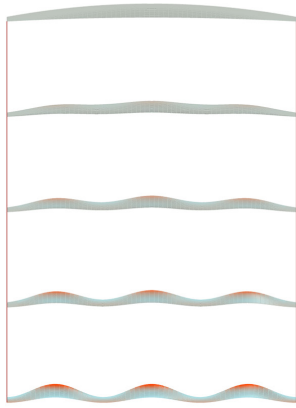


Figure 79. Transformation from flat to curved surface.



COMPOSITION 02
PARABOLIC SURFACE

COMPOSITION 03
SINUSOIDAL SURFACE

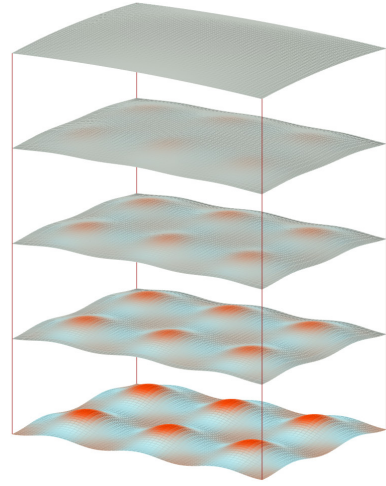


Figure 80. Transformation from panel composition 2 to 3.

4.3. PROTOTYPING

4.3.1. DESIGN CONCEPT

The material used for the prototype is a solid plate of plywood, which is perfectly suitable for traditional CNC milling machines. The diameter of the available milling bits determined the scale of the used pattern. The smallest available milling bit with a diameter of 5 mm has been used to cut out the pattern of a plate with a thickness of 6 mm. A segment width of 10 mm results in an open surface area of approximately 30%. The dimensions of the entire panel are 1045 by 595 mm (Figure 81).

The black dots in the image indicate the positions of the supports at the knots of the pattern. They lie at a distance of 450 mm from each other. An area of 25 by 25 mm each is large enough to fit the bolt and nuts, and allow the panel to maintain its required stiffness at that point. The rounded corners of the kerfing pattern are due to the circular

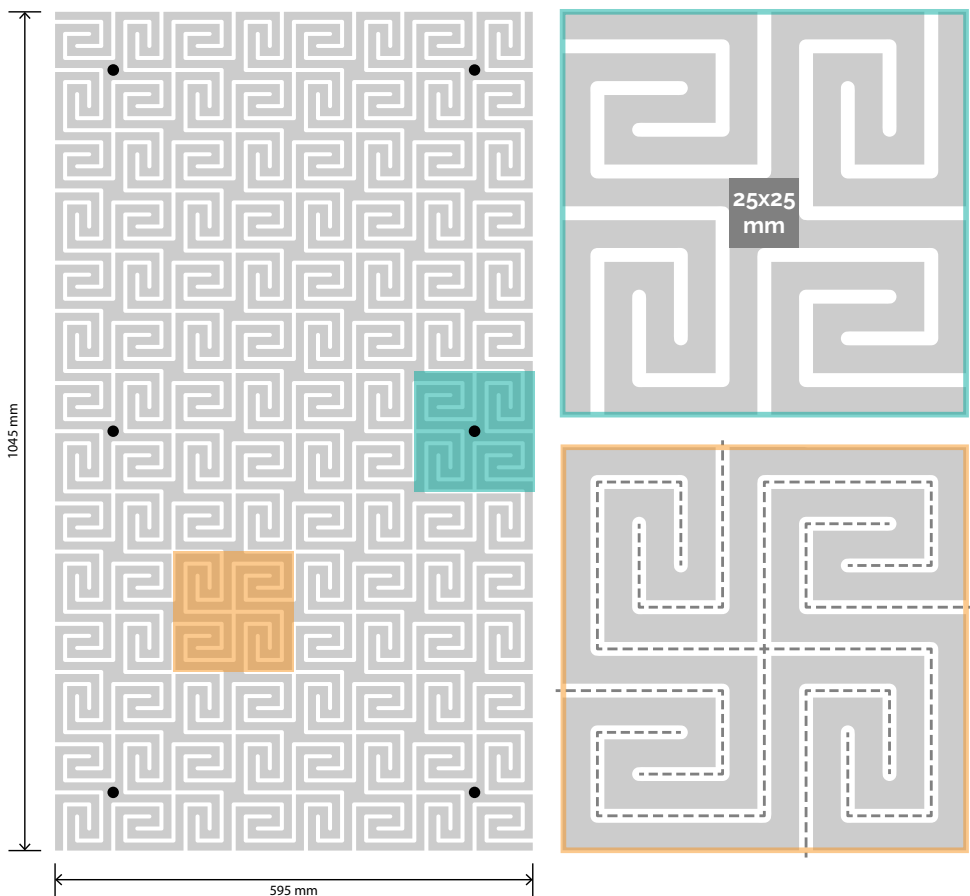


Figure 81. Pattern design for the constructed prototype.

shape of the milling bit following the constructed path of the kerfs, visualized as a dotted line.

The production of the prototype involved several issues related to the milling process. The diameter of the milling bit that was used at the first attempt was too large. Instead of the requested 5 mm, a diameter of 10 mm was used, which damaged the panel and resulted in a broken and useless pattern. Due to the diameter of 10 mm, the width of the segments in the resulting pattern would have been only 5 mm. It became clear that the vibrations of the milling machine can cause significant damage to the material, especially when the dimensions of the individual segments become too small.

The second attempt was a small test to investigate the effect when the right milling bit with a diameter of 5 mm was used. The result was significantly better than the first attempt, but still showed little damage across the surface.

At the third and last attempt, the remaining part of the plywood sheet had been fastened to limit the vibrations. Combined with a moderate milling speed, the resulting panel was successfully made. Milling the pattern onto the plywood sheet resulted in a panel with splintering edges, as can be seen in Figure 82 . Due to the high quality of the plywood and the applied milling speed, the material did not show much tear-out, exposing the ply underneath. The splinters however needed to be removed by sanding all edges of the panel to improve the appearance of the wooden surface.

After this time consuming job, the layer of foam was tailored to match the dimensions of the panel. The bolts and nuts hold the layer of foam in place, This material is soft and flexible, which allows it to deform collectively with the curvature of the wooden surface. Photos of the completed prototype can be seen in Figure 85 to Figure 92.



Figure 82. Close-up from the constructed panel, directly coming from the milling machine.

A simulation model of the built prototype shows a small displacement of 12 mm when all supports are enabled (Figure 83). The maximum surface curvature has a radius of approximately 70 cm, when the two supports at the center are disabled (Figure 84).

The flexibility of the physical model did show similar results, which indicates that the results from the simulation are quite accurate and reliable.

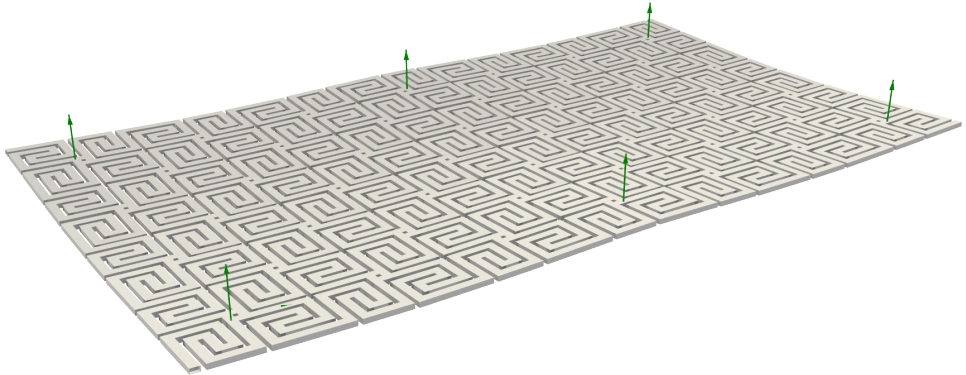


Figure 83. Simulation model of the built prototype has a maximum displacement of 12 mm.

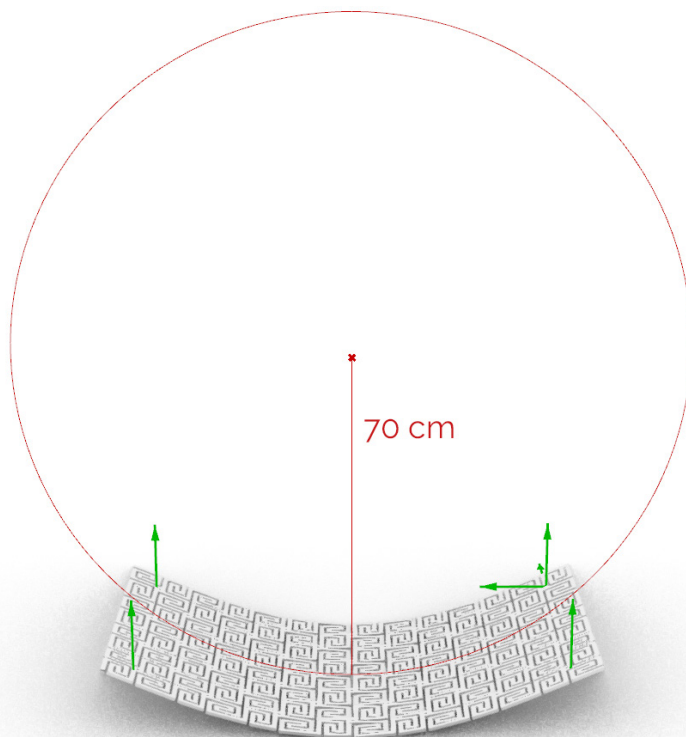


Figure 84. The radius of the maximum surface curvature of this prototype is approximately 70 cm.

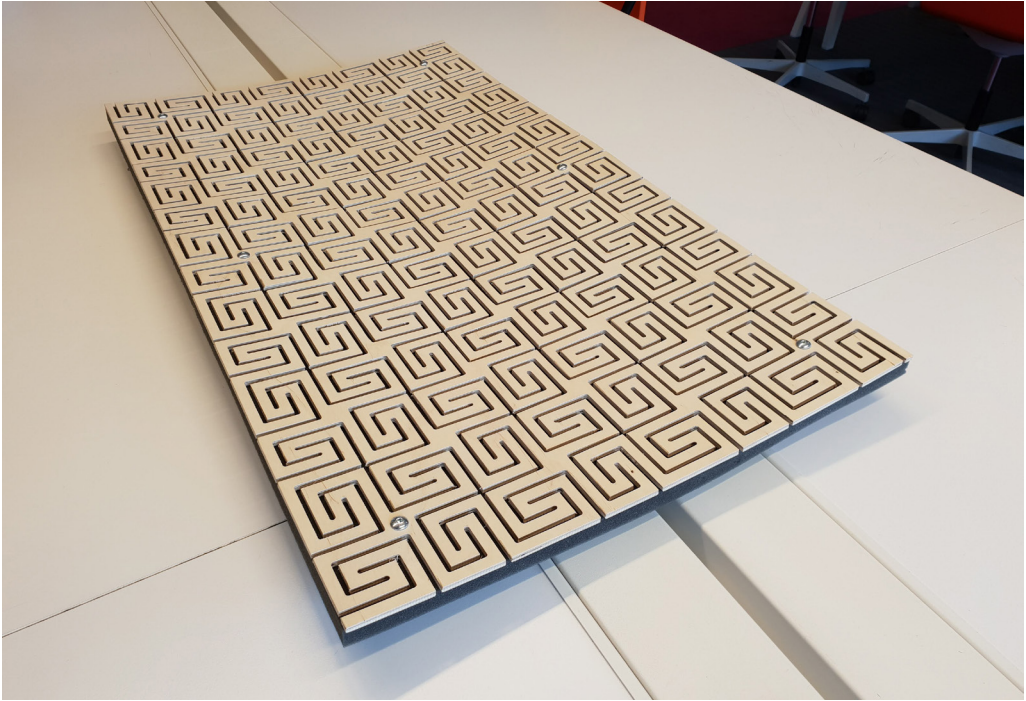


Figure 85. Completed prototype laid down flat.

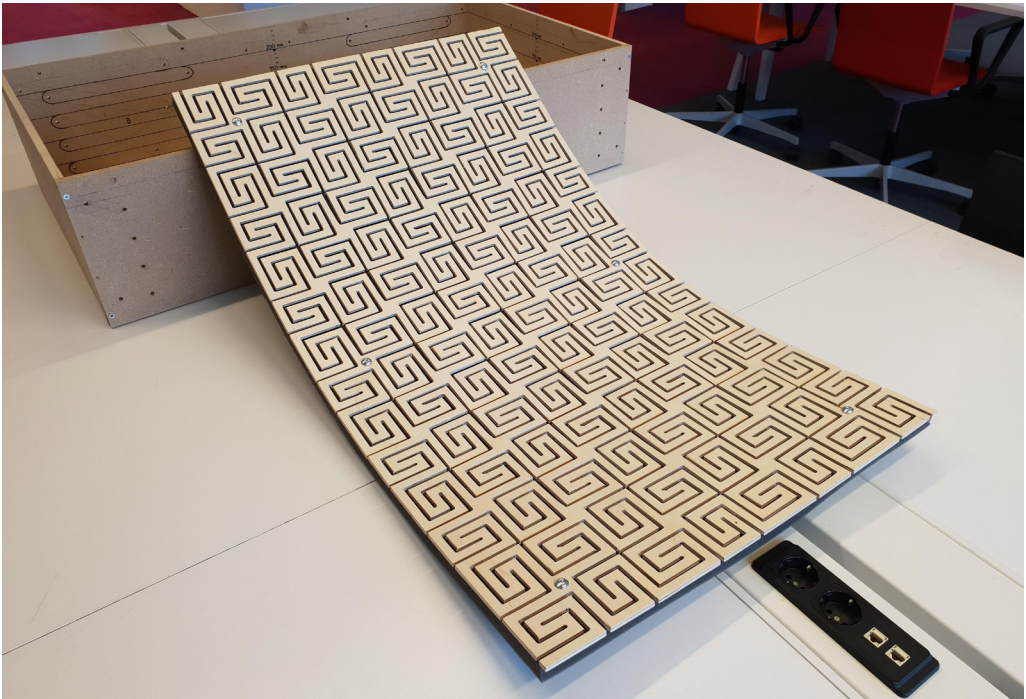


Figure 86. Completed prototype laid down with curved surface.

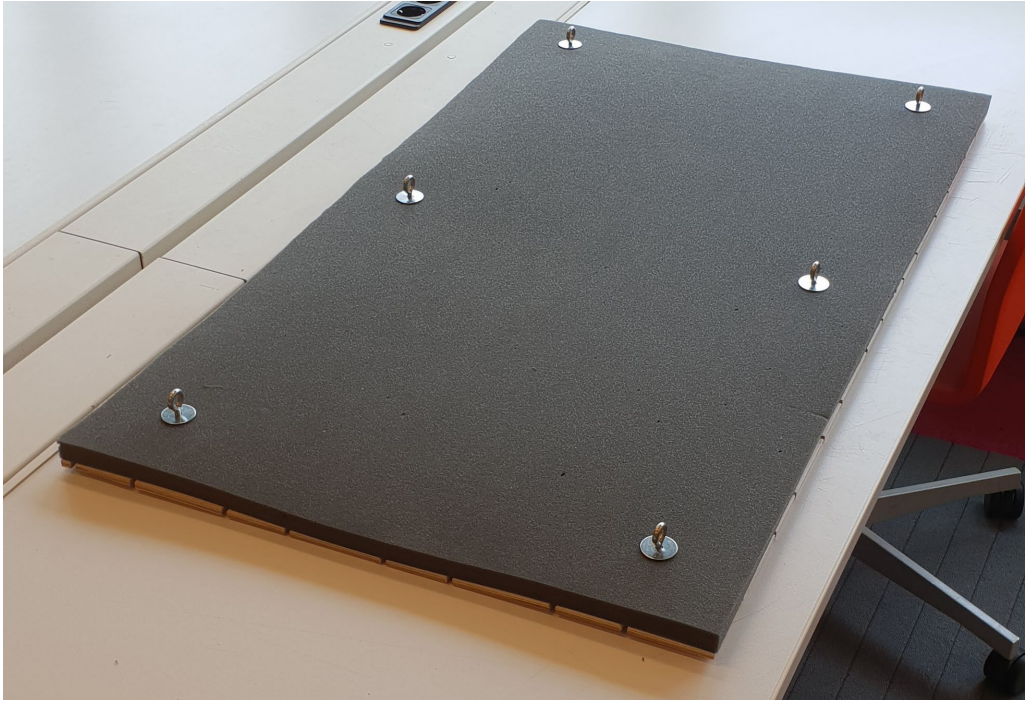


Figure 87. Completed prototype with the absorbent layer fixed by bolts and nuts.

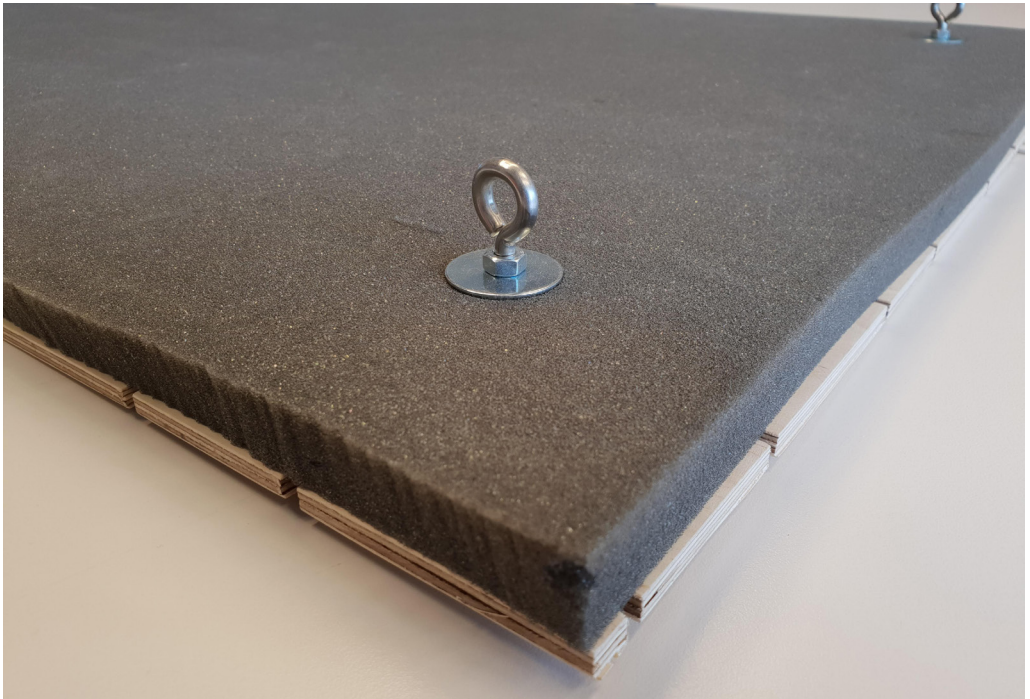


Figure 88. Close-up from the support point at the completed prototype.



Figure 89. Hanging prototype with a convex surface.



Figure 90. Hanging prototype with a concave surface.



Figure 91. Hanging prototype with a freeform surface.

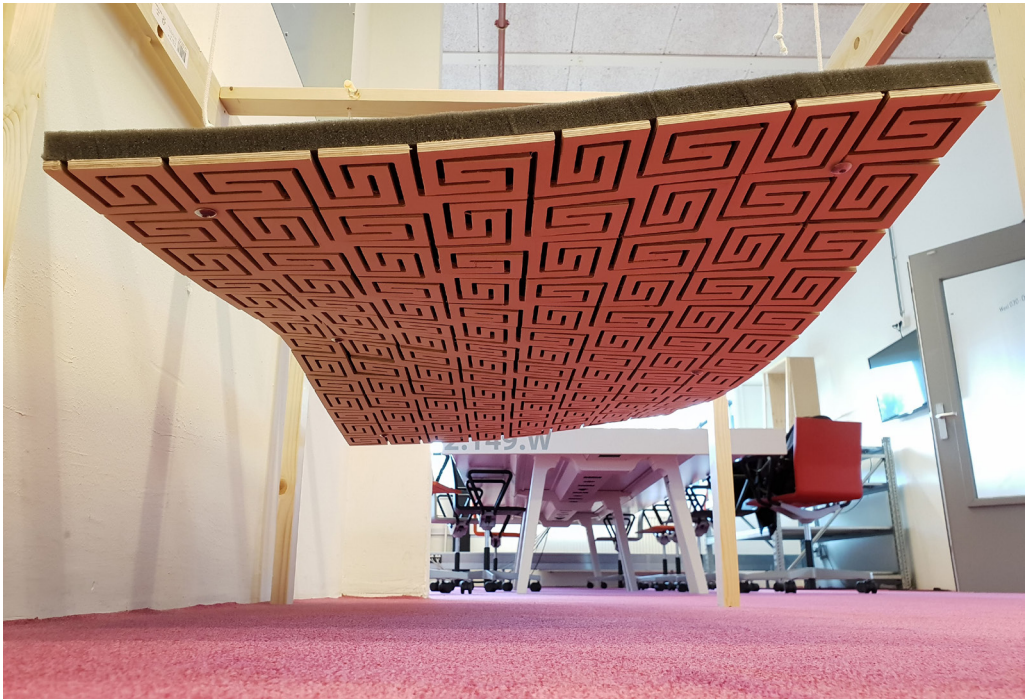


Figure 92. Close-up from the hanging prototype with a freeform surface.

4.3.2. PROCEEDING TO A FINAL PRODUCT

Before this conceptual design proceeds to the final design and product manufacturing, additional factors have to be included in the process. Plywood as the used type of material is definitely suitable, but there are more materials that meet the requirements for this product. Choosing the right material also includes the factors of fire safety, geometric capabilities, applicable manufacturing techniques and durability. A detailed structural analysis and accurate acoustic measurements are essential for pattern optimization to improve the flexibility and the acoustic performance. Lastly, the production costs of the entire system are not to be forgotten, including the entire process of design, manufacturing and installation.

Furthermore, there are several design challenges that need to be overcome. To cover an entire ceiling with adjustable acoustic panels, it is preferable and probably essential to divide the surface into smaller segments. The dimensions of the panels are limited due to production, transportation and management of the product. The challenge here is to combine these smaller segments into an apparent uniform surface, with a continuous surface curvature. That brings us to the next question: How can additional features, such as lighting and ventilation outlets be integrated and how does that affect the flexibility of the entire panel? What might be even more challenging is the combination of a ceiling covered in adjustable acoustic panels with a sprinkler system. All these questions apply to the installation, but also to the maintenance of the system.

4.4. CASE STUDY

4.4.1. INTRODUCTION

The findings of the research within geometric design and fabrication will be applied and presented in a case study. A regular lecture room at the faculty of Architecture is chosen for the application of the system. A typical setting will be created to approximate a real situation and show how responsive acoustic panels will influence the appearance of a room.

4.4.2. SCENARIOS

The chosen lecture room is mainly used in three different setups, of which each requires a different acoustic setup. The first scenario is a setup for traditional classes, with a single speaker at the front of the room talking to the audience. The second setup is meant for a round-table discussion, where all people participate in a large group conversation. The last setup involves a more dynamic use of the space in the form of small groupwork sessions.

The room will be redesigned and equipped with acoustic panels which are produced using the proposed pattern kerfing techniques and which can adapt to the changing acoustic needs of the space in different setups. The different compositions are shown in Figure 93. Besides the standard flat surface composition, the half parabolic, full parabolic and sinusoidal surface are defined for the three mentioned scenarios.

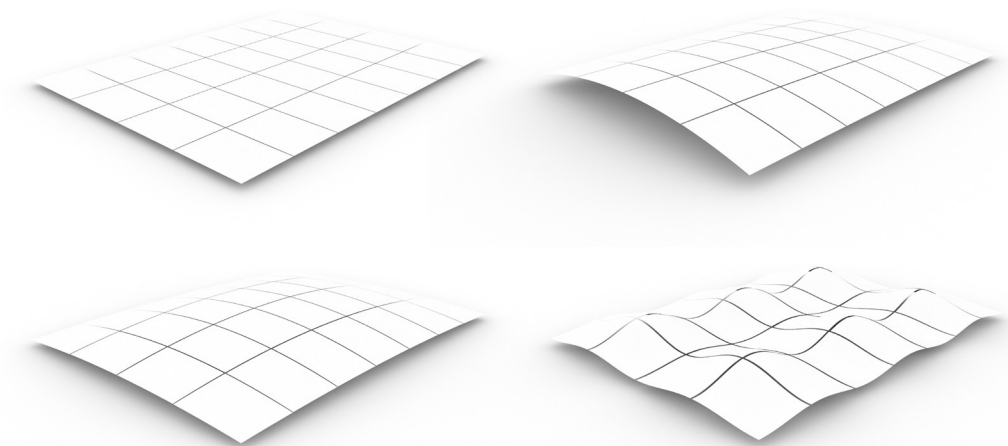


Figure 93. The four basic panel compositions: Flat, half parabolic, full parabolic and sinusoidal.



Figure 94. Acoustic panels applied in the lecture room, with a flat surface.

Standard composition

Figure 94 shows the standard position of the responsive panels, where they form a uniform and flat surface. The gap between the panels is here at its minimum, not more than two centimeters. The height of the panels is adjustable, which can decrease the room volume in order to reduce the reverberation time. The wooden surface with its natural texture and style gives a warm and comfortable appearance to the room.



Figure 95. Acoustic panels applied in the lecture room, with a half parabolic surface.

Scenario 1

The first scenario in Figure 95 is meant for the traditional lecture setup, with a single speaker at the front of the room in front of an audience. The sound absorption by the panels reduces the reverberation time in the room. With the used absorbent, not all incoming sound will be absorbed, a part also gets reflected from the wooden surface. The placement of the panels distributes the sound reflections across the room with a focus on the central area where the audience is seated. The parabolic shape of the surface is able to redirect more of the early reflections directly to the audience instead of to the walls. In combination with the direct sound, this will improve the speech intelligibility in the room.



Figure 96. Acoustic panels applied in the lecture room, with a full parabolic surface.

Scenario 2

In Figure 96 the panels are placed in the composition which is suitable for a round-table group discussion, where the conversations happen within a larger group of people, facing each other while seated in a circle. The acoustic panels are positioned in a double parabolic shape, causing the majority of the reflected sound to be directed towards the opposite side of the group. In the center, the panels are placed close to the ceiling to minimize the depth of the air cavity and increase the amount of reflection in that particular area. This is based on the principle that the particle velocity is low close to the room boundaries, reducing the amount of sound absorption and consequently cause an increased amount of reflection. Closer to the sides, the parabolic shape creates a larger distance between the panel and the ceiling, which increases the amount of absorption and consequently reduces the reverberation time.



Figure 97. Acoustic panels applied in the lecture room, with a sinusoidal surface.

Scenario 3

The sinusoidal shape of the responsive surface in Figure 97 is meant for the third scenario, which involves working in small groups, spread across the room. It is desired that the sound levels of other groups should be kept low in order to reduce unwanted noise and to improve the comprehension of the group conversation. Due to the concave shape of the panels above each group, sound reflections will be redirected back while the convex part distributes the reflections in a diffuse pattern, reducing distinct echoes and reflections. The varying distance between the panels and the ceiling allows for an averaged sound absorption of multiple sound frequencies. The gaps between the panels will be at its maximum in this composition, because of the large deformation of the individual panels.

4.5. CONCLUSIONS

4.5.1. PROTOTYPE

During the milling process, it became clear that the vibrations of the milling machine can cause significant damage to the material, especially when the dimensions of the individual segments become too small. Although several issues occurred during the process, the resulting panel is proof that this technique is still suitable for kerfing a pattern into a sheet of plywood. Combined with a moderate milling speed, the resulting panel was successfully made. Further processing however, is time consuming, when all splintering edges need to be sanded by hand.

Fixing the sound absorbing foam onto the finished surface completes the prototype of the acoustic panel. The layer of foam does not seem to affect the flexibility of the panel, as it is self a soft and flexible material that deforms collectively with the curvature of the wooden surface. The used bolts to fasten the foam and act as attachment points, appear to be a suitable solution for this type of panel. They contain the right stiffness and strength to support the panel.

The attainable curvature of the prototype corresponds to the results of the simulation in Karamba. This does not only confirm the reliability of the simulation, it also indicates that the chosen pattern parameters in combination with the position of the attachment points appear to be suitable for this design.

For the manufacturing of the panel, it is recommended to use a laser cutter instead of a CNC milling machine, despite the lack of tear-outs in the resulting panel. The vibrations of a milling machine cause potential damage to the material. Combined with a minimum diameter for the milling bit, means that the pattern will have minimum dimensions for certain parameters. A laser cutter does not have the mentioned issues and comes with additional benefits. It is more accurate and allows to apply small scale patterns with high detail. Local adjustments can be applied with ease and high accuracy. The absence of splintering edges is also convenient and user friendly.

4.5.2. DESIGN

The design is still a concept and not yet abundantly developed for proceeding to a manufactured product. A detailed structural analysis and accurate acoustic measurements will lead to a pattern optimization, to improve the flexibility and acoustic performance of the panel. Multiple aspects such as fire safety, production costs and durability need to be elaborated.

Besides the aspects that are mostly material related, there remain certain essential design challenges that need to be overcome. How can multiple panels create an apparent uniform surface with a continuous intrinsic curvature? How can additional

features, such as lighting and ventilation outlets, be integrated and how does that affect the flexibility of the entire surface?

4.5.3. FINAL REMARKS

At the beginning of this chapter one sub-question has been asked that can now be answered:

What are potential uses of responsive surfaces on acoustic performance?

The designed responsive surfaces are theoretically applicable in any situation. The adjustable curvature of the surface is beneficial for the changing acoustic needs in a room. It allows for changes in the absorption coefficients at specific frequencies and can adapt to the required acoustic composition. The deformation of the panels redirects the sound waves into different directions, depending on the local surface curvature. Furthermore, due to vertical movement of these panels, they are able to decrease the volume of a room and thus the reverberation time.

When there is no specific need for changing acoustics, they can also be applied when only an aesthetic pleasing design for static acoustic performance is desired. The actual acoustic performance of a full scale panel however, needs further research, as the results of the Impulse Response measurement were not entirely reliable to give accurate conclusions on the performance of this acoustic panel. Due to the lack of reliable data, an acoustic simulation has not been performed.

5. CONCLUSIONS

5.1. CONCLUSIONS

The final design meets the essential requirements: it is flexible, covers a wide range of frequencies and is adaptable for changing acoustic needs, has a pleasant appearance and can easily be manufactured using traditional CNC machines. Creating the panels from flat sheets of plywood allows the transformation of flat wooden plates into three-dimensional curved objects. An additional advantage is that the manufactured panels can be positioned in their original flat shape which makes transport and storage simple and efficient.

5.1.1. FLEXIBILITY

The attainable curvature of a panel with a meander pattern is determined by three main pattern parameters: the size of a meander unit, the number of iterations and the kerf width. The pattern divides the surface into multiple interconnected segments, which are able to enhance the attainable surface curvature by means of torsion and bending. The pattern parameters determine the dimensions of these segments, and thus the flexibility of the panel.

Simulations within the plugin Karamba confirmed the theoretical assumptions based on the literature study and the observations with physical models. The results showed that the height of the segments is of greater influence than the width, indicating that the surface curvature is caused by both torsion and bending. The exact share of both aspects to the final curvature is currently unknown, as the individual angle of displacement could not be determined.

5.1.2. ACOUSTICS

Based on the three pattern parameters, four acoustic parameters have been determined that could affect the acoustic performance: the type of pattern, open surface area, the depth of the air cavity and the surface curvature. From these parameters, the type of pattern has no significant effect on the acoustic performance. And neither does the open surface area have significant effect on the average absorption coefficient, as for any value above 20%, the absorption is entirely controlled by the porous absorbent with no additional effect by the perforated panel. The depth of the air cavity varies, depending on the surface curvature of the panel, and is the most influential aspect. It determines the exact position of the crests and troughs of the absorption curve, and the distance between them. The resulting sound absorption of the panel will be an average of the individual values, related to the depth of the air cavity and the used sound absorption material.

Besides the varying depth of the air cavity, additional effects of a curved surface of a panel on its acoustic performance cannot be mentioned explicitly. Due to the broadband measurement and inaccurate results, no detailed information can be given on the acoustic performance of individual compositions of the acoustic panel. The effects on sound reflection were not measured, but it is expected that a surface curvature is able to redirect the reflected sound due to the variable position of the wooden surface.

5.1.3. DESIGN

The attainable curvature of the prototype corresponds to the results of the simulation in Karamba. This does not only confirm the reliability of the simulation, it also indicates that the chosen pattern parameters in combination with the position of the attachment points appear to be suitable for a responsive acoustic panel.

The production of the prototype showed that CNC milling is a suitable technique for kerfing a pattern into a sheet of plywood. However, it is recommended to use a laser cutter instead of a milling machine, because it is more accurate, allows small scale patterns with high detail and lacks the potential damage caused by vibrations of the milling machine.

The design is still in a conceptual phase, which means that further research is necessary. A detailed structural analysis and accurate acoustic measurements will lead to a pattern optimization to improve the flexibility and acoustic performance of the panel. Multiple aspects such as fire safety, production costs and durability need to be elaborated. There also remain certain essential design challenges that need to be overcome. How can multiple panels create an apparent uniform surface with a continuous intrinsic curvature? How can additional features, such as lighting and ventilation outlets, be integrated and how does that affect the flexibility of the entire surface?

However, the designed responsive surfaces are theoretically applicable in any situation, where the adjustable curvature of the surface is beneficial for the changing acoustic needs in a room and gives an aesthetically pleasing appearance.

5.1.4. FINAL REMARKS

The application of kerfing meander patterns allows sheets of plywood to transform into three-dimensional geometries with freeform surface curvatures. Changing the various pattern parameters modifies the flexibility of a panel, with the ability of local adjustments. It comes with practical and functional benefits that support efficient manufacturing, transportation and improved acoustic performance.

The changes in acoustic performance with this concept however appear to be quite limited. The attainable sound absorption for each frequency is mainly dependent on the

thickness and type of the used sound absorbing material, which is fixed in advance and cannot be altered once the acoustic panels have been placed. The only thing that can be adjusted real time, is the depth of the air cavity by changing the surface curvature, and thus the position of the absorption crests and troughs in the frequency spectrum. Due to the varying air cavity it is expected that application of such acoustic panels will result in an averaged sound absorption coefficient that falls within the frequency range of human speech with an upward trend towards higher frequencies. Regarding sound reflection, it is expected that a surface curvature is able to redirect the reflected sound due to the variable position of the wooden surface.

This thesis provides an answer to the main research question:

How can we formalize the pattern kerfing techniques in order to produce responsive wooden surfaces for better acoustic performance?

In conclusion, deliberate pattern kerfing techniques enhance the flexibility of a responsive wooden surface towards better acoustic performance, but provide limited possibilities to respond to specific acoustic needs of a room.

5.2. RECOMMENDATIONS FOR FUTURE WORK

The used meander pattern proved to be a suitable solution for the production of flexible panels, but a more detailed structural analysis can be done for pattern optimization in order to improve the flexibility. Pattern optimization can be done by manipulating the different pattern parameters to adjust local flexibility, but there might be a different type of pattern that is more efficient and comes with better opportunities. Varying the complexity of the patterns may require a more sophisticated milling technique with a higher degree of freedom (DOF). To this end, a 6-axis robotic arm can be used for testing more complex patterns in order to see if a higher DOF can provide more efficient geometric solutions. But when small adjustments are required to modify the local flexibility, it is recommended to use a laser cutter instead of a milling machine, because of its higher accuracy.

Further development of the responsive acoustic panels requires the inclusion of additional (material) aspects, such as fire safety, environmental conditions and production costs. Instead of choosing only one material, multilayered plates could have potential benefits above single layered materials. This also applies for the acoustic performance: combining multiple absorbent materials with different characteristics can improve the overall acoustical performance of the panel.

Doing the Impulse Response measurement in a suitable space with larger samples gives more detailed and more reliable results, which can be used as input for acoustic simulations. This can also include the effect of a surface curvature on the sound reflections. The acoustic performance of the design can be tested and improved by using the Pachyderm Acoustic plug-in with Grasshopper.

A ceiling covered with responsive acoustic panels comes with design challenges like the integration of additional features, such as lighting and ventilation outlets, or the creation of an apparent uniform surface built from a series of panels. The designed responsive panels are suspended from the ceiling with the proposed retractable cable system, but to include the option for responsive panels to be mounted on a wall, a different approach is required for the underlying construction.

6. REFLECTION

Introduction

This master's thesis is the outcome of the research done within the chairs of Design Informatics and Climate Design, with focus on acoustics. This topic for my graduation was not the one I had in mind in the first place, where I started out with the combination of Design Informatics with Structural Design. One month before my P2 presentation, I decided to let go of this subject and to continue with a different topic: Pattern Kerfing for Responsive Wooden Surfaces.

Objective

The main objective for this research was to combine the technique of pattern kerfing with acoustic design in order to create a flexible acoustic panel. The idea of pattern kerfing to increase the flexibility of rigid flat panels is relatively new, meaning that actual applications based on this technique began just over a decade ago. The amount of scientific research on this technique is still scarce, which makes it a challenging subject that demands further research. The combination with acoustic design brings new opportunities for acoustic panels to change and adapt to the desired acoustic performance.

Methodology

This research starts with a literature study on the subject of pattern kerfing and acoustics. While few scientific reports are available on pattern kerfing, more can be found on acoustics. The study into the literature about the first subject was limited and left more to be explored and defined by myself. Research by design was done by creating physical models and study the bending behavior of different models each of which having a unique set of pattern parameters. The designed patterns were created within a parametric model, that used the defined pattern parameters as input.

Creating the algorithm for the parametric model was taking up more time than expected. This has probably to do with the fact that I liked working on this model and tried to optimize it continuously, by adding and experimenting on additional features. It resulted however in a model with extra features, that allow for various local adjustments in the pattern and is for example capable of creating sample pieces of a pattern automatically, which were used for acoustic measurements. Several other aspects I wanted to include as well have not made it into the model due to the complexity of these parts and the limited amount of time left. But the effort put into it resulted in a better understanding and new insights of the possibilities of the software and opens up new opportunities for further elaboration in the future.

Acoustic measurements were done to analyze the influence of the pattern parameters on the acoustic performance. The pattern parameters have been translated to four different acoustic parameters, which relate to the pattern design and the surface curvature of the panel. The measurements with the Impedance Tube gave accurate and reliable results, as they were almost identical in repetitive measurements. This type of measurement is quite convenient, as only small samples are required and there are only few possibilities for flaws and errors in the results. A minor downside with this measurement is that it only measures with normal incidence and does not give any information on acoustic performance with random incidence. That means that the effect of one of the four acoustic parameters, the surface curvature, could not be measured.

All collected data from the research and the measurements was then combined to create a full scale prototype of the panel. The constructed prototype has been used for Impulse Response measurements, which should give more insight in the fourth acoustic parameter, how the surface curvature affects the acoustic performance. Unfortunately, this measurement ended up in results that were not so accurate and therefore not useful to give detailed information on the acoustic performance of a full scale panel and the effect of a curved surface. The resulting values were meant to be the input for acoustic simulations, which have not been performed due to the unreliable results and a lack of time.

Based on the available results, it can be concluded that the adaptation of the panel to changing acoustic needs is quite limited. However, the results of the research, the measurements and the built prototype, showed that the principle of responsive acoustic panels is definitely promising and demands further development.

Relevance

Acoustic panels are already widely available, but only few of them are capable to change its acoustic performance in order to meet the changing acoustic needs in a multi-purpose room. The relatively simple technique of kerfing a pattern onto a wooden sheet to transform it into a three-dimensional geometry, is a cost efficient approach to create responsive acoustic panels. This technique is relatively young and currently still under development, which makes it a suitable topic for this research.

Sustainability

Besides the fact that wood is a durable and renewable material, it can also be easily processed, either by CNC laser cutters, milling machines or by hand. The possibility of transforming a flat wooden sheet into a three-dimensional geometry is cost efficient and reduces the amount of waste compared to building a 3D geometry straightaway. The manufactured panel can be placed in its original flat position, which allows for compact storage and transportation. Once placed, it has an aesthetically pleasing appearance that keeps its quality with little care and maintenance.

The main research question has been answered during this research, but there is more to discover in this field of work. There is plenty of room to overcome several design challenges, optimize the pattern design and include other design aspects to create an actual product that can be applied in any room and responds to changing acoustic needs.

7. BIBLIOGRAPHY

- Acoustical Surfaces Inc. (2018). Acoustics 101. Retrieved 2017, 21-12 from https://www.acousticalsurfaces.com/acoustic_IOI/101home.htm
- AMA Alexi Marmot Associates in association with haa design. (2006). *Spaces for learning: a review of learning spaces in further and higher education*. Retrieved from <http://aleximarmot.com/userfiles/file/Spaces%20for%20learning.pdf>
- Arenas, J. P., & Crocker, M. J. (2010). Recent trends in porous sound-absorbing materials. *Sound & vibration*, 44(7), 12-18.
- Arie. (2013). Jones Hall. Retrieved from <https://thecoog.wordpress.com/2013/08/27/pictures-from-the-20th-annual-theater-district-open-house-houston/>
- Belforte, D. A., & Jafferson, J. M. (2016). Laser Cutting. In *Reference Module in Materials Science and Materials Engineering*: Elsevier.
- Bies, D. A., & Hansen, C. H. (2003). *Engineering Noise Control: Theory and Practice* (3rd ed.). London: Spon Press.
- Breaz, R. E., Bologa, O., & Racz, S. G. (2017). Selecting between CNC milling, robot milling and DMLS processes using a combined AHP and fuzzy approach. *Procedia Computer Science*, 122, 796-803. doi:<https://doi.org/10.1016/j.procs.2017.11.439>
- Callens, S. J. P., & Zadpoor, A. A. (2017). From flat sheets to curved geometries: Origami and kirigami approaches. *Materials Today*. doi:<https://doi.org/10.1016/j.matod.2017.10.004>
- Cavanaugh, W. J., & Wilkes, J. A. (1999). *Architectural acoustics: principles and practice*. New York: Wiley.
- Collins, D. (2016). Detent torque and holding torque. Retrieved 2018, October 15 from <https://www.motioncontroltips.com/faq-whats-the-difference-between-detent-torque-and-holding-torque/>
- Couden, C. (2013). Laser-Cut Book Covers. Retrieved from <https://makezine.com/projects/make-33/laser-cut-book-covers/>
- Cox, T. J., & D'Antonio, P. (2009). *Acoustic absorbers and diffusers : theory, design and application* (2nd ed. ed.). London :: Taylor & Francis.
- Cremer, L., & Muller, H. A. (1982). *Principles and Applications of Room Acoustics* (T. J. Schultz, Trans.): Peninsula Publishing/Olympia Books.
- Cutting Plywood. (Unknown). Retrieved from <https://i.pinimg.com/originals/e5/e5/a2/e5e5a2df0a3e20cac0d5bf5ada522b2f.jpg>

- De Vries, D. (2001). *Variable Acoustics in Auditoria yesterday, today and tomorrow*. Paper presented at the ICA, Rome.
- Dionne, C. (2012). EJ Thomas Hall, Akron, Ohio. Retrieved from <https://www.flickr.com/photos/dionnemusic/8207761565/in/photostream/>
- Downtown Houston. (2010). Downtown Houston Guides. Retrieved from https://www.downtownhouston.org/site_media/uploads/photos/2010-05-05/jones-newtheater-102208_800x600.JPG
- dukta. (2018a). dukta flexible wood. Retrieved 2018, February 19 from <https://dukta.com/en/about-us/>
- dukta. (2018b). Wooden Knot. Retrieved from <https://dukta.com/en/products/objets-dart/>
- Dunn, F., Hartmann, W. M., Campbell, D. M., & Fletcher, N. H. (2015). *Springer handbook of acoustics*: Springer.
- Ermann, M. (2014). *Architectural acoustics illustrated*. Hoboken, New Jersey: Wiley.
- Godbold, O. (2008). *Investigating Broadband Acoustic Absorption Using Rapid Manufacturing*. (Doctoral Thesis), Loughborough University, Loughborough.
- Goldberg, S. A. (2006). Computational Design of Parametric Scripts for Digital Fabrication of Curved Structures. *International Journal of Architectural Computing*, 4(3), 99-117. doi:10.1260/147807706778658801
- Ivanišević, D. (2014). Super flexible laser cut plywood. Retrieved 2018, April 9 from <http://lab.kofaktor.hr/en/portfolio/super-flexible-laser-cut-plywood/>
- JISC. (n.d.). *Designing Spaces for Effective Learning: A guide to 21st century learning space design*. Retrieved from http://webarchive.nationalarchives.gov.uk/20140702233839/http://www.jisc.ac.uk/publications/programmerelated/2006/pub_spaces.aspx
- Kaushish, J. (2010). *Manufacturing processes*: PHI Learning Pvt. Ltd.
- Kingston University London. (Unknown). Laser cutting. Retrieved from <https://store.kingston.ac.uk/product-catalogue/kingston-school-of-art/3d-workshop/cnc3d-printing>
- Madbouly, A. I., Noaman, A. Y., Ragab, A. H. M., Khedra, A. M., & Fayoumi, A. G. (2016). Assessment model of classroom acoustics criteria for enhancing speech intelligibility and learning quality. *Applied Acoustics*, 114, 147-158. doi:<https://doi.org/10.1016/j.apacoust.2016.07.018>
- MaterialDistrict. (2017). New Metamaterial Based On Japanese Art Of Kirigami. Retrieved from <https://materialdistrict.com/article/new-metamaterial-kirigami/>

- Nieweglowski, T. Cutting wood with a CNC milling machine. Retrieved from <http://www.rt-cnc.ee/en-gb/cncmachines/cncrouters/miniteh.aspx>
- Ohshima, T., Igarashi, T., Mitani, J., & Tanaka, H. (2013). Fabricating curved objects without moulds or glue.
- Pääkkönen, R., Vehviläinen, T., Jokitulppo, J., Niemi, O., Nenonen, S., & Vinha, J. (2015). Acoustics and new learning environment – A case study. *Applied Acoustics*, 100, 74-78. doi:<https://doi.org/10.1016/j.apacoust.2015.07.001>
- Panier des Touches, O. (2014). Espace de projection. Retrieved from <http://web4.ircam.fr/cursus.html?event=1286&L=1>
- Porterfield, A. (2014). Madera curvada con un cortador láser. Retrieved from <http://www.instructables.com/howto/bent+plywood/>
- Puglisi, G. E., Cutiva, L. C. C., Pavese, L., Castellana, A., Bona, M., Fasolis, S., . . . Astolfi, A. (2015). Acoustic Comfort in High-school Classrooms for Students and Teachers. *Energy Procedia*, 78, 3096-3101. doi:<https://doi.org/10.1016/j.egypro.2015.11.763>
- Rational Acoustics. (2015). *Smaart 7 Impulse Response Measurement and Analysis Guide*. Retrieved from <https://www.rationalacoustics.com/wp-content/uploads/2015/04/Smaart-v7-IR-Guide.pdf>
- Roohnia, M. (2016). Wood: Acoustic Properties. In *Reference Module in Materials Science and Materials Engineering*: Elsevier.
- Sala, E., & Rantala, L. (2016). Acoustics and activity noise in school classrooms in Finland. *Applied Acoustics*, 114, 252-259. doi:<https://doi.org/10.1016/j.apacoust.2016.08.009>
- Scannell, L., Hodgson, M., Villarreal, J. G. M., & Gifford, R. (2016). The Role of Acoustics in the Perceived Suitability of, and Well-Being in, Informal Learning Spaces. *Environment and Behavior*, 48(6), 769-795. doi:10.1177/0013916514567127
- Schattschneider, D. (1978). The plane symmetry groups: their recognition and notation. *The American Mathematical Monthly*, 85(6), 439-450.
- Sharma, A., & Yadava, V. (2017). Experimental analysis of Nd-YAG laser cutting of sheet materials – A review. *Optics & Laser Technology*, 98(Supplement C), 264-280. doi:<https://doi.org/10.1016/j.optlastec.2017.08.002>
- Shyu, T. C., Damasceno, P. F., Dodd, P. M., Lamoureux, A., Xu, L., Shlian, M., . . . Kotov, N. A. (2015). A kirigami approach to engineering elasticity in nanocomposites through patterned defects. *Nature Materials*, 14, 785. doi:10.1038/nmat4327
- Thomasnet. (2018). About CNC Milling. Retrieved 2018, 05-03-2018 from <https://www.thomasnet.com/about/cnc-milling-51276103.html>

- Unknown. (2010). Architectural Acoustics. Retrieved 2018, April 14 from <http://www.industrial-electronics.com/measurement-testing-com/architectual-acoustics-3-2.html>
- US Craft Company. (Unknown). Baltic Birch Plywood. Retrieved from <https://www.bayou.com.tr/>
- Wikipedia contributors. (2018, March 21). Meander (art). In *Wikipedia, The Free Encyclopedia*. Retrieved 2018, April 9 from [https://en.wikipedia.org/wiki/Meander_\(art\)](https://en.wikipedia.org/wiki/Meander_(art))
- Zarrinmehr, S., Akleman, E., Ettehad, M., Kalantar, N., & Borhani, A. (2017). Kerfing with Generalized 2D Meander-Patterns: Conversion of Planar Rigid Panels into Locally-Flexible Panels with Stiffness Control. In G. Çagdas, M. Özkar, L. F. Gül, & E. Gürer (Eds.), *Future Trajectories of Computation in Design* (pp. 276-293). Istanbul, Turkey.
- Zarrinmehr, S., Akleman, E., Ettehad, M., Kalantar, N., Haghighi, A. B., & Sueda, S. (2017). An Algorithmic Approach to Obtain Generalized 2D Meander-Patterns. In D. Swart, C. H. Séquin, & K. Fenyvesi (Eds.), *Proceedings of Bridges 2017: Mathematics, Art, Music, Architecture, Education, Culture* (pp. 87-94). Phoenix, Arizona: Tessellations Publishing.
- Zarrinmehr, S., Ettehad, M., Kalantar, N., Borhani, A., Sueda, S., & Akleman, E. (2017). Interlocked archimedean spirals for conversion of planar rigid panels into locally flexible panels with stiffness control. *Computers & Graphics*, 66, 93-102. doi:<https://doi.org/10.1016/j.cag.2017.05.010>

APPENDICES

A. ACOUSTIC DATA AND MEASUREMENT RESULTS

A.1. PROJECT SETUP IMPEDANCE TUBE - LARGE SAMPLES

Impedance Tube

Type	Large
Microphone Spacing	0,05 m
Distance to Sample from Mic. B, Pos. 3	0,1 m
Distance to Source from Mic. A, Pos. 2	0,15 m
Diameter	0,100 m
Lower Frequency Limit	50 Hz

Measurement

Lines	800
Span	1,6 kHz
Averages	150
Center Frequency	800 Hz

Generator

Waveform	Random
Signal Level	2000 Vrms
Pink Filter	Off

Environment

Atmospheric Pressure	1013,25 hPa
Temperature	20 °C
Relative Humidity	80,0 %
Velocity of Sound	343,24 m/s
Density of Air	1202 kg/m ³
Characteristic Impedance of Air	412,6 Pa/(m/s)

Options

Signal-to-Noise Ratio Below	10,0 dB
Autospectrum (Max-Min) Above	60,0 dB
Calibration Factor exceeds	2,0 dB
Calibration Factor exceeds	2,0 degrees
Transfer Function Estimate	H1

A.2. PROJECT SETUP IMPEDANCE TUBE - SMALL SAMPLES

Impedance Tube

Type	Small
Microphone Spacing	0,02 m
Distance to Sample from Mic. B, Pos. 3	0,035 m
Distance to Source from Mic. A, Pos. 2	0,37 m
Diameter	0,029 m
Lower Frequency Limit	500 Hz

Measurement

Lines	800
Span	6,4 kHz
Averages	150
Center Frequency	3200 Hz

Generator

Waveform	Random
Signal Level	1414 Vrms
Pink Filter	Off

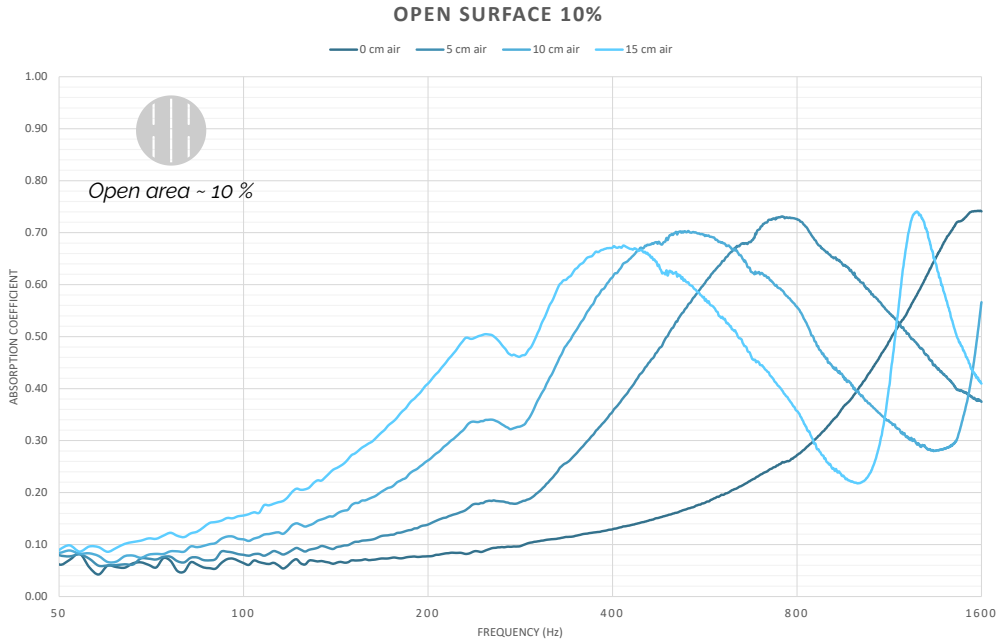
Environment

Atmospheric Pressure	1013,25 hPa
Temperature	20 °C
Relative Humidity	80,0 %
Velocity of Sound	343,24 m/s
Density of Air	1202 kg/m ³
Characteristic Impedance of Air	412,6 Pa/(m/s)

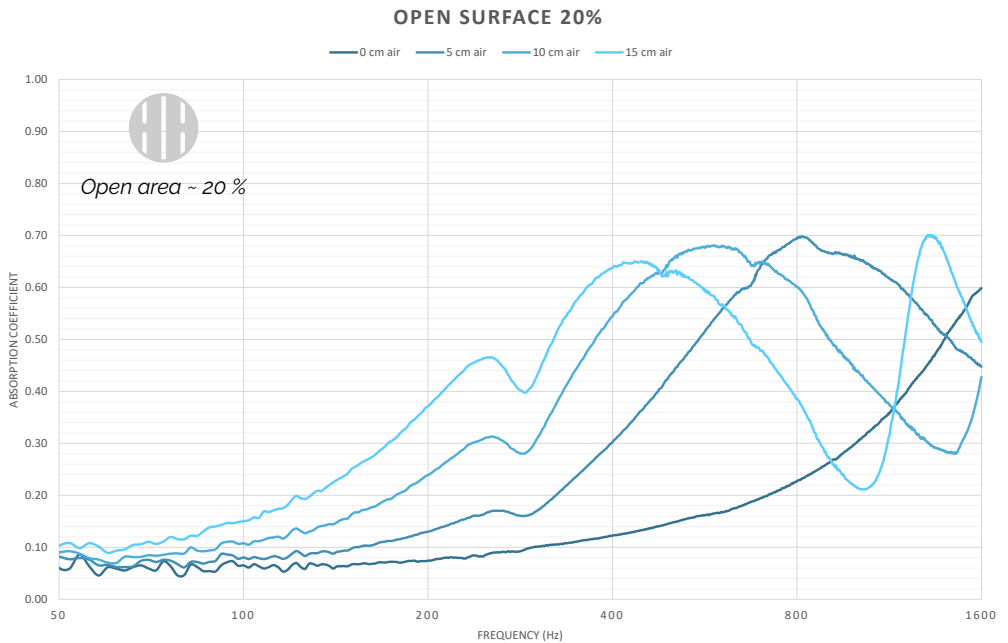
Options

Signal-to-Noise Ratio Below	10,0 dB
Autospectrum (Max-Min) Above	60,0 dB
Calibration Factor exceeds	2,0 dB
Calibration Factor exceeds	2,0 degrees
Transfer Function Estimate	H1

A.3. INDIVIDUAL GRAPHS IMPEDANCE TUBE MEASUREMENT

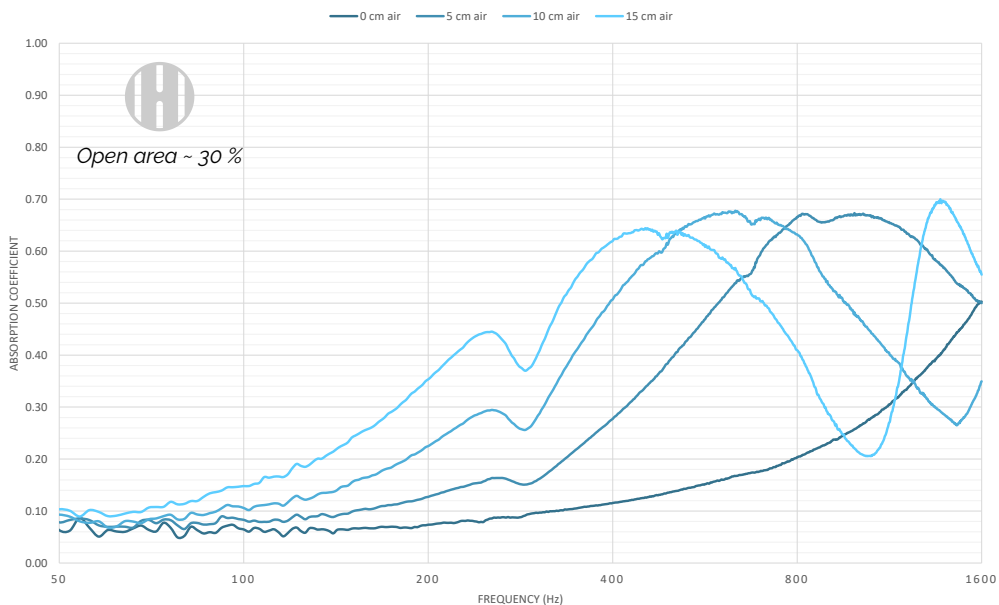


NOTE: Graph is in logarithmic scale



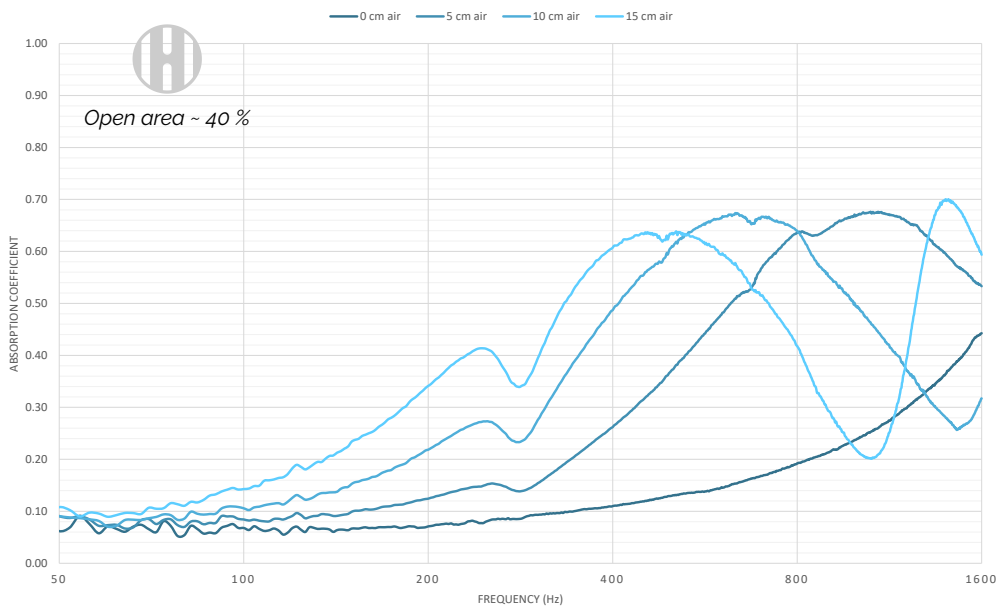
NOTE: Graph is in logarithmic scale

OPEN SURFACE 30%



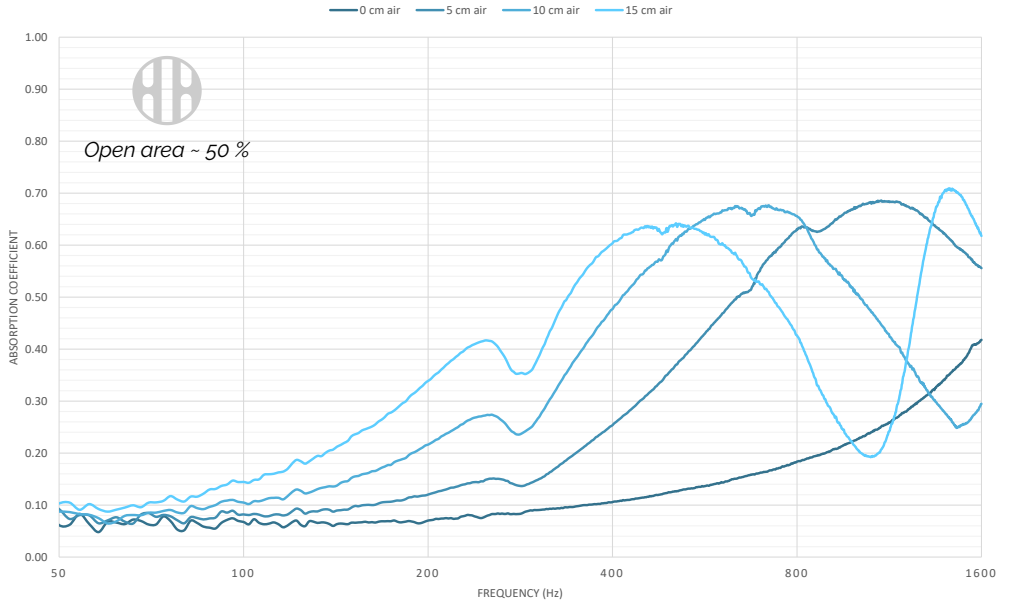
NOTE: Graph is in logarithmic scale

OPEN SURFACE 40%



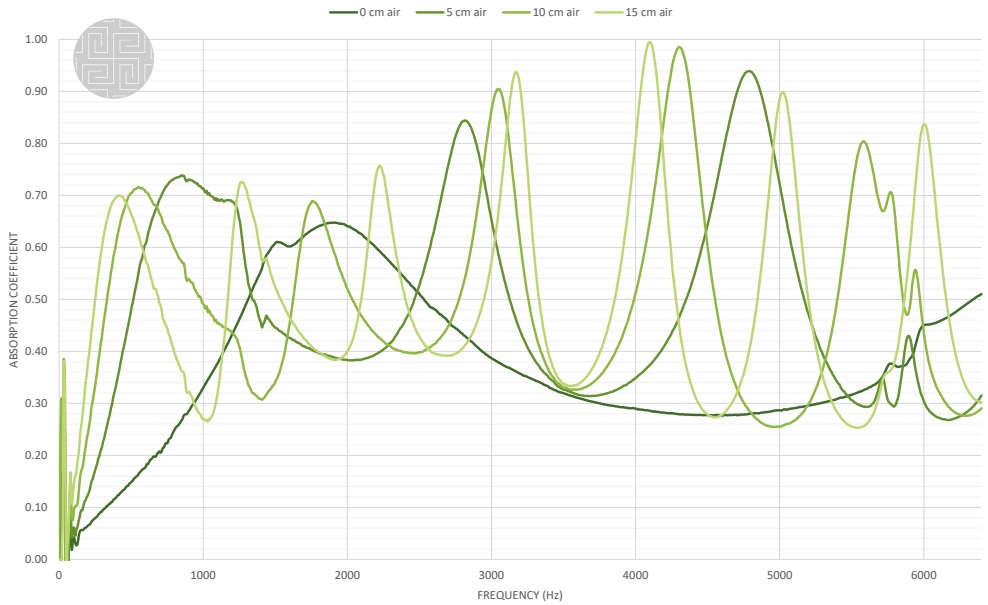
NOTE: Graph is in logarithmic scale

OPEN SURFACE 50%



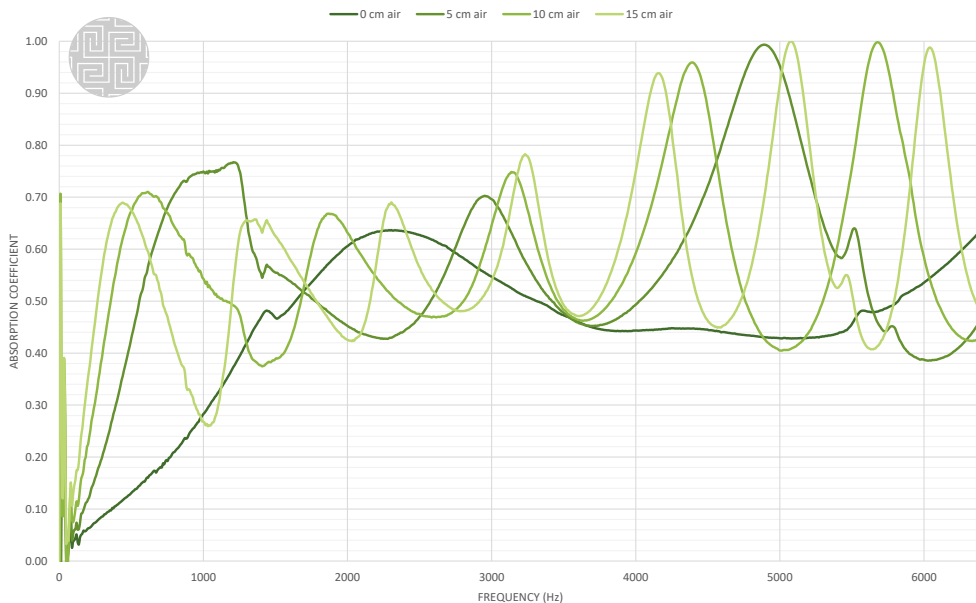
NOTE: Graph is in logarithmic scale

OPEN SURFACE 10%



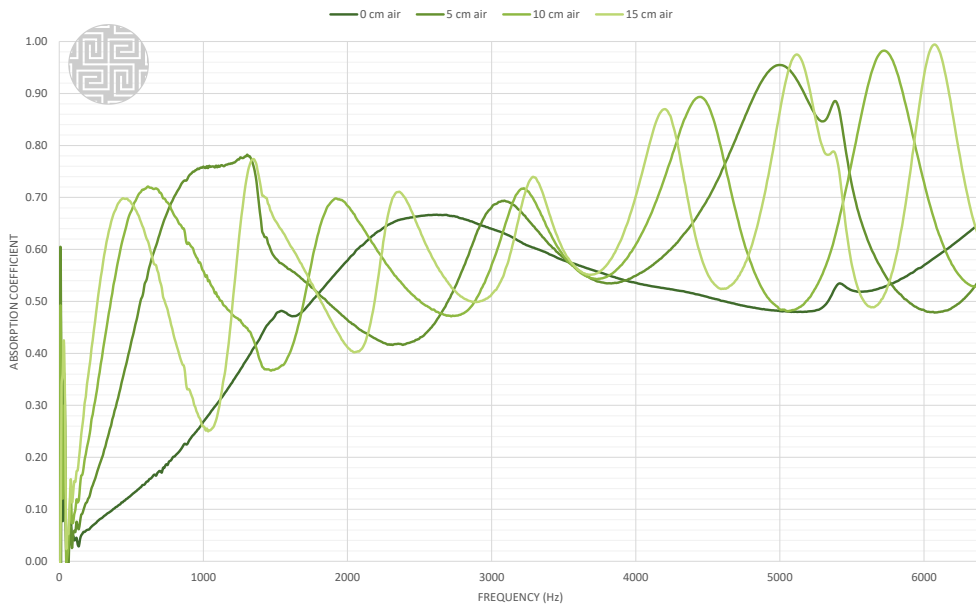
NOTE: Graph is in linear scale

OPEN SURFACE 20%



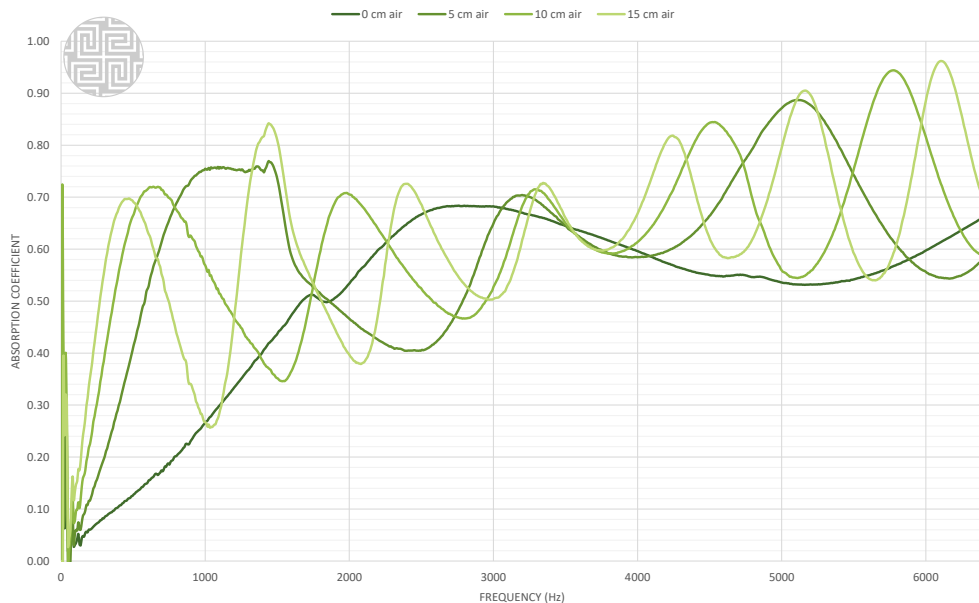
NOTE: Graph is in linear scale

OPEN SURFACE 30%



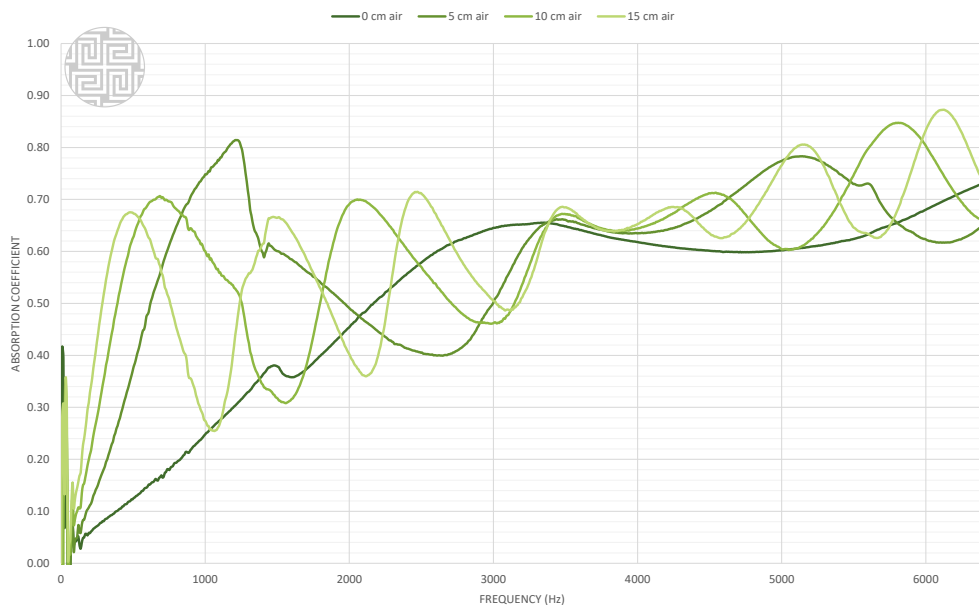
NOTE: Graph is in linear scale

OPEN SURFACE 40%



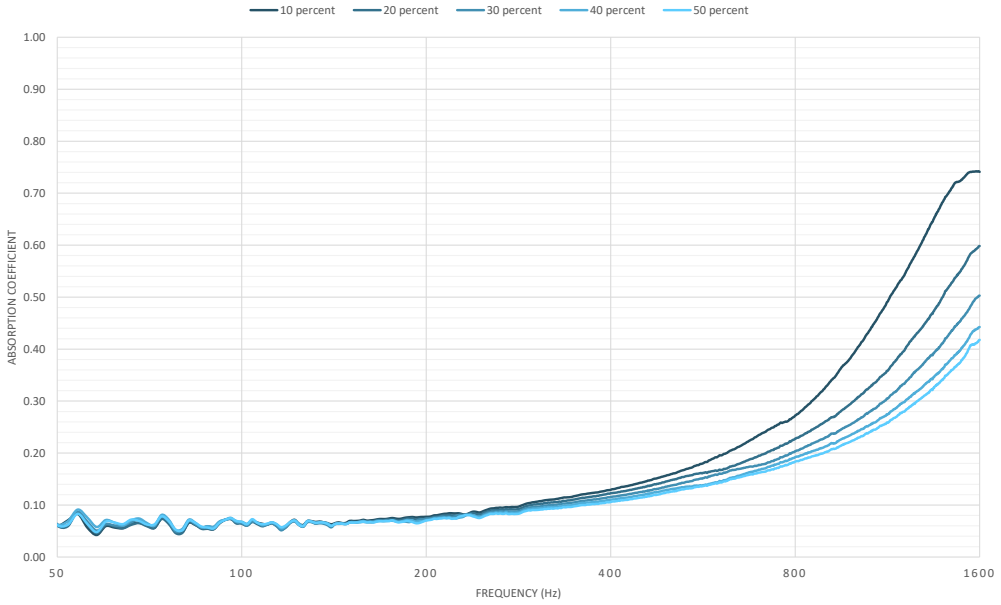
NOTE: Graph is in linear scale

OPEN SURFACE 50%



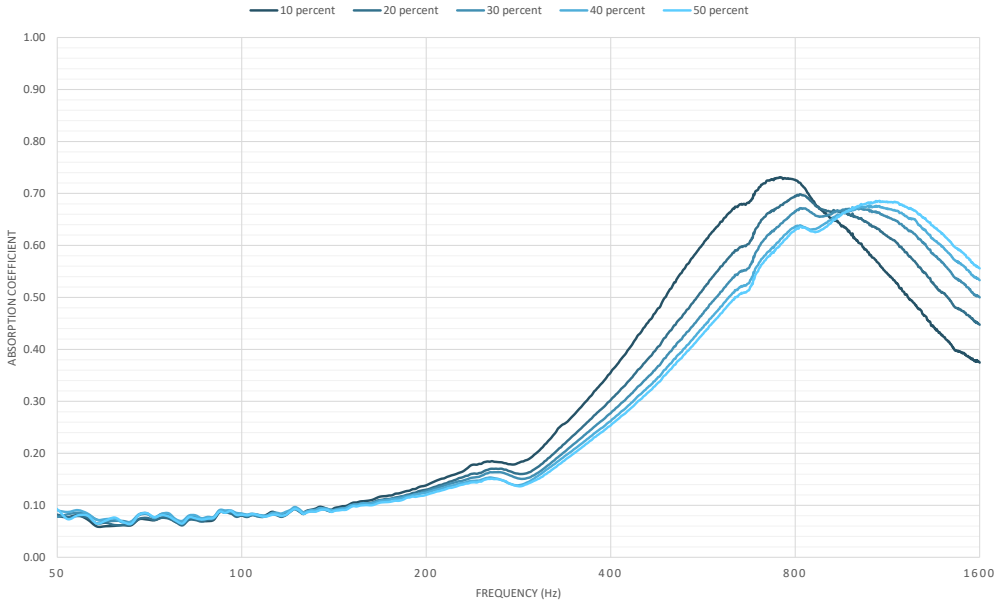
NOTE: Graph is in linear scale

AIR GAP 0 CM



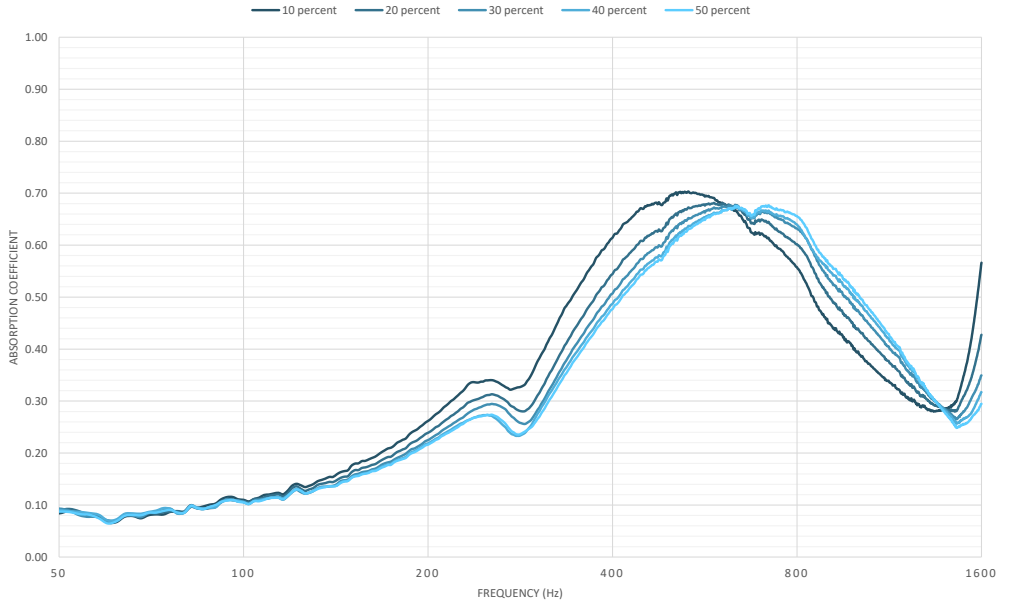
NOTE: Graph is in logarithmic scale

AIR GAP 5 CM



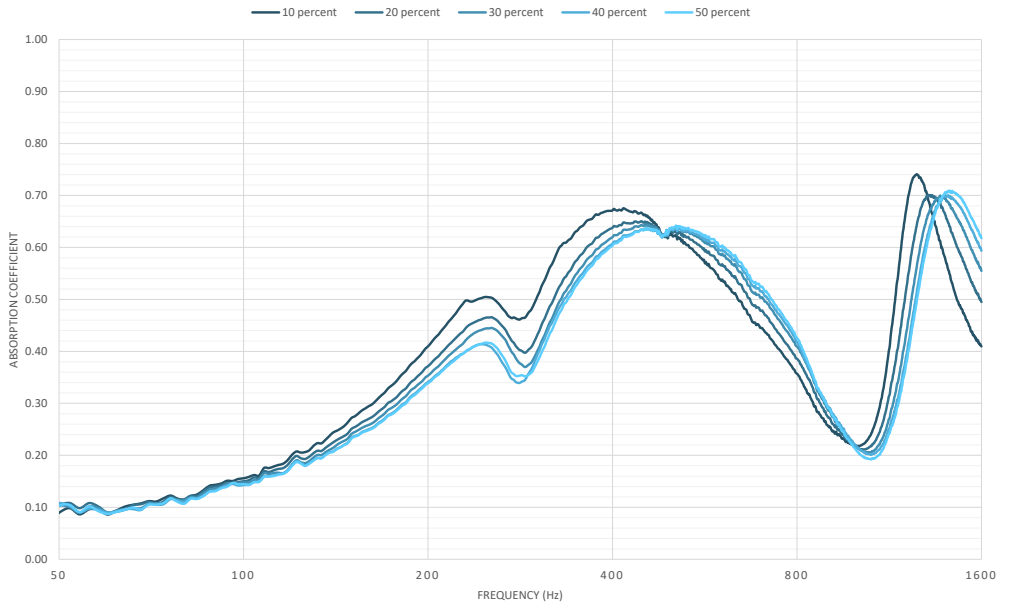
NOTE: Graph is in logarithmic scale

AIR GAP 10 CM



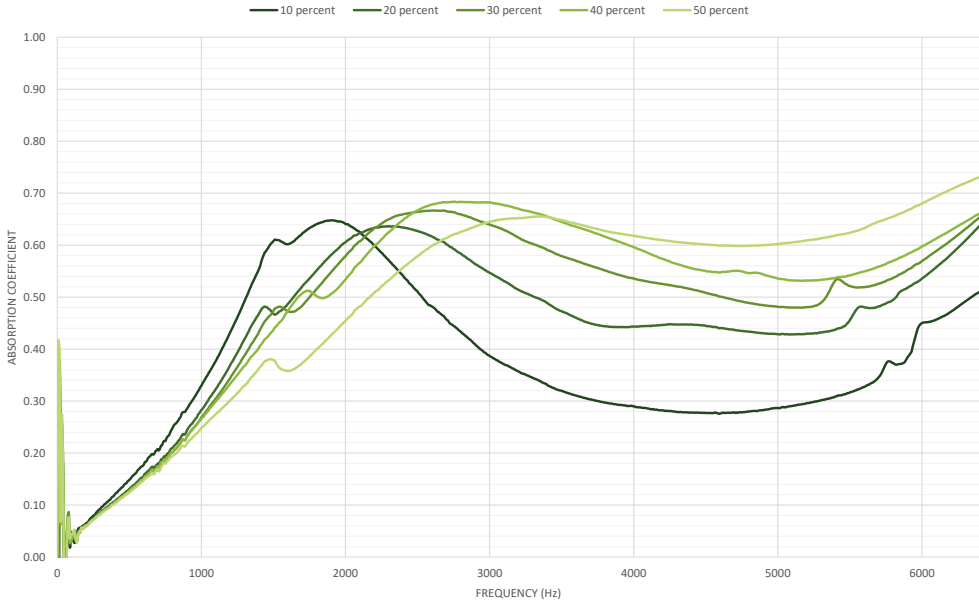
NOTE: Graph is in logarithmic scale

AIR GAP 15 CM



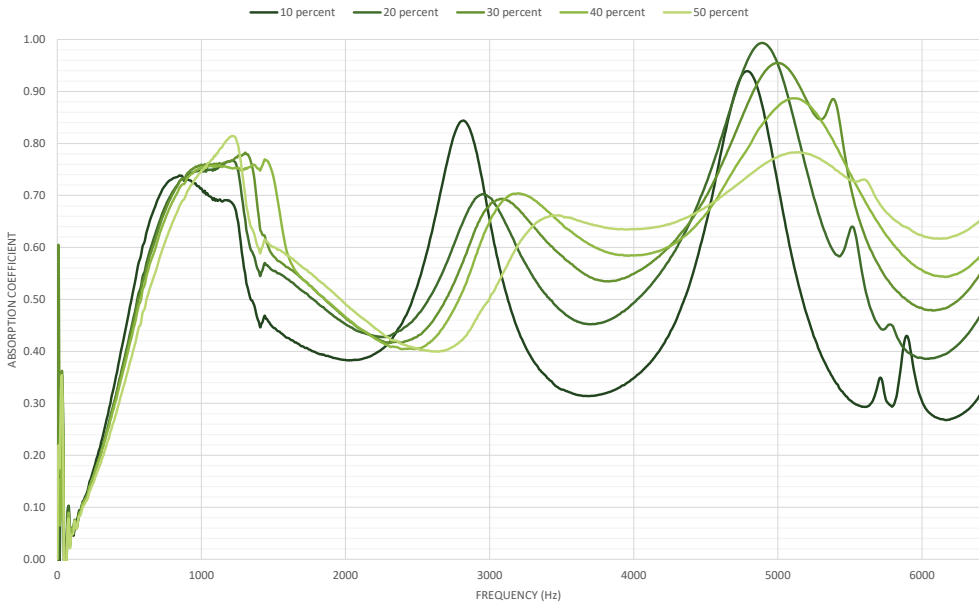
NOTE: Graph is in logarithmic scale

AIR GAP 0 CM

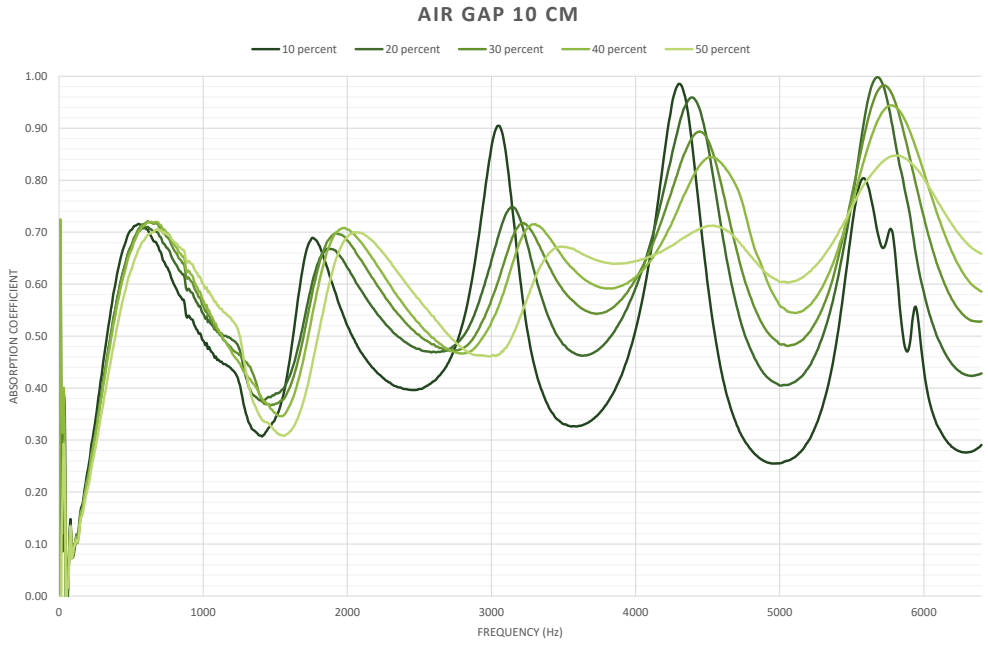


NOTE: Graph is in linear scale

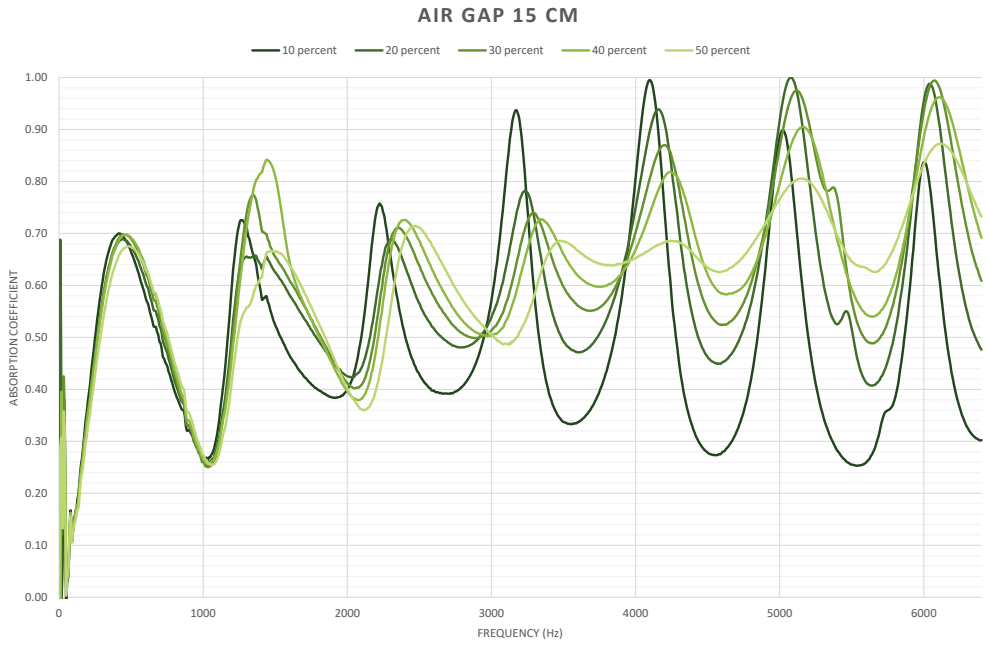
AIR GAP 5 CM



NOTE: Graph is in linear scale



NOTE: Graph is in linear scale



NOTE: Graph is in linear scale

